ISSN 2095-8137 CN 53-1229/Q
Volume 40 Issue 2
18 March 2019

ZR

Zoological Research

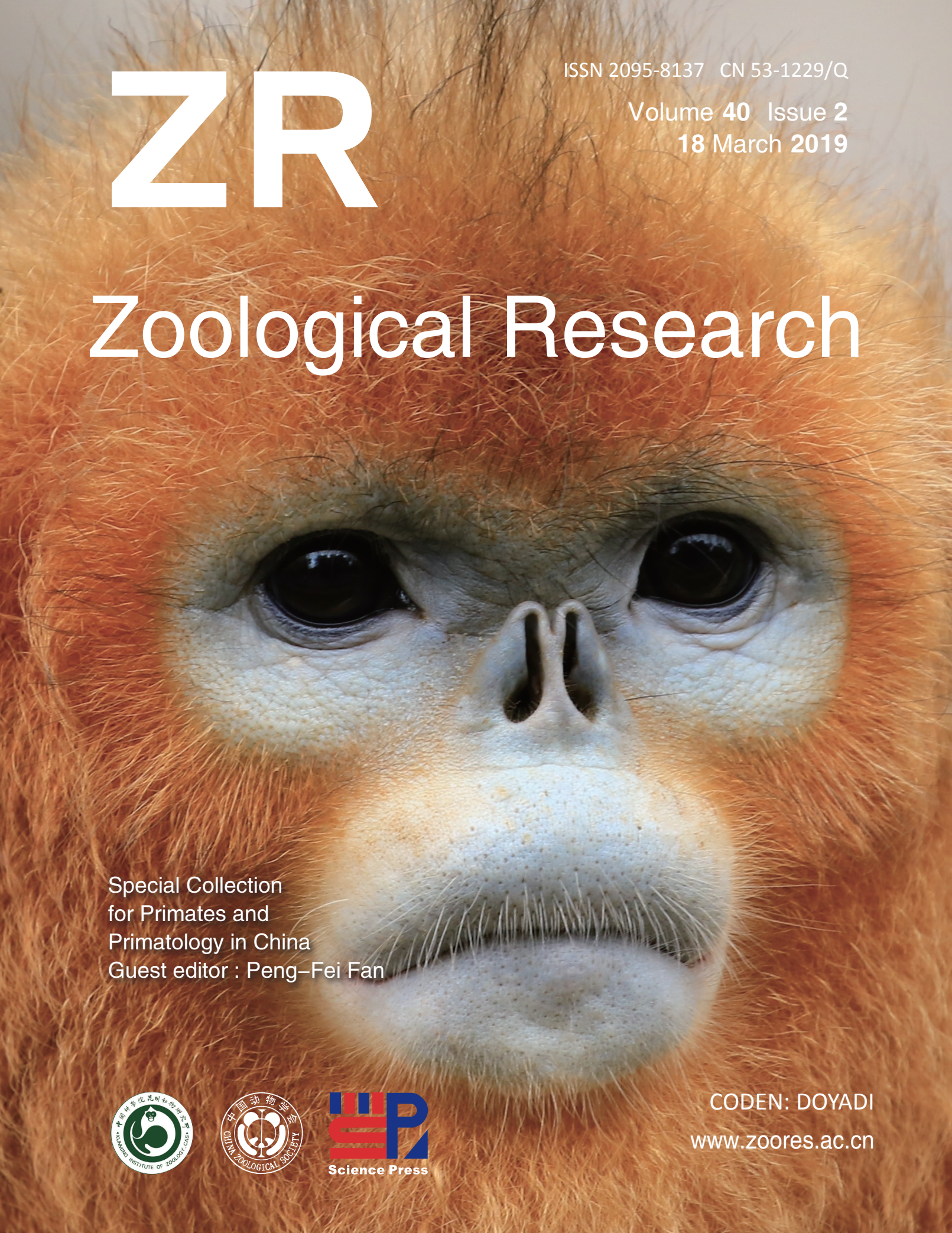

Special Collection
for Primates and
Primatology in China
Guest editor : Peng–Fei Fan

Science Press

CODEN: DOYADI
www.zoores.ac.cn

ZOOLOGICAL RESEARCH

Volume 40, Issue 2 18 March 2019

CONTENTS

Special Collection: Primates and Primatology in China

The special collection for “Primates and Primatology in China” was edited by Prof. Peng-Fei Fan

Cover image: Golden snub-nosed monkey (*Rhinopithecus roxellana*). Photo by Xiao-Feng Ma

Cover design: Li-Bin Wu

Current understanding on the roles of gut microbiota in fish disease and immunity

Intensive aquaculture has increased the severity and frequency of fish diseases. Given the functional importance of gut microbiota in various facets of host physiology, modulation of this microbiota is a feasible strategy to mitigate emerging diseases in aquaculture. To achieve this, a fundamental understanding of the interplay among fish health, microbiota, and invading pathogens is required. This commentary focuses on current knowledge regarding the associations between fish diseases, dysbiosis of gut microbiota, and immune responses. Furthermore, updated research on fish disease from an ecological perspective is discussed, including colonization resistance imposed by commensals and strategies used by pathogens to overcome resistance. We also propose several directions for future research, such as exploration of the causal links between fish diseases and specific taxa, and identification of universal gut microbial biomarkers for rapid disease diagnosis.

Fish aquaculture is the fastest growing animal food sector to support the growing human population, with a year-on-year growth rate of 10.4% (FAO, 2013). However, fish production is threatened by numerous diseases (Lafferty et al., 2015). This is particularly pertinent to aquacultural systems that impose various stressors on aquatic animals (Lafferty et al., 2015; Li et al., 2017a). Traditionally, antibiotics have been widely applied to prevent and treat diseases in aquacultures. However, antibiotic abuse has been highlighted in the transfer of resistance genes among pathogens, and has raised concerns regarding environmental pollution and consumer safety (Brandt et al., 2015). In recent years, the introduction of probiotics has been considered a sustainable strategy to improve fish health and protect them from emerging diseases (de Bruijn et al., 2017). Despite the extensive list of candidate probiotics investigated in previous studies (Dawood et al., 2016; Liu et al., 2018; Ramesh et al., 2017), successful application has been limited, as reported in a survey of farmers (Xiong et al., 2016). The lack of consistency in probiotic performance may be due to unsuccessful colonization as a result of sudden changes in habitats, e.g., from aerobic culture conditions to the anaerobic intestines (Giatsis et al., 2016). In addition, the fish gut is a main pathogen transmission route and a portal of entry (de Bruijn et al., 2017; Li et al., 2017a; Ringø et al., 2007; Zhang et al., 2015). Therefore, understanding the factors that dictate the invasion of pathogens and establishment of probiotics in the intestine will provide an initial step towards predicting and treating fish diseases.

Gut microbiota can affect fish physiology, development, life span, immunity, and barriers against pathogens (Burns et al., 2016; Nie et al., 2017; Smith et al., 2017; Yan et al., 2016). Therefore, the gut microbiota plays an indispensable role in fish fitness. Several recent reviews have centered on the diversity and functions of bacterial communities in healthy fish (de Bruijn et al., 2017), as well as on the external factors that affect fish gut microbiota (Wang et al., 2017) and interactions between gut microbiota and innate immunity in fish (Gómez & Balcázar, 2008; Nie et al., 2017). However, most previous studies have focused on factors that govern healthy gut microbiota, such as diet, rearing conditions, and fish genotype (Schmidt et al., 2015; Sullam et al., 2012; Yan et al., 2016). In contrast, few studies have reported on the interplay among gut microbiota, fish immunity, and disease (Nie et al., 2017). In this commentary, we summarize current knowledge on the associations between fish immunity, gut microbiota, and invading intestinal pathogens. We also highlight recent progress in uncovering the ecological processes of fish diseases.

According to the diversity resistance hypothesis, a more diverse microbial community harbors greater probability of having a species with an antagonistic trait toward an invader or pathogen (Fargione & Tilman, 2005). Consistent with this assertion, higher alpha diversity (mean species diversity at the habitat level) is frequently detected in healthy fish compared with diseased fish, such as largemouth bronze gudgeon (*Coreius guichenoti*) (Li et al., 2016), crucian carp

Received: 05 April 2018; Accepted: 23 May 2018; Online: 03 July 2018
Foundation items: This project was supported by the Program for the National Natural Science Foundation of China (31772876; 31372555), Natural Science Foundation of Zhejiang Province (LZ18C190001), Natural Science Foundation of Ningbo City of China (2017A610284), Scientific Innovation Team Project of Ningbo (2015C110018), and K.C. Wong Magna Fund in Ningbo University
DOI: 10.24272/j.issn.2095-8137.2018.069

(*Carassius auratus*) (Li et al., 2017a), and ayu (*Plecoglossus altivelis*) (Nie et al., 2017). One possible explanation for this pattern is that the invading pathogens out-compete the gut commensals, thereby reducing diversity. Similarly, gnotobiotic zebrafish (*Danio rerio* Hamilton, 1822) have been shown to be more sensitive to pathogenic infections (Oyarbide et al., 2015). In addition, antibiotic administration generally reduces diversity of the gut microbiota, which, in turn, facilitates colonization by external pathogens (He et al., 2017). Indeed, gut microbial diversity has been used as a biomarker of fish health and metabolic capacity (Clarke et al., 2014), with low diversity and stability of the microbiota closely associated with fish disease (He et al., 2017; Li et al., 2017a; Nie et al., 2017). A preponderance of evidence has demonstrated that more diverse gut communities exert greater protective effects on the host (De Schryver & Vadstein, 2014; Johnson et al., 2008; Zhu et al., 2016). In this regard, gut microbial diversity in fish should be maximized to reduce pathogenic invasions in aquaculture systems.

Fish are in continual contact with a complex and dynamic planktonic microbiota. Therefore, it is expected that gut microbiota in fish will be largely affected by microbes in the environment. This has been demonstrated by the high similarity between water and gut microbiotas of Atlantic cod larvae (*Gadus morhua*) (Bakke et al., 2013), rainbow trout (*Oncorhynchus mykiss*) (Wong et al., 2013), and tilapia larvae (Giatsis et al., 2015). Based on the co-evolution theory, however, to improve host fitness, mutualistic relationships between fish and gut microbiota should be tightly regulated to ensure suitable bacterial colonization (McFall-Ngai et al., 2013). As a result, gut bacterial communities between recently caught and domesticated fish share similar community structures (Roeselers et al., 2011). Intriguingly, reciprocal gut microbiota transplants between zebrafish and mice have shown that the relative abundance of lineages changes to resemble normal gut microbiota of the recipient host (Rawls et al., 2006). Similarly, previous meta-analysis has revealed that host phylogeny determines the composition of fish gut bacteria, even at the bacterial phylum level (Sullam et al., 2012). For example, the gut microbiota of largemouth bronze gudgeon is dominated by phyla *Proteobacteria*, *Actinobacteria*, and *Tenericutes* (Li et al., 2016), whereas *Gammaproteobacteria*, *Alphaproteobacteria*, *Firmicutes*, and *Bacteroides* are predominant in the gut of ayu (Nie et al., 2017). This pattern also holds true for different fish species (herbivorous *Ctenopharyngodon idellus*, carnivorous *Siniperca chuatsi*, and *Silurus meridionalis*) reared in the same pond (Yan et al., 2016). Indeed, it has been suggested that gut microbiotas of fish are distinct from those in rearing water and/or sediment (Li et al., 2017a; Schmidt et al., 2015; Zhang et al., 2018). However, this does not mean that the gut microbiota is temporally stable during the entire lifetime of the fish; rather, gut bacterial communities vary significantly during the developmental stages in healthy fish (Li et al., 2017b; Stephens et al., 2016; Yan et al., 2016; Zhang et al., 2018). This high temporal pattern is largely contributed to by maturation of the host (Burns et al., 2016; Zhang et al., 2018) as selection of gut microbiota is reinforced with time. Intriguingly, several species of fish exhibit core gut microbiota, including zebrafish (Roeselers et al., 2011), rainbow trout (Wong et al., 2013), channel catfish (*Ictalurus punctatus*), largemouth bass (*Micropterus salmoides*), and bluegill (*Lepomis macrochirus*) (Larsen et al., 2014), though location-dependent variations in gut microbiota also exist. These core lineages may be used as baselines for future probiotic trials.

It is worth emphasizing, however, that the tight link between fish and their gut microbiota can be disrupted by diverse variables, with host disease being the primary factor (Li et al., 2017a; Nie et al., 2017). Gut bacteria reside on mucosal surfaces, which provide the first line of defense against pathogens. Specifically, commensal bacteria compete for or modify the ecological niche and available nutrients to inhibit the colonization and proliferation of incoming pathogens in the intestine (Kamada et al., 2013). For example, well-known probiotic *Bifidobacterium* prevents pathogenic *Escherichia coli* invasion via acidification of the intestinal environment (interspecies barrier effect) (Fukuda et al., 2012). In addition, gut commensals can produce bacteriocins and proteinaceous toxins that specifically inhibit members of the same or similar bacterial species (intraspecies barrier effect). Therefore, susceptibility to pathogenic infection seems to rely, at least in part, on the structure of the host's gut microbial community (Galindo-Villegas et al., 2012; He et al., 2017). Indeed, dysbiosis in the gut microbiota is frequently associated with fish disease (He et al., 2017; Nie et al., 2017). However, it is currently unclear whether changes in the microbial community are a cause or consequence of these diseases.

Responses of a community to disturbance (e.g., disease) are not solely the sum of the traits of individual species but are also dependent on interspecies interactions (Faust & Raes, 2012; Zhu et al., 2016). Our recent work showed that pathogenic infections have a significant impact on the gut microbiota, with diseased ayu exhibiting less complex and diverse interspecies interactions (Nie et al., 2017). Indeed, interspecies interaction analysis has been applied to identify candidate pathogens and/or probiotics in gut diseases (Buffie et al., 2015; Dai et al., 2018). Furthermore, it is apparent that populations, not clones, are the causal agents of some aquaculture diseases (Hou et al., 2018; Lemire et al., 2015). This idea overturned the traditional view that only a pathogen and/or virulence gene result in disease (Falkow, 1988), and led to the 'ecological Koch's postulates', which aims to untangle the interplay between host health, microbiota, invading pathogens, and diseases (Vonaesch et al., 2018). However, current understanding on the ecological processes that govern the gut microbiota in fish is still in its infancy, and no consensus has yet emerged. For example, it has been reported that the relative importance of determinism increases as zebrafish mature (Burns et al., 2016), whereas other studies have shown the opposite trend (Li et al., 2017b; Yan et al., 2016). Understanding the factors that govern the gut microbiota provides an initial step to establishing and maintaining a healthy fish microbiome (de Bruijn et al., 2017; De Schryver & Vadstein, 2014). In this regard, exploring the underlying mechanisms of

fish diseases will provide an integrated approach to systems biology and ecology.

Going a further step, gut signatures can also be associated with fish diseases. For example, taxa affiliated with genera *Vibrio*, *Aeromonas*, and *Shewanella* are overrepresented in the gut microbiota of "red-operculum" disease in crucian carp, whereas *Cetobacterium* species are indicators of healthy fish (Li et al., 2017a). Similarly, *Aeromonas* is a biomarker for largemouth bronze gudgeon suffering from furunculosis (Li et al., 2016). This phenomenon suggests that certain gut microbial signatures are indicative of host health status irrespective of disease pathogeny, as has been demonstrated in human gut diseases (Mancabelli et al., 2017). Recent mechanistic studies suggest that the inflammatory host response produces reactive oxygen species, which facilitate a competitive advantage to facultative anaerobic lineages, such as *Aeromonas* (Winter & Bäumler, 2014). To date, however, surprisingly few studies have examined the association between disease severity and degree of dysbiosis in the gut microbiota during disease progression in fish. As a result, it is unclear whether the transition from healthy to diseased gut microbiota is gradient-like or a discrete process (Knights et al., 2014). If the transition is gradual, gut microbial signatures could serve as independent variables for predicting the incidence of fish disease, similar to that observed in shrimp diseases (Xiong et al., 2017; Xiong et al., 2018).

In addition to direct inhibition, the fish gut microbiota also plays critical roles in epithelial renewal and maturation, which, in turn, regulate immune responses (Gómez & Balcázar, 2008; Wang et al., 2017). Under normal conditions, goblet cells secrete mucus, which functions as a barrier to inhibit migration of microorganisms out of the intestinal lumen (Ringø et al., 2007). A mature gut mucosa is also essential for distinguishing pathogens from commensals through pattern recognition receptors (PRRs, such as toll-like receptors, RIG-I-like receptors, NOD-like receptors and AIM2-like receptors), which detect bacterial antigens and activate signaling cascades to regulate immune responses (cytokines) (Pérez et al., 2010). For example, the toll-like receptor family, a representative member of PRRs, recognizes conserved structures in pathogens, which can recruit and regulate the immune and inflammatory cells that initiate and mediate systemic immune responses (Fasano & Sheadonohue, 2005). Additionally, commensals can protect the host by depriving invading pathogens of nutrients, secreting a range of antimicrobial substances and occupying the niche (de Bruijn et al., 2017; Gómez & Balcázar, 2008; Pérez et al., 2010). However, if this balance is disrupted, such as during pathogenic infections, the innate and adaptive immune systems are activated to prevent disease exacerbation. Conversely, there is a correlation between colonization of probiotics and innate immune responses, such as phagocytic and alternative complement pathway activities, which protect fish against pathogens (Balcázar et al., 2007; Kim & Austin, 2006).

Studies on gnotobiotic zebrafish demonstrate that the gut microbiota enhances the stability of β-catenin via activation of Wnt signaling, thereby promoting intestinal cell proliferation over normal ontogenesis (Cheesman et al., 2011; Rawls et al., 2006). Compared with germ-free zebrafish, conventionally raised zebrafish exhibit a greater abundance of genes associated with epithelial proliferation and innate immune response (Rawls et al., 2004). However, germ-free zebrafish with a commensal microbiota can robustly activate NF-κB and its target genes in intestinal and extra-intestinal tissues (Kanther et al., 2011). Similarly, colonization of commensals in larvae stimulates neutrophils and activates pro-inflammatory genes through the TLR/MyD88 signaling pathway and phagocytes, which can enhance disease resistance in zebrafish (Galindo-Villegas et al., 2012). Specifically, the gut microbiota induces intestinal macrophages by upregulating pro-IL-1β. The mature form of IL-1β (activated by pathogen infection) recruits neutrophils, thereby priming macrophages to eradicate pathogens (Kamada et al., 2013). Significant association between the gut microbiota and transcription level of secreted immunoglobulin M (sIgM, a proxy for adaptive immune development) has been reported during healthy zebrafish development (Stephens et al., 2016). Compared with functional B- and T-cell receptor immune-deficient zebrafish, wild-type zebrafish exhibit an individualized gut microbiota and increased determinism of gut microbiota assembly (Stagaman et al., 2017). Our recent work also showed pro-inflammatory cytokines IL-1β and TNF-α to be activated in response to pathogenic infections in ayu (Nie et al., 2017). On the other hand, administration of probiotics to sea bass (*Dicentrarchus labrax* L.) results in the downregulation of IL-1β and transforming growth factor-β (Picchietti et al., 2008). Collectively, these results indicate a normal gut microbiota contributes indispensable roles in regulating the fish immune system, and vice versa.

As described above, the host and gut microbiota have co-evolved multiple strategies to not only prevent colonization by external pathogens, but also suppress resident pathogens. However, pathogens have developed various strategies to overcome these barriers, including entry into the host, occupation of a unique niche, circumvention of commensals and host defense barriers, and acquisition of nutrients from fish hosts (Ringø et al., 2007). Specifically, pathogens express sortases and adhesins for anchoring to host intestinal cells. After attachment to the intestinal tract, pathogens produce toxins and hemolysins to aggressively damage the intestinal lining and induce inflammatory responses (Mazmanian et al., 2001; Ringø et al., 2007). There is evidence that the inflamed environment induces production of reactive oxygen and/or nitrogen species by the host, resulting in a bloom of facultative anaerobic bacteria (e.g., *Proteobacteria*) and reduction in obligate anaerobic bacteria (Winter & Bäumler, 2014). This shift in community composition compromises colonization resistance imposed by gut microbiota, thereby facilitating the overgrowth of potentially harmful indigenous bacterial species (Galindo-Villegas et al., 2012; He et al., 2017). To escape from host immune clearance, some enteric pathogens harbor a modified form of siderophore (chelating iron under iron-limiting

conditions) that is not inhibited by host cell-secreted lipocalin 2, which can further promote the growth of pathogens (Fischbach et al., 2006). Additionally, pathogenic capsules promote virulence by reducing host immune responses (Singh et al., 2011). Gram-negative pathogens commonly encode the type 6 secretion system (T6SS), which enables pathogens to attack the resident microbiota and to confer them with a competitive advantage (Russell et al., 2014; Vonaesch et al., 2018). In addition, to counteract nutritional competition by commensals, some pathogens can use alternative or pathogen-specific nutrients, which expand the nutrient niche for their colonization (Fabich et al., 2008). Alternatively, invaders can also occupy a distinct niche during replication to reduce competition with commensals. For example, pathogenic *Citrobacter rodentium* expresses intimin, which enables its localization to the intestinal epithelial surface, where commensals do not normally occur (Kamada et al., 2012). Intriguingly, pathogens can sense cues (e.g., bile acids, temperature, and nutrient availability) from their host to regulate virulence genes at the appropriate location (Fraser & Brown, 2017; Vonaesch et al., 2018). This regulatory mechanism can therefore maximize the chance of successful invasion.

Once a pathogen escapes colonization resistance imposed by gut commensals and host immunity, it can replicate and further express diverse virulence factors to attack fish and cause disease. There is increasing evidence that pathogenic infections cause profound disturbances to the fish gut microbiota and immune responses (He et al., 2017; Nie et al., 2017; Ringø et al., 2007). Notably, variations in the gut microbiota of ayu are significantly associated with TNF-α and IL-1β expression levels (Nie et al., 2017). Similarly, antibiotic administration can also cause imbalance in the gut microbiota of zebrafish, resulting in a compromised immune response, which further increases susceptibility to infections (He et al., 2017). Molecular experiments further suggest that decreased water quality can promote pathogen virulence (Penttinen et al., 2016). Therefore, disease onset in fish can be attributed to a variety of disturbances, such as environmental stress and antibiotic administration, which disrupt the gut microbiota in stressed fish and enhance the virulence of pathogens.

In summary, the introduction of pathogens into hosts is antagonized by environmental pressure, fish filtering, and colonization resistance of gut commensals (Mallon et al., 2015). In healthy fish, the gut microbiota directly antagonizes the colonization or overgrowth of pathogens (Nie et al., 2017). These effects include competition for resources, niche exclusion, and suppression of virulence factors. In addition, pathogens are suppressed by immune clearance. In diseased fish, balances in the protective commensal microbial community and host immunity are disturbed by external factors. For example, antibiotic usage can decrease species diversity and alter gut microbial community structure in fish (He et al., 2017). Pathogenic infections have been shown to significantly disrupt interspecies interactions in the fish gut microbiota (Nie et al., 2017). These alterations may open up ecological niches for pathogenic invasions. Furthermore, environmental stresses may impose additional pressure on fish, leading to compromised immunity. Lastly, the expression of virulence genes in pathogens can also be induced by poor water quality (Penttinen et al., 2016; Zhou et al., 2012). These detrimental effects cumulatively attenuate resistance to colonization by pathogens and allow overgrowth of harmful colonies that may lead to disease.

Given the functional importance of the gut microbiota in improving host fitness, introduction or augmentation of beneficial microbes may be a promising approach for protecting fish from emerging diseases (de Bruijn et al., 2017). However, various studies have identified long lists of implicated microbes that may contribute to the gut microbiota dysbiosis-disease relationship, and these associations may reflect biomarkers of disease. Therefore, future work is required to explore the causal links between fish disease and specific taxa, which may enable us to optimize gut microbiota composition to mitigate fish disease. Pathogenic infections involve several phases: introduction, establishment, spread, and impact, which are governed by the environment, host, and gut microbiota (Mallon et al., 2015). To understand the mechanisms underlying fish disease, one should focus on the infection process from an ecological prospective (De Schryver & Vadstein, 2014; Xiong et al., 2016) instead of isolating potential pathogens from diseased fish. Next generation sequencing has allowed the identification of universal gut microbial biomarkers (common features of affected individuals) in various fish diseases from different regions. Therefore, we recommend that relevant information should be deposited into a public database, which could enable convenient cross-disease comparisons. This would facilitate rapid diagnosis as well as promote prediction of the course and prognosis of disease.

COMPETING INTERESTS

The authors declare that they have no competing interests.

AUTHORS' CONTRIBUTIONS

J.C. and J.B.X. designed the study. J.B.X. wrote the manuscript with help from J.C. and L.N.. All authors read and approved the final version of the manuscript.

Jin-Bo Xiong[1], Li Nie[1,2], Jiong Chen[1,2,*]

[1] *Laboratory of Biochemistry and Molecular Biology, School of Marine Sciences, Ningbo University, Ningbo Zhejiang* 315211*, China*

[2] *Key Laboratory of Applied Marine Biotechnology of Ministry of Education, Ningbo University, Ningbo Zhejiang* 315211*, China*

[*]Corresponding author, E-mail: jchen1975@163.com

REFERENCES

Bakke I, Skjermo J, Vo TA, Vadstein O. 2013. Live feed is not a major determinant of the microbiota associated with cod larvae (*Gadus morhua*). *Environmental Microbiology Reports*, **5**(4): 537–548.

Balcázar JL, De BI, Ruiz-Zarzuela I, Vendrell D, Calvo AC, Márquez I, Gironés O, Muzquiz JL, 2007. Changes in intestinal microbiota and humoral

immune response following probiotic administration in brown trout (*Salmo trutta*). *British Journal of Nutrition*, **97**(3): 522–527.

Brandt KK, Amézquita A, Backhaus T, Boxall A, Coors A, Heberer T, Lawrence JR, Lazorchak J, Schönfeld J, Snape JR, 2015. Ecotoxicological assessment of antibiotics: A call for improved consideration of microorganisms. *Environment International*, **85**: 189–205.

Buffie CG, Bucci V, Stein RR, McKenney PT, Ling L, Gobourne A, No D, Liu H, Kinnebrew M, Viale A, Littmann E, van den Brink MR, Jenq RR, Taur Y, Sander C, Cross JR, Toussaint NC, Xavier JB, Pamer EG. 2015. Precision microbiome reconstitution restores bile acid mediated resistance to *Clostridium difficile*. *Nature*, **517**(7533): 205–208.

Burns AR, Stephens WZ, Stagaman K, Wong S„ Rawls JF, Guillemin K, Bohannan BJ. 2016. Contribution of neutral processes to the assembly of gut microbial communities in the zebrafish over host development. *ISME Journal*, **10**(3): 655–664.

Cheesman SE, Neal JT, Mittge E, Seredick BM, Guillemin K. 2011. Epithelial cell proliferation in the developing zebrafish intestine is regulated by the wnt pathway and microbial signaling via myd88. *Proceedings of the National Academy of Sciences of the United States of America*, **108** (Suppl 1): 4570–4577.

Clarke SF, Murphy EF, O'Sullivan O, Lucey AJ, Humphreys M, Hogan A, Hayes P, O'Reilly M, Jeffery IB, Wood-Martin R, Kerins DM, Quigley E, Ross RP, O'Toole PW, Molloy MG, Falvey E, Shanahan F, Cotter PD. 2014. Exercise and associated dietary extremes impact on gut microbial diversity. *Gut*, **63**(12): 1913–1920.

Dai WF, Yu WN, Xuan LX, Tao Z, Xiong JB, 2018. Integrating molecular and ecological approaches to identify potential polymicrobial pathogens over a shrimp disease progression. *Applied Microbiology and Biotechnology*, **102**(8): 3755–3764.

Dawood MA, Koshio S, Ishikawa M, El-Sabagh M, Esteban MA, Zaineldin AI. 2016. Probiotics as an environment-friendly approach to enhance red sea bream, *Pagrus major* growth, immune response and oxidative status. *Fish & Shellfish Immunology*, **57**: 170–178.

de Bruijn I, Liu Y, Wiegertjes GF, Raaijmakers JM. 2017. Exploring fish microbial communities to mitigate emerging diseases in aquaculture. *FEMS Microbiology Ecology*, **94**(1): fix161.

De Schryver P, Vadstein O. 2014. Ecological theory as a foundation to control pathogenic invasion in aquaculture. *ISME Journal*, **8**(12): 2360–2368.

Fabich AJ, Jones SA, Chowdhury FZ, Cernosek A, Anderson A, Smalley D, McHargue JW, Hightower GA, Smith JT, Autieri SM, Leatham MP, Lins JJ, Allen RL, Laux DC, Cohen PS, Conway T. 2008. Comparison of carbon nutrition for pathogenic and commensal *Escherichia coli* strains in the mouse intestine. *Infection & Immunity*, **76**(3): 1143–1152.

Falkow S. 1988. Molecular Koch's postulates applied to microbial pathogenicity. *Reviews of Infectious Diseases*, **10** (Suppl 2): S274–S276.

FAO. 2013. FAO Fisheries and Aquaculture Department has published the Global Aquaculture Production Statistics for the Year 2011. 2013 ed. http://cape-eaprac.co.za/projects/NMM101%20Marine%20Aquaculture/DEIR/Appendix%20F%20GlobalAquacultureProductionStatistics2011.pdf.

Fargione JE, Tilman D. 2005. Diversity decreases invasion via both sampling and complementarity effects. *Ecology Letters*, **8**(6): 604–611.

Fasano A, Sheadonohue T. 2005. Mechanisms of disease: The role of intestinal barrier function in the pathogenesis of gastrointestinal autoimmune diseases. *Nature Clinical Practice Gastroenterology & Hepatology*, **2**(9): 416–422.

Faust K, Raes J. 2012. Microbial interactions: From networks to models. *Nature Reviews Microbiology*, **10**(8): 538–550.

Fischbach MA, Lin H, Liu DR, Walsh CT. 2006. How pathogenic bacteria evade mammalian sabotage in the battle for iron. *Nature Chemical Biology*, **2**(3): 132–138.

Fraser T, Brown PD, 2017. Temperature and oxidative stress as triggers for virulence gene expression in pathogenic *Leptospira* spp. *Frontiers in Microbiology*, **8**: 783.

Fukuda S, Toh H, Hase K , Oshima K, Nakanishi Y, Yoshimura K, Tobe T, Clarke JM , Topping DL, Suzuki T, Taylor TD , Itoh K, Kikuchi J, Morita H, Hattori M, Ohno H. 2012. Bifidobacteria can protect from enteropathogenic infection through production of acetate. *Nature*, **469**(5): 543–547.

Gómez GD, Balcázar JL. 2008. A review on the interactions between gut microbiota and innate immunity of fish. *FEMS Immunology Medical Microbiology*, **52**(2): 145–154.

Galindo-Villegas J, García-Moreno D, de Oliveira S, Meseguer J, Mulero V. 2012. Regulation of immunity and disease resistance by commensal microbes and chromatin modifications during zebrafish development. *Proceedings of the National Academy of Sciences of the United States of America*, **109**(39): E2605–E2614.

Giatsis C, Sipkema D, Ramiro-Garcia J, Bacanu GM, Abernathy J, Verreth J, Smidt H, Verdegem M. 2016. Probiotic legacy effects on gut microbial assembly in tilapia larvae. *Scientific Reports*, **6**: 33965.

Giatsis C, Sipkema D, Smidt H , Heilig H, Benvenuti G, Verreth J, Verdegem M. 2015. The impact of rearing environment on the development of gut microbiota in tilapia larvae. *Scientific Reports*, **5**: 18206.

He SX, Wang QM, Li SN, Ran C, Guo XZ, Zhang Z, Zhou ZG. 2017. Antibiotic growth promoter olaquindox increases pathogen susceptibility in fish by inducing gut microbiota dysbiosis. *Science China Life Sciences*, **60**(11): 1260–1270.

Hou D, Huang Z, Zeng S, Liu J, Wei D, Deng X, Weng S, Yan Q, He J. 2018. Intestinal bacterial signatures of white feces syndrome in shrimp. *Applied Microbiology and Biotechnology*, **102**(8): 3701–3709.

Johnson PT, Hartson RB, Larson DJ, Sutherland DR. 2008. Diversity and disease: Community structure drives parasite transmission and host fitness. *Ecology Letters*, **11**(10): 1017–1026.

Kamada N, Chen GY, Inohara N, Núñez G. 2013. Control of pathogens and pathobionts by the gut microbiota. *Nature Immunology*, **14**(7): 685–690.

Kamada N, Kim YG, Sham HP, Vallance BA, Puente JL, Martens EC, Núñez G. 2012. Regulated virulence controls the ability of a pathogen to compete with the gut microbiota. *Science*, **336**(6086): 1325–1329.

Kanther M, Sun X, Mühlbauer M, Mackey LC, Flynn EJ 3rd, Bagnat M, Jobin C, Rawls JF. 2011. Microbial colonization induces dynamic temporal and spatial patterns of NF-κB activation in the zebrafish digestive tract. *Gastroenterology*, **141**(1): 197–207.

Kim DH, Austin B. 2006. Innate immune responses in rainbow trout (*Oncorhynchus mykiss*, Walbaum) induced by probiotics. *Fish & Shellfish Immunology*, **21**(5): 513–524.

Knights D, Ward TL, McKinlay CE, Miller H, Gonzalez A, McDonald D, Knight

R. 2014. Rethinking “enterotypes”. *Cell Host Microbe*, **16**(4): 433.

Lafferty KD, Harvell CD, Conrad JM, Friedman CS, Kent ML, Kuris AM, Powell EN, Rondeau D, Saksida SM. 2015. Infectious diseases affect marine fisheries and aquaculture economics. *Annual Review of Marine Science*, **7**(1): 471–496.

Larsen AM, Mohammed HH, Arias CR. 2014. Characterization of the gut microbiota of three commercially valuable warmwater fish species. *Journal of Applied Microbiology*, **116**(6): 1396–1404.

Lemire A, Goudenège D, Versigny T, Petton B, Calteau A, Labreuche Y, Le Roux F. 2015. Populations, not clones, are the unit of *Vibrio* pathogenesis in naturally infected oysters. *ISME Journal*, **9**(7): 1523–1531.

Li T, Li H, Gatesoupe FJ, She R, Lin Q, Yan X, Li J, Li X. 2017a. Bacterial signatures of “red-operculum” disease in the gut of crucian carp (*Carassius auratus*). *Microbial Ecology*, **74**(3): 510–521.

Li T, Long M, Ji C, Shen Z, Gatesoupe FJ, Zhang X, Zhang Q, Zhang L, Zhao Y, Liu X, Li A. 2016. Alterations of the gut microbiome of largemouth bronze gudgeon (*Coreius guichenoti*) suffering from furunculosis. *Scientific Reports*, **6**: 30606.

Li X, Zhou L, Yu Y, Ni J, Xu W, Yan Q. 2017b. Composition of gut microbiota in the gibel carp (*Carassius auratus gibelio*) varies with host development. *Microbial Ecology*, **74**(1): 239–249.

Liu CH, Wu K, Chu TW, Wu TM. 2018. Dietary supplementation of probiotic, *Bacillus subtilis* e20, enhances the growth performance and disease resistance against *Vibrio alginolyticus* in parrot fish (*Oplegnathus fasciatus*). *Aquaculture International*, **26**(1): 63–74.

Mallon CA, Elsas JDV, Salles JF. 2015. Microbial invasions: The process, patterns, and mechanisms. *Trends in Microbiology*, **23**(11): 719–729.

Mancabelli L, Milani C, Lugli GA, Turroni F, Cocconi D, van Sinderen D, Ventura M. 2017. Identification of universal gut microbial biomarkers of common human intestinal diseases by meta-analysis. *FEMS Microbiology Ecology*, **93**(12): fix153.

Mazmanian SK, Ton-That H, Schneewind O. 2001. Sortase-catalysed anchoring of surface proteins to the cell wall of *Staphylococcus aureus*. *Molecular Microbiology*, **40**(5): 1049–1057.

McFall-Ngai M, Hadfield MG, Bosch TC, Carey HV, Domazet-Lošo T, Douglas AE, Dubilier N, Eberl G, Fukami T, Gilbert SF, Hentschel U, King N, Kjelleberg S, Knoll AH, Kremer N, Mazmanian SK, Metcalf JL, Nealson K, Pierce NE, Rawls JF, Reid A, Ruby EG, Rumpho M, Sanders JG, Tautz D, Wernegreen JJ. 2013. Animals in a bacterial world, a new imperative for the life sciences. *Proceedings of the National Academy of Sciences of the United States of America*, **110**(9): 3229–3236.

Nie L, Zhou QJ, Qiao Y, Chen J. 2017. Interplay between the gut microbiota and immune responses of ayu (*Plecoglossus altivelis*) during *Vibrio anguillarum* infection. *Fish & Shellfish Immunology*, **68**: 479–487.

Oyarbide U, Iturria I, Rainieri S, Pardo MA. 2015. Use of gnotobiotic zebrafish to study *Vibrio anguillarum* pathogenicity. *Zebrafish*, **12**(1): 71–80.

Pérez T, Balcázar JL, Ruiz-Zarzuela I, Halaihel N, Vendrell D, de Blas I, Múzquiz JL. 2010. Host-microbiota interactions within the fish intestinal ecosystem. *Mucosal Immunology*, **3**(4): 355–360.

Penttinen R, Kinnula H, Lipponen A, Bamford JK, Sundberg LR. 2016. High nutrient concentration can induce virulence factor expression and cause higher virulence in an environmentally transmitted pathogen. *Microbial Ecology*, **72**(4): 955–964.

Picchietti S, Fausto AM, Randelli E, Carnevali O, Taddei AR, Buonocore F, Scapigliati G, Abelli L. 2008. Early treatment with *Lactobacillus delbrueckii* strain induces an increase in intestinal t-cells and granulocytes and modulates immune-related genes of larval *Dicentrarchus labrax* (L.). *Fish & Shellfish Immunology*, **26**(3): 368–376.

Ramesh D, Souissi S, Ahamed TS. 2017. Effects of the potential probiotics *Bacillus aerophilus* kadr3 in inducing immunity and disease resistance in *Labeo rohita*. *Fish & Shellfish Immunology*, **70**(6): 408–415.

Rawls JF, Mahowald MA, Ley RE, Gordon JI. 2006. Reciprocal gut microbiota transplants from zebrafish and mice to germ-free recipients reveal host habitat selection. *Cell*, **127**(2): 423–433.

Rawls JF, Samuel BS, Gordon JI. 2004. Gnotobiotic zebrafish reveal evolutionarily conserved responses to the gut microbiota. *Proceedings of the National Academy of Sciences of the United States of America*, **101**(13): 4596–4601.

Ringø E, Myklebust R, Mayhew TM, Olsen RE. 2007. Bacterial translocation and pathogenesis in the digestive tract of larvae and fry. *Aquaculture*, **268**(1–4): 251–264.

Roeselers G, Mittge EK, Stephens WZ, Parichy DM, Cavanaugh CM, Guillemin K, Rawls JF. 2011. Evidence for a core gut microbiota in the zebrafish. *ISME Journal*, **5**(10): 1595–1608.

Russell AB, Wexler AG, Harding BN, Whitney JC, Bohn AJ, Goo YA, Tran BQ, Barry NA, Zheng H, Peterson SB, Chou S, Gonen T, Goodlett DR, Goodman AL, Mougous JD. 2014. A type vi secretion-related pathway in bacteroidetes mediates interbacterial antagonism. *Cell Host Microbe*, **16**(2): 227–236.

Schmidt VT, Smith KF, Melvin DW, Amaral-Zettler LA. 2015. Community assembly of a euryhaline fish microbiome during salinity acclimation. *Molecular Ecology*, **24**(10): 2537–2550.

Singh A, Wyant T, Anaya-Bergman C, Aduse-Opoku J, Brunner J, Laine ML, Curtis MA, Lewis JP. 2011. The capsule of *Porphyromonas gingivalis* leads to a reduction in the host inflammatory response, evasion of phagocytosis, and increase in virulence. *Infection Immunity*, **79**(11): 4533–4542.

Smith P, Willemsen D, Popkes M, Metge F, Gandiwa E, Reichard M, Valenzano DR. 2017. Regulation of life span by the gut microbiota in the short-lived african turquoise killifish. *eLife*, **6**: e27014.

Stagaman K, Burns AR, Guillemin K, Bohannan BJ. 2017. The role of adaptive immunity as an ecological filter on the gut microbiota in zebrafish. *ISME Journal*, **11**(7): 1630–1639.

Stephens WZ, Burns AR, Stagaman K, Wong S, Rawls JF, Guillemin K, Bohannan BJ. 2016. The composition of the zebrafish intestinal microbial community varies across development. *ISME Journal*, **10**(3): 644–654.

Sullam KE, Essinger SD, Lozupone CA, O’Connor MP, Rosen GL, Knight R, Kilham SS, Russell JA. 2012. Environmental and ecological factors that shape the gut bacterial communities of fish: A meta-analysis. *Molecular Ecology*, **21**(13): 3363–3378.

Vonaesch P, Anderson M, Sansonetti PJ. 2018. Pathogens, microbiome and the host: Emergence of the ecological koch’s postulates. *FEMS Microbiology Reviews*, **42** (3):273–292.

Wang AR, Ran C, Ringø E, Zhou ZG. 2017. Progress in fish gastrointestinal microbiota research. *Reviews in Aquaculture*, doi: 10.1111/raq.12191.

Winter SE, Bäumler AJ. 2014. Why related bacterial species bloom

simultaneously in the gut: Principles underlying the 'like will to like' concept. *Cellular Microbiology*, **16**(2): 179–184.

Wong S, Waldrop T, Summerfelt S, Davidson J, Barrows F, Kenney B, Welch T, Wiens GD, Snekvik K, Rawls JF, Good C. 2013. Aquacultured rainbow trout (*Oncorhynchus mykiss*) possess a large core intestinal microbiota that is resistant to variation in diet and rearing density. *Applied Environmental Microbiology*, **79**(16): 4974–4984.

Xiong J, Dai W, Li C. 2016. Advances, challenges, and directions in shrimp disease control: The guidelines from an ecological perspective. *Applied Microbiology and Biotechnology*, **100**(16): 6947–6954.

Xiong J, Yu W, Dai W, Zhang J, Qiu Q, Ou C. 2018. Quantitative prediction of shrimp disease incidence via the profiles of gut eukaryotic microbiota. *Applied Microbiology Biotechnology*, **102**(7): 3315–3326.

Xiong J, Zhu J, Dai W, Dong C, Qiu Q, Li C. 2017. Integrating gut microbiota immaturity and disease-discriminatory taxa to diagnose the initiation and severity of shrimp disease. *Environmental Microbiology*, **19**(4): 1490–1501.

Yan Q, Li J, Yu Y, Wang J, He Z, Van Nostrand JD, Kempher ML, Wu L, Wang Y, Liao L, Li X, Wu S, Ni J, Wang C, Zhou J. 2016. Environmental filtering decreases with fish development for the assembly of gut microbiota. *Environmental Microbiology*, **18**(12): 4739–4754.

Zhang X, Yang W, Zhang D, Li T, Gong X, Li A. 2015. Does the gastrointestinal tract serve as the infectious route of aeromonas hydrophila in crucian carp (*Carassius carassius*)? *Aquaculture Research*, **46**(1): 141–154.

Zhang ZM, Li DP, Refaey MM, Xu WT, Tang R, Li L. 2018. Host age affects the development of southern catfish gut bacterial community divergent from that in the food and rearing water. *Frontier in Microbiology*, **9**: 495.

Zhou JF, Fang WH, Yang XL, Zhou S, Hu LL, Li XC, Qi XY, Su H, Xie LY. 2012. A nonluminescent and highly virulent vibrio harveyi strain is associated with "bacterial white tail disease" of *Litopenaeus vannamei* shrimp. *PLoS One*, **7**(2): e29961.

Zhu J, Dai W, Qiu Q, Dong C, Zhang J, Xiong J. 2016. Contrasting ecological processes between intestinal bacterial community in healthy and diseased shrimp. *Microbial Ecology*, **72**(4): 975–985.

Involvement of ayu NOD2 in NF-κB and MAPK signaling pathways: Insights into functional conservation of NOD2 in antibacterial innate immunity

Yi Ren[1,#], Shui-Fang Liu[1,#], Li Nie[1,*], Shi-Yu Cai[1], Jiong Chen[1,2,*]

[1] *Laboratory of Biochemistry and Molecular Biology, School of Marine Sciences, Ningbo University, Ningbo Zhejiang* 315211*, China*
[2] *Key Laboratory of Applied Marine Biotechnology of Ministry of Education, Ningbo University, Ningbo Zhejiang* 315211*, China*

ABSTRACT

Nucleotide oligomerization domain 2 (NOD2) is a major cytoplasmic sensor for pathogens and is critical for the clearance of cytosolic bacteria in mammals. However, studies regarding NOD2, especially the initiated signaling pathways, are scarce in teleost species. In this study, we identified a NOD2 molecule (PaNOD2) from ayu (*Plecoglossus altivelis*). Bioinformatics analysis showed the structure of NOD2 to be highly conserved during vertebrate evolution. Dual-luciferase reporter assays examined the activation of NF-κB signaling and Western blotting analysis detected the phosphorylation of three MAP kinases (p-38, Erk1/2, and JNK1/2). Functional study revealed that, like its mammalian counterparts, PaNOD2 was the receptor of the bacterial cell wall component muramyl dipeptide (MDP), and the leucine-rich repeat motif was responsible for the recognition and binding of PaNOD2 with the ligand. Overexpression of PaNOD2 activated the NF-κB signaling pathway, leading to the upregulation of inflammatory cytokines, including TNF-α and IL-1β in HEK293T cells and ayu head kidney-derived monocytes/macrophages (MO/MΦ). Particularly, we found that PaNOD2 activated the MAPK signaling pathways, as indicated by the increased phosphorylation of p-38, Erk1/2, and JNK1/2, which have not been characterized in any teleost species previously. Our findings proved that the NOD2 molecule and initiated pathways are conserved between mammals and ayu. Therefore, ayu could be used as an animal model to investigate NOD2-based diseases and therapeutic applications.

Keywords: Ayu NOD2; NF-κB signaling; MAPK signaling; Inflammatory cytokines; *Vibrio anguillarum* infection

INTRODUCTION

Microorganisms that invade a host are initially recognized and cleared by the innate immune system and related immune responses (Medzhitov, 2007a). Innate immune responses are the first line of host defense and are primed upon recognizing pathogen-associated molecular patterns (PAMPs) by germline-encoded pattern recognition receptors (PRRs). Several classes of PRRs, including Toll-like receptors, retinoic acid-inducible gene I (RIG-I)-like receptors, nucleotide oligomerization domain (NOD)-like receptors (NLRs), and cytosolic viral DNA sensors, recognize distinct microbial components and directly activate immune cells (Brubaker et al., 2015; Keating et al., 2011; Medzhitov, 2007b; Sabbah et al., 2009; Yoneyama et al., 2004). Exposure of these receptors to their corresponding PAMPs activates intracellular signaling cascades that induce the expression of a variety of inflammatory-related genes and cytokines.

Nucleotide oligomerization domain 2 (NOD2), a member

Received: 14 March 2018; Accepted: 27 April 2018; Online: 25 May 2018

Foundation items: This project was supported by the National Natural Science Foundation of China (31772876, 31702374), Natural Science Foundation of Zhejiang Province (LZ18C190001, LQ17C190001), Zhejiang Xinmiao Talents Program (2017R405023), and K.C. Wong Magna Fund in Ningbo University

[#]Authors contributed equally to this work

[*]Corresponding authors, E-mail: nieli@nbu.edu.cn; jchen1975@163.com

DOI: 10.24272/j.issn.2095-8137.2018.066

of the NLR family, is a major cytoplasmic sensor for a peptidoglycan fragment existing in both gram-positive and gram-negative bacteria, named muramyl dipeptide (MDP) (Kufer et al., 2006). Structurally, NOD2 contains two N-terminal tandem caspase activation and recruitment domains (CARDs), a central nucleotide-binding domain (NBD), and multiple C-terminal leucine-rich repeats (LRRs). In resting cells, NOD2 is held in an autoinhibited monomeric state by intramolecular inhibition of the NBD domain through the LRR motifs. After recognizing MDP by LRRs, NOD2 oligomerizes through its NBD domain and recruits the downstream adaptor receptor-interacting serine/threonine kinase 2 (RIPK2) by homotypic CARD-CARD interactions to activate NF-κB and mitogen-activated protein kinase (MAPK) signaling pathways, thus inducing a series of immune responses (Girardin et al., 2003; Tanabe et al., 2004; Windheim et al., 2007). These pathways are essential for bacterial clearance, the disruption of which increases host susceptibility to various kinds of pathogens.

Despite the substantial information about NOD2 in mammals, knowledge of this molecule in lower vertebrates, especially in teleosts, remains limited. Compared with other teleost species, studies on NOD2 in zebrafish (*Danio rerio*) are the most comprehensive. For example, the structural model of the NACHT domain and ATP binding orientations, antibacterial and protective functions, induced NF-κB signaling pathways, and mutual regulation between NOD2 and RIG-I signaling in zebrafish have been well studied (Maharana et al., 2015; Nie et al., 2017; Oehlers et al., 2011; Zou et al., 2016). Other than zebrafish, preliminary studies on NOD2 in other teleosts, including grass carp (*Ctenopharyngodon idella*), Nile tilapia (*Oreochromis niloticus*), Indian major carp (*Catla catla*), rohu (*Labeo rohita*), orange-spotted grouper (*Epinephelus coioides*), miiuy croaker (*Miichthys miiuy*), and rainbow trout (*Oncorhynchus mykiss*) have been carried out (Basu et al., 2016; Chang et al., 2011; Chen et al., 2010; Gao et al., 2018; Hou et al., 2012; Li et al., 2015; Maharana et al., 2013). However, most studies have focused on bioinformatics analysis of this protein, tissue expression levels and inflammatory gene expression levels under different stress. Hence, comprehensive study regarding signaling pathways, especially whether teleost NOD2 can also activate MAPK signaling pathways like in mammals, is required.

Ayu (*Plecoglossus altivelis*) is an economically important and widely cultured fish in East Asia. However, the development of the ayu aquaculture is challenged by bacterial and viral fish diseases that have caused production and animal welfare problems (Zhang et al., 2015). Given the importance of NOD2 in antibacterial innate immune responses, studying the ligands, functions, and induced signaling pathways of ayu NOD2 is important. In the present study, we identified a NOD2 gene from ayu (PaNOD2), which, like its mammalian counterparts, contains all functional domains. The mRNA expression patterns of PaNOD2 were examined in various tissues under normal conditions and after *Vibrio anguillarum* challenge. The subcellular localization and ligands of PaNOD2 were analyzed. Importantly, we demonstrated the conserved involvement of PaNOD2 in the NF-κB and MAPK signaling pathways. This study will hopefully enrich current understanding of teleost NLRs in antibacterial immunity and provide valuable insights into the evolutionary history of cytosolic PRRs in innate immunity from teleosts to mammals.

MATERIALS AND METHODS

Experimental fish

All experimental ayu (45.0±2.4 g, *n*=250) used in the present study were purchased from a fishery in Ninghai County, Ningbo City, China. Healthy fish were temporarily maintained in a recirculating water system (21.0±1.0 °C) with regular feeding, as described previously (Zhang et al., 2018). The fish were acclimatized to laboratory conditions for two weeks before the experiments. All experiments were performed according to the Experimental Animal Management Law of China and approved by the Animal Ethics Committee of Ningbo University.

Molecular characterization of PaNOD2

The cDNA sequence of PaNOD2 was retrieved from the transcriptome data of the ayu head kidney-derived monocytes/macrophages (MO/MΦ). Specific primers were designed to amplify the open reading frame (ORF) of PaNOD2 using reverse transcription PCR (NOD2 F1/R1, Table 1), followed by cloning and sequencing. Multiple sequence alignment was performed using ClustalW with homologous sequences retrieved by BLAST (http://blast.ncbi.nlm.nih.gov/Blast.cgi). Functional motifs in proteins were analyzed using the SMART (http://smart.embl-heidelberg.de/) and Pfam databases (http://smart.embl-heidelberg.de/; http://pfam.xfam.org/) (Letunic et al., 2012). The phylogenies of the protein sequences were estimated with MEGA 5.0 software using parsimony and the neighbor-joining method (Tamura et al., 2011). Sequences used in this study are listed in Table 2.

Plasmid constructions

The ORF of PaNOD2 was inserted into EGPF-N1 (Clontech, USA) between the *Eco*R I and *Bam*H I sites to construct EGFP fusion proteins (pEGFP-PaNOD2, NOD2 F2/R2), and was inserted into pcDNA3.1-FLAG (kind gift from Prof. Zong-Ping Xia) between *Not* I and *Sfa*A I to construct eukaryotic expression vectors (pcDNA3.1-PaNOD2, NOD2 F3/R3). The LRR motif-deleted mutant (ΔLRR) constructs [pcDNA3.1-PaNOD2 (ΔLRR), NOD2 F3/R4] were cloned and inserted into pcDNA3.1-FLAG between the *Not* I and *Sfa*A I sites. The NF-κB luciferase construct was purchased from Clontech (Palo Alto, USA) and the pRL-TK vector was obtained from Promega (Madison, USA). All constructed sequences were confirmed by sequencing analysis. The plasmids for transfection were prepared at the endotoxin-free level using an EZNA™ Plasmid Midi Kit (Omega Bio-Tek, USA).

In vivo bacterial challenge and expression analysis of PaNOD2

The *V. anguillarum* challenge was carried out as reported previously (Zhang et al., 2018). Briefly, *V. anguillarum* were grown

at 28 °C in nutrient broth and harvested at the logarithmic phase before washing, resuspending, and diluting to the appropriate concentration in sterile phosphate-buffered saline (PBS). The final bacterial concentration was confirmed by plating serial dilutions on solid media. Each ayu was intraperitoneally injected with 1.2×10^4 colony forming units (CFUs) of live *V. anguillarum* (in 100 μL PBS), with PBS injected alone used as the control group. Ayu were sacrificed at 4, 8, 12, 24, or 48 h post-infection (hpi) and the gill, spleen, head kidney, liver, and intestine were collected for total RNA extraction (Chen et al., 2018). The RNA of healthy fish tissues, including the muscle, skin, heart, gill, spleen, head kidney, liver, and intestine, were also extracted for tissue expression pattern analysis. Real-time quantitative PCR (RT-qPCR) was performed on an ABI StepOne Real-Time PCR System (Applied Biosystems, USA) using SYBR premix Ex Taq II (TaKaRa, Japan) with the following protocol: (1) 40 cycles of amplification at 95 °C for 30 s and 60 °C for 20 s; (2) melting curve analysis at 95 °C for 5 s, 65 °C for 15 s, and 95 °C for 15 s; and (3) cooling at 40 °C for 30 s. Relative gene expression was calculated using the $2^{-\Delta\Delta CT}$ method with PaNOD2 initially normalized against Pa18S rRNA. The primers used are listed in Table 1 (NOD2 qRT F/R). Each PCR trial was performed in triplicate and repeated at least three times.

Cell culture and transient transfection

Ayu head kidney-derived MO/MΦ were isolated as described previously (He et al., 2013). The isolated MO/MΦ were seeded into 35-mm dishes (2×10^7/mL) and cultured in RPMI 1640 medium (Invitrogen, China) supplemented with 5% (v/v) fetal bovine serum (FBS) (Gibco, Life Technologies, USA), 5% (v/v) ayu serum, penicillin (100 U/mL), and streptomycin (100 μg/mL) at 24 °C in 5% CO_2 after washing off non-adherent cells. The HEK293T cells were maintained in Dulbecco's modified Eagle's medium (DMEM, Invitrogen, China) supplemented with 10% (v/v) FBS, penicillin (100 U/mL), and streptomycin (100 μg/mL) at 37 °C in 5% CO_2. The HEK293T cells (1×10^5/mL) were seeded into multi-well plates (Corning, USA) to allow growth until 70%–90% confluence on the day of transfection. Both cell types were transiently transfected with DNA using lipofectamine 3000 (Invitrogen, China) according to the manufacturer's instructions.

Subcellular localization

The HEK293T cells were cultured and seeded onto cover slips in 6-well plates before transfection. After 24 h of culture, the cells were transfected with pEGFP-PaNOD2 (1 μg/mL). At 36 h post-transfection (hpt), the cells were washed twice with PBS and fixed for 20 min in 4% (v/v) paraformaldehyde, followed by staining with DiI (Beyotime, China) for 10 min. After twice washing with PBS, the nuclei were stained with DAPI (Sigma, USA) for 5 min. Fluorescence images of cells were obtained using a confocal microscope (Zeiss LSM710 NLO, Carl Zeiss, Germany).

Table 1 Oligonucleotide primers used in this work

Primer	Gene	GenBank accession No.	Nucleotide sequence (5′–3′)	Amplicon size (bp)	Usage of primer pairs
NOD2 F1	*PaNOD2*	MG674830	ATGAGTGCCCAGCAGTTGGTGCTAAG	2 964	Cloning of PaNOD2
NOD2 R1			TCAGAACGTTAGTCGGGA		
NOD2 F2	*PaNOD2*	MG674830	GAATTCATGAGTGCCCAGCAGTTGGTGCTAA	2 964	Construct EGFP fusion plasmid
NOD2 R2			GGATCCCGGAACGTTAGTCGGGACTCT		
NOD2 F3	*PaNOD2*	MG674830	ATGCGCGGCCGCTATGAGTGCCCAGCAGTTGGTGCTAA	2 964	Construct eukaryotic expression plasmid
NOD2 R3	*PaNOD2*	MG674830	ATGCGCGATCGCGAACGTTAGTCGGGACTCT		
NOD2 R4	*PaNOD2*	MG674830	ATGCGCGATCGCGATTGCCAGAGGAACGATGGCG	2 205	Construct ΔLRR mutant
NOD2 qRT F	*PaNOD2*	MG674830	GGATGACATTTACACCGAAGG	244	Quantification of NOD2 gene expression
NOD2 qRT R			TCTGCGACAACTGAATGGA		
TNF-α qRT F	*PaTNF-α*	JP740414	ACATGGGAGCTGTGTTCCTC	115	Quantification of TNF-α gene expression
TNF-α qRT R			GCAAACACACCGAAAAAGGT		
IL-1β qRT F	*PaIL-1β*	HF543937	TACCGGTTGGTACATCAGCA	104	Quantification of IL-1β gene expression
IL-1β qRT R			TGACGGTAAAGTTGGTGCAA		
18S rRNA qRT F	*Pa18S rRNA*	FN646593	GAATGTCTGCCCTATCAACT	103	Quantification of 18S rRNA gene expression
18S rRNA qRT R			GATGTGGTAGCCGTTTCT		

Table 2 NOD1 and NOD2 sequences used in this study

GenBank accession No.	Species		Protein
	Latin name	English name	
MG674830	*Plecoglossus altivelis*	Ayu	NOD2
XP_022597963.1	*Seriola dumerili*	Amberjack	NOD2
XP_022522840.1	*Astyanax mexicanus*	Mexican tetra	NOD2
ERE77544.1	*Cricetulus griseus*	Chinese hamster	NOD2
XP_020797036.1	*Boleophthalmus pectinirostris*	Mudskipper	NOD2
XP_015236187.1	*Cyprinodon variegatus*	Sheepshead minnows	NOD2
XP_008335431.1	*Cynoglossus semilaevis*	Half-smooth tongue sole	NOD2
XP_012715032.1	*Fundulus heteroclitus*	Killifish	NOD2
ACX71753.1	*Ctenopharyngodon idella*	Grass carp	NOD2
AFV53358.1	*Epinephelus coioides*	Orange-spotted grouper	NOD2
AEG89706.1	*Labeo rohita*	Rohu	NOD2
AKR76246.1	*Miichthys miiuy*	Miiuy croaker	NOD2
XP_003437591.1	*Oreochromis niloticus*	Nile tilapia	NOD2
XP_014031576.1	*Salmo salar*	Atlantic salmon	NOD2
ADV31549.1	*Oncorhynchus mykiss*	Rainbow trout	NOD2a
ADV31550.1	*Oncorhynchus mykiss*	Rainbow trout	NOD2b
XP_017314821.1	*Ictalurus punctatus*	Channel catfish	NOD2
XP_018522174.1	*Larimichthys crocea*	Large yellow croaker	NOD2
XP_020481540.1	*Labrus bergylta*	Ballan wrasse	NOD2
NP_001314973.1	*Danio rerio*	Zebrafish	NOD2
XP_017548715.1	*Pygocentrus nattereri*	Red-bellied piranhas	NOD2
XP_019935411.1	*Paralichthys olivaceus*	Japanese flounder	NOD2
NP_001035913.1	*Takifugu rubripes*	Pufferfish	NOD2
NP_001002889.1	*Bos taurus*	Cattle	NOD2
NP_665856.2	*Mus musculus*	Mouse	NOD2
NP_001280486.1	*Homo sapiens*	Human	NOD2
XP_020792937.1	*Boleophthalmus pectinirostris*	Mudskipper	NOD1
XP_004571362.1	*Maylandia zebra*	Zebra mbuna	NOD1
XP_002665106.3	*Danio rerio*	Zebrafish	NOD1
AII73558.1	*Oncorhynchus mykiss*	Rainbow trout	NOD1
XP_018418247.1	*Nanorana parkeri*	Tibetan frog	NOD1
NP_001002889.1	*Bos taurus*	Cattle	NOD1
NP_001164478.1	*Mus musculus*	Mouse	NOD1
NP_006083.1	*Homo sapiens*	Human	NOD1

Dual-luciferase report assay

The HEK293T cells and ayu MO/MΦ were transfected with relative plasmids (1 μg/mL) and NF-κB luciferase reporter vectors (200 pg/mL). The pRL-TK Renilla luciferase reporter plasmid was used as an internal control. The empty control plasmid pcDNA3.1-FLAG was added to ensure the same amounts of total DNA. Cells were lysed at 24 hpt and dual-luciferase reporter assay was performed (Nie et al., 2015). Luciferase activity was normalized to pRL-TK activity and expressed as fold stimulation relative to the control.

Role of PaNOD2 in activating NF-κB signaling pathway

NF-κB activation was examined in both HEK293T cells and ayu MO/MΦ using luciferase assay and RT-qPCR according to above description. For luciferase assay, pcDNA3.1-FLAG, pcDNA3.1-PaNOD2, or pcDNA3.1-PaNOD2 (ΔLRR), together with the NF-κB luciferase reporter gene, were transfected into both cell types, with the pRL-TK Renilla luciferase reporter plasmid used as an internal control. At 24 hpt, cells were harvested and firefly and Renilla luciferase activities were assayed with three replicates according to the manufacturer's instructions. Luciferase activity was normalized to pRL-TK activity and expressed as fold stimulation relative to the control. For RT-qPCR, pcDNA3.1-FLAG or pcDNA3.1-PaNOD2 (1 μg/mL) were transfected into HEK293T cells or ayu MO/MΦ and the expression of TNF-α and IL-1β were analyzed at 6, 12, and 24 hpt. Each trial was performed in triplicate and repeated at least three times. Results were displayed relative to the

corresponding Pa18S rRNA values to calculate relative copy numbers.

Recognition assay

As HEK293T cells do not express endogenous NOD2, they are the perfect system to investigate the ligands of PaNOD2. The HEK293T cells were transfected with pcDNA3.1-PaNOD2 (1 μg/mL) or MDP (10 ng/mL) or both with PaNOD2 at gradient levels, together with NF-κB luciferase reporter vector. The pRL-TK Renilla luciferase reporter plasmid was used as the internal control. Empty control plasmid pcDNA3.1-FLAG was added to ensure the same amounts of total DNA. At 24 hpt, cells were lysed, and dual-luciferase reporter assay was conducted, as described above.

Role of PaNOD2 in activating MAPK signaling pathways

Both cell types were transfected with pcDNA3.1-FLAG or pcDNA3.1-PaNOD2 (1 μg/mL). At 12, 24, 36, and 48 hpt, the activation of the MAPK signaling pathways was examined by Western blotting using antibodies against three representative MAP kinases (p-38, ERK1/2, and JNK1/2). The primary antibodies used were rabbit phospho-p38 MAPK (Thr180/Tyr182), rabbit p38 MAPK, rabbit phospho-SAPK/JNK1/2 (Thr183/Tyr185), rabbit SAPK/JNK1/2, rabbit phospho-p44/42 MAPK (ERK1/2) (Thr202/Tyr204), and rabbit p44/42 MAPK (ERK1/2) (Cell Signaling Technology, China). The secondary antibody used was HRP-conjugated goat anti-rabbit IgG (Life Technologies, China). The blot was then incubated with enhanced chemiluminescence (ECL) reagents (Life Technologies, China) according to the manufacturer's protocols.

Statistical analyses

Data from three independent experiments were expressed as means±*SEM*. Statistical analysis was conducted by one-way analysis of variance (ANOVA) with SPSS version 13.0 (SPSS Inc, Chicago, USA). $P<0.05$ and $P<0.01$ were considered statistically significant.

RESULTS

Molecular characterization of PaNOD2

The ORF of PaNOD2 was 2 964 bp in length and encoded a protein with 987 amino acids. The molecular weight (MW) of the protein was 1.1036×10^5 and the putative isoelectric point (*p*I) was 6.20. The PaNOD2 protein also contained two N-terminal tandem CARD domains, central NBD domain, and multiple C-terminal LRRs. Multiple sequence alignment showed that the protein sequence and domains of NOD2 were conserved among vertebrates, and PaNOD2 shared highest amino acid identity and similarity (67% identity and 81% similarity) with the large yellow croaker homolog (Figure 1). Phylogenetic tree analysis showed that all teleost NOD2 proteins were clustered together with their higher vertebrate counterparts and formed a distinct group with the NOD1 proteins, which also belonged to the NLR family (Figure 2).

Tissue distribution and expression analysis of PaNOD2

The mRNA expression pattern of PaNOD2 was detected in the skin, heart, gill, spleen, head kidney, liver, and intestine of ayu. The highest expression of PaNOD2 was observed in the intestine, followed by the liver and head kidney (Figure 3A). Upon *V. anguillarum* infection, PaNOD2 mRNA expression was upregulated in all examined immune-related tissues in a time-dependent manner. The PaNOD2 transcript in the gill was dramatically upregulated at 12 hpi, then gradually decreased and returned to normal status at 48 hpi (Figure 3B). In the spleen, head kidney, liver, and intestine, PaNOD2 expression was upregulated at 8 hpi and gradually increased as the infection continued. The highest expression in the spleen, liver, and intestine was observed at 24 hpi, whereas that in the head kidney was detected at 48 hpi (Figure 3B–F).

Subcellular localization of PaNOD2

Before functional characterization, subcellular localization of PaNOD2 was initially evaluated by introducing an EGFP-fused construct (EGFP-PaNOD2) into the HEK293T cells. PaNOD2 was clearly distributed in the cytoplasm of the transfected cells, with no colocalized signals with DiI (membrane indicator) or DAPI (nucleus indicator) (Figure 4).

Role of PaNOD2 in activating NF-κB signaling pathway

As an important pathway initiated by NOD2 signaling, activation of the NF-κB signaling pathway was examined to provide evidence for the conserved role of PaNOD2 in antibacterial immunity. Luciferase reporter activity and inflammatory cytokine (TNF-α and IL-1β) expression were detected to evaluate the activation of the NF-κB signaling pathway. Results showed that overexpression of PaNOD2 in both the HEK293T cells and ayu MO/MΦ for 24 h significantly ($P<0.05$ and $P<0.01$) induced NF-κB activation, as determined by the dual-luciferase report assay (Figure 5A, B). In addition, the expressions of TNF-α and IL-1β were also upregulated in the PaNOD2 overexpression group (Figure 5C, D). The LRR-deleted mutant PaNOD2 (ΔLRR) construct was used to examine whether the LRR domain in PaNOD2 acted to keep this molecule in an autoinhibited status. As expected, overexpression of the ΔLRR mutant in both HEK293T cells and ayu MO/MΦ greatly enhanced the extent of NF-κB activation compared with the wild group (Figure 5A, B). Clearly, PaNOD2 played a conserved role in the NF-κB signaling pathway and the LRR structure acted as an autoinhibition domain, which was regulated by recognition of the receptor to bacterial PAMPs.

Recognition of PaNOD2 to bacterial PAMPs

For recognition analysis, HEK293T cells (with no endogenous expression of NOD2) were used for ectopic expression of PaNOD2; and MDP, a typical PAMP molecule on the cell walls of both gram-negative and gram-positive bacteria, was used for stimulation of PaNOD2-dependent NF-κB activation. Results showed that activation of NF-κB could be induced ($P<0.05$) with increased administration of the PaNOD2-expression vector and significantly higher with the co-administration of MDP ($P<0.05$ and $P<0.01$, Figure 6). Thus, PaNOD2 is an intracellular PRR participating in the recognition of bacterial MDP, whose performance is similar to that of mammalian NOD2s.

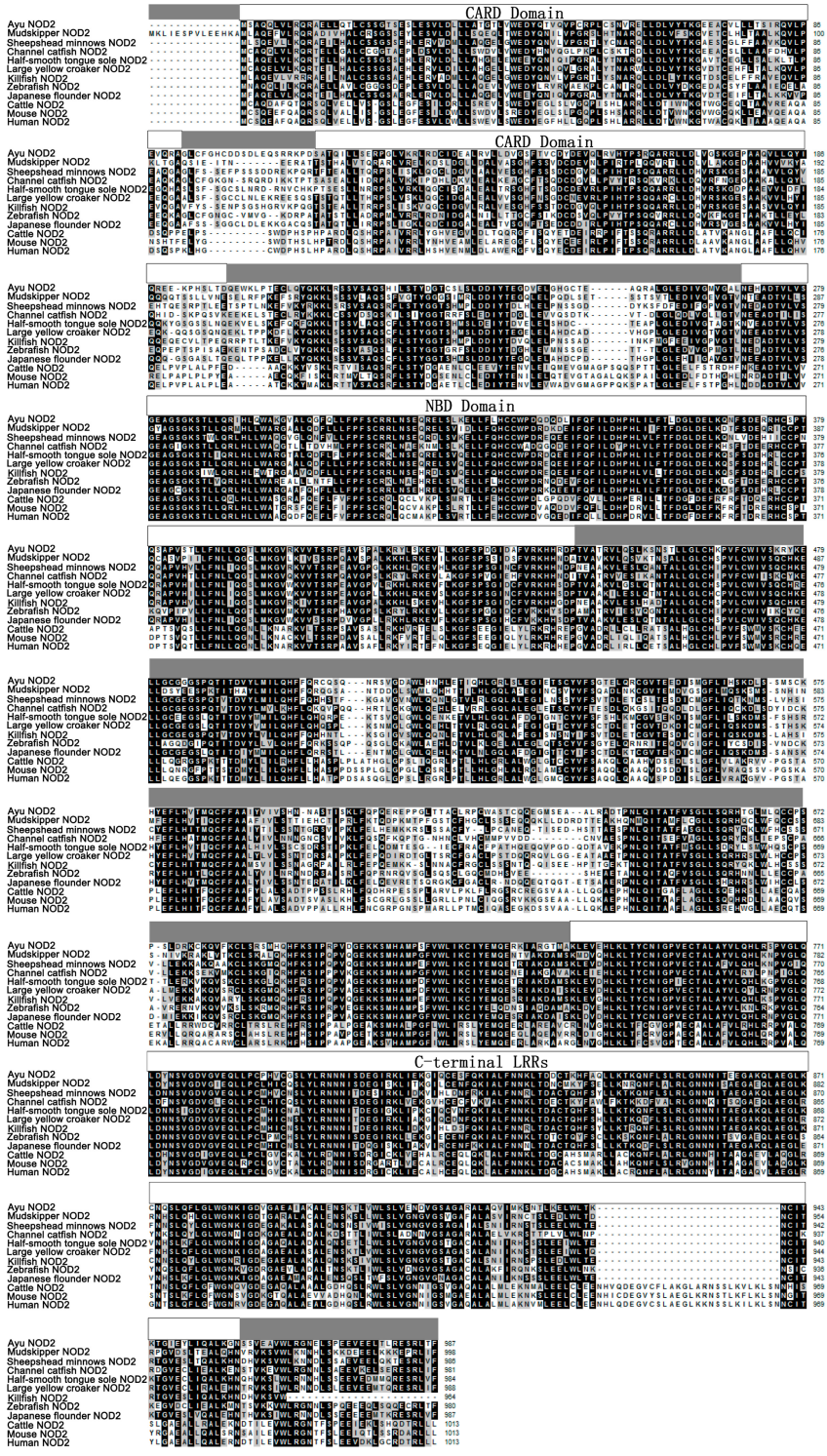

Figure 1 Multiple sequence alignment of PaNOD2 with other homologues

The threshold for shading is >60%; similar residues are marked with gray shading, identical residues are marked with black shading, and alignment gaps are marked as "–". Accession numbers of sequences used are listed in Table 2. Two N-terminal tandem CARD domains, central NBD domain, and multiple C-terminal LRRs are indicated above the alignment.

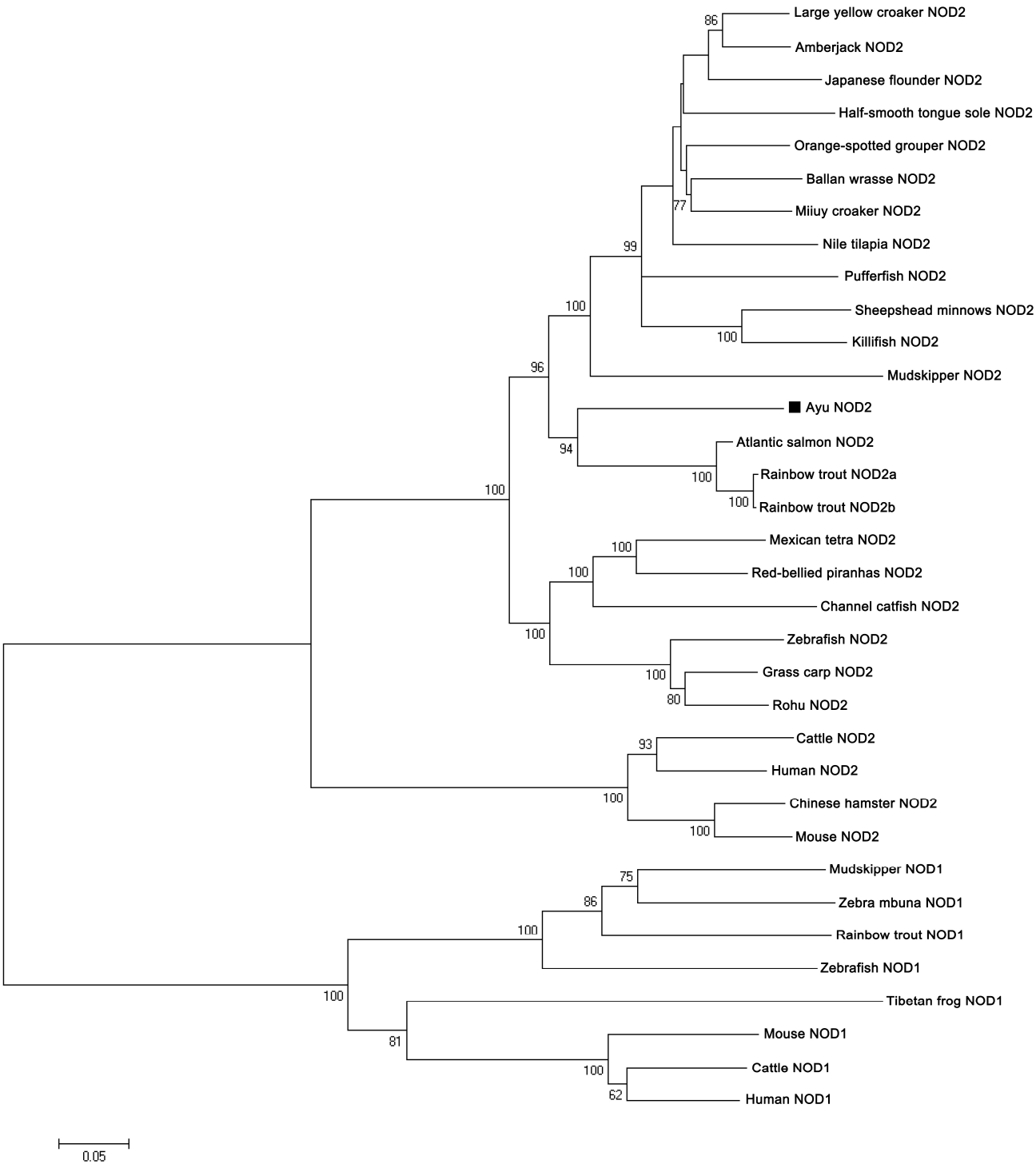

Figure 2 Phylogenetic tree showing relationship of PaNOD2 with other known NOD2 homologues and other NLR family members using MEGA 5.0

Values at forks indicate the percentage of trees in which this grouping occurred after bootstrapping (1 000 replicates; shown only when >60%). Scale bar shows number of substitutions per base. GenBank accession Nos. of sequences are listed in Table 2. The ayu NOD2 site is marked with ■.

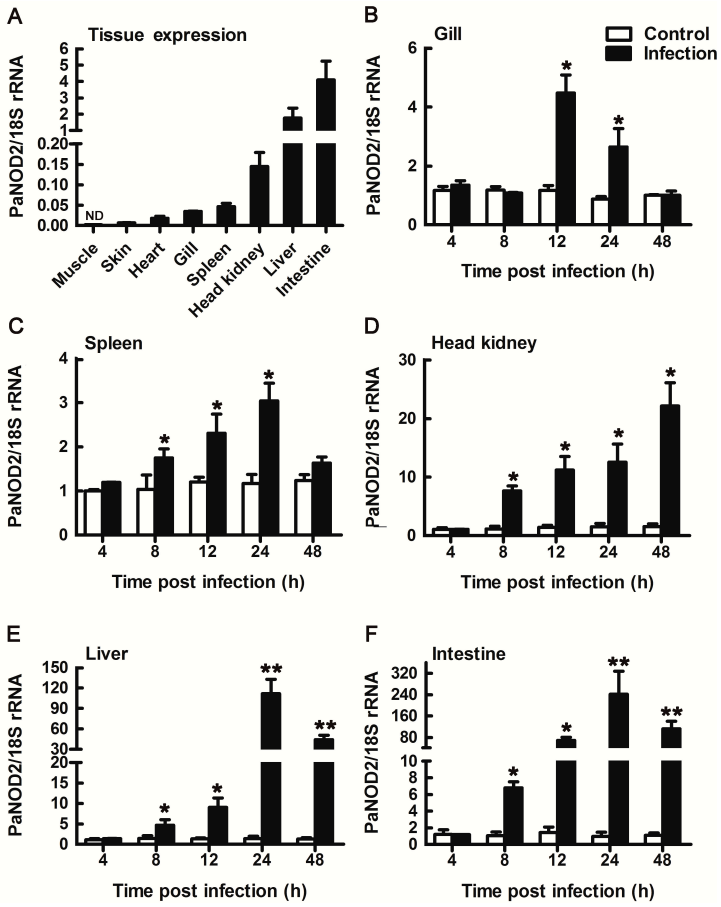

Figure 3 RT-qPCR analysis of PaNOD2 expression patterns in healthy ayu tissues and immune tissues after *V. anguillarum* infection

A: Relative PaNOD2 expression in various healthy ayu tissues (muscle, skin, heart, gill, spleen, head kidney, liver, intestine) against 18S rRNA, ND is not detected. Relative expression was calculated as the average of three replicates, each consisting of four fish samples. B–F: PaNOD2 transcripts in immune tissues of ayu challenged with *V. anguillarum*. Tissues were collected at 4, 8, 12, 24, and 48 hpi. Relative PaNOD2 transcript levels to 18S rRNA were quantified, and the mRNA level in the 4-h PBS-injected group was normalized to 1. Data are means±*SEM* of results from three replicates *: $P<0.05$, **: $P<0.01$.

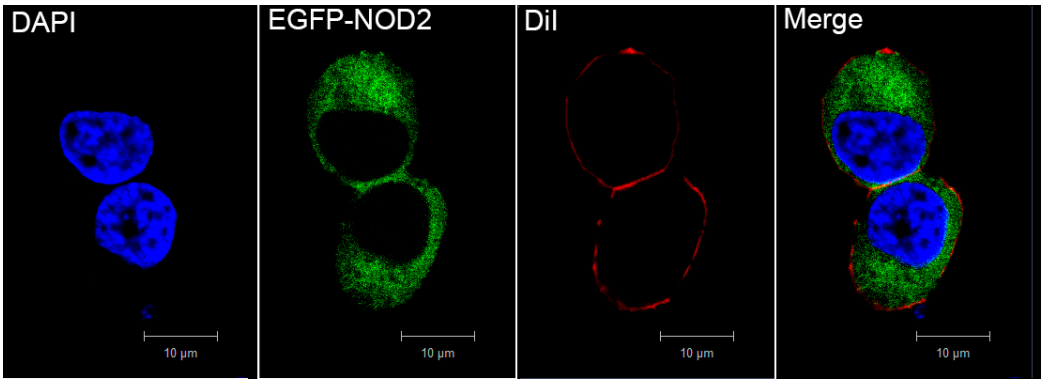

Figure 4 Subcellular localization of PaNOD2

Cytoplasmic localization of PaNOD2 in HEK293T cells observed using confocal microscopy. Nucleus was stained by DAPI and cell membrane was stained by DiI. Scale bars: 10 μm, original magnification ×640.

Conserved role of PaNOD2 in activating MAPK signaling pathways

As another important pathway activated by NOD2 signaling, activation of the MAPK signaling pathway was further examined to verify the conserved role of PaNOD2 in antibacterial processes. The phosphorylation of three conventional MAP kinases (p-38, ERK1/2, and JNK1/2) was examined in both HEK293T cells and ayu MO/MΦ when PaNOD2 was overexpressed, representing the activation of corresponding MAPK signaling. Results showed that the three MAP kinases were not phosphorylated in naïve HEK293T cells, the phosphorylation of which was clearly observed at 12, 24, 36, and 48 h post PaNOD2 transfection (Figure 7A–C). The phosphorylation of p-38 and JNK1/2 but not Erk1/2 was observed in naïve ayu MO/MΦ, but at a relatively low level. After the overexpression of PaNOD2, phosphorylation of p38 was significantly upregulated at 12 hpt, then gradually decreased and returned to the control level at 48 hpt (Figure 7D). Phosphorylation of Erk1/2 was observed at 12 hpt, and reached the highest level at 48 hpt, with a slight decrease at 24 hpt (Figure 7E). Phosphorylation of JNK1/2 was significantly upregulated at 12 hpt and remained at a similar level till 48 hpt (Figure 7F).

DISCUSSION

The NLRs are a large family of cytosolic receptors involved in innate immune responses (Kanneganti et al., 2007; Proell et al., 2008). Bioinformatics have revealed that 23 NLR genes exist in the human genome and at least 34 NLR genes exist in mice (Harton et al., 2002; Kanneganti et al., 2007). The NLR family can be divided into three groups, one of which consists of NOD1 and NOD2, which sense cytosolic peptidoglycan fragments iE-DAP (dipeptide γ-D-glutamyl-*meso*-diaminopimelic acid) and MDP, respectively, driving the activation of the NF-κB and MAPK signaling pathways. The second group consists of NLRs required for the assembly of inflammasomes, leading to the activation of caspase-1 and maturation of IL-1β. The last group consists of the CIITA transcription factor, which is involved in the transcription of genes encoding MHC I (Fitzgerald, 2010; Meissner et al., 2010).

NOD2 is an essential NLR that participates in the recognition of bacterial invasion and viral infection. It initiates the NF-κB and MAPK signaling pathways to induce the production of various proinflammatory cytokines as well as apoptosis and autophagy to eliminate invading pathogens (Shaw et al., 2011). Although the NOD2 gene has been cloned from several fish species, studies regarding its functions and signaling pathways in teleosts are limited, especially the activation of MAP kinases. In the present study, we described the functional characterization of a NOD2 homologue (PaNOD2) in an ayu model. Structural analysis showed that PaNOD2 shared conserved functional domains with its mammalian counterparts, including N-terminal tandem CARD domains, central NBD domain, and multiple C-terminal LRRs. The structural similarity indicates that functional conservation may also exist between PaNOD2 and its higher species homologues.

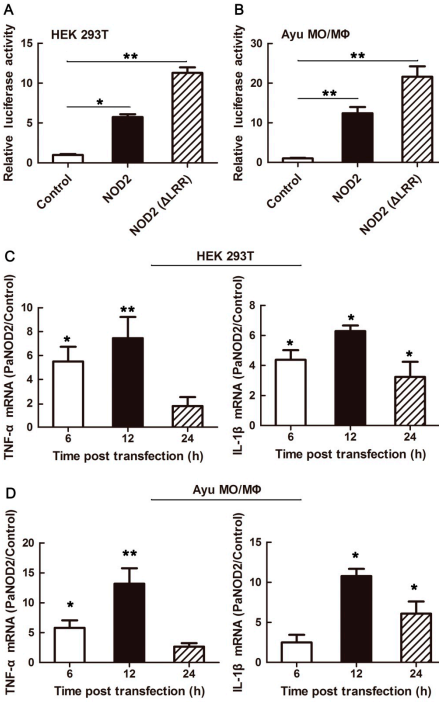

Figure 5 Activation of NF-κB signaling pathway by PaNOD2 and LRR-deleted mutant PaNOD2 (ΔLRR)

HEK293T cells (A) and ayu MO/MΦ (B) were transfected with pcDNA3.1-PaNOD2 or pcDNA3.1-PaNOD2 (ΔLRR), together with the NF-κB luciferase reporter vector, with an empty plasmid transfected group used as the control. Luciferase reporter assays were conducted at 24 hpt. C, D: Examination of the expression of inflammatory cytokines (TNF-α and IL-1β). HEK293T cells (C) and ayu MO/MΦ (D) were transfected with pcDNA3.1-PaNOD2 or empty plasmid, with cells collected at 6, 12, and 24 hpt for RNA extraction and real-time PCR to measure the expression of TNF-α and IL-1β. Values are means±*SEM*; *: $P<0.05$, **: $P<0.01$.

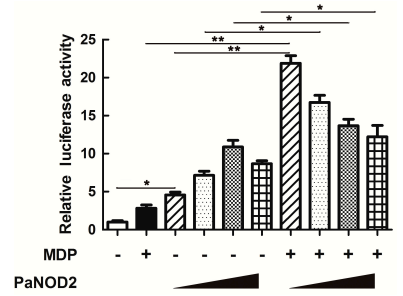

Figure 6 Functional evaluation of PaNOD2 as a receptor of MDP

Non-endogenous NOD2-expression HEK293T cells were used for this purpose. HEK293T cells were transfected with pcDNA3.1-PaNOD2 or MDP (10 ng/mL) or both with PaNOD2 at gradient levels (up to 1 μg/mL), together with NF-κB luciferase reporter vector. Empty-plasmid transfected group was used as the control. Luciferase reporter assays were conducted at 24 hpt. Values are means±*SEM*; *: $P<0.05$, **: $P<0.01$.

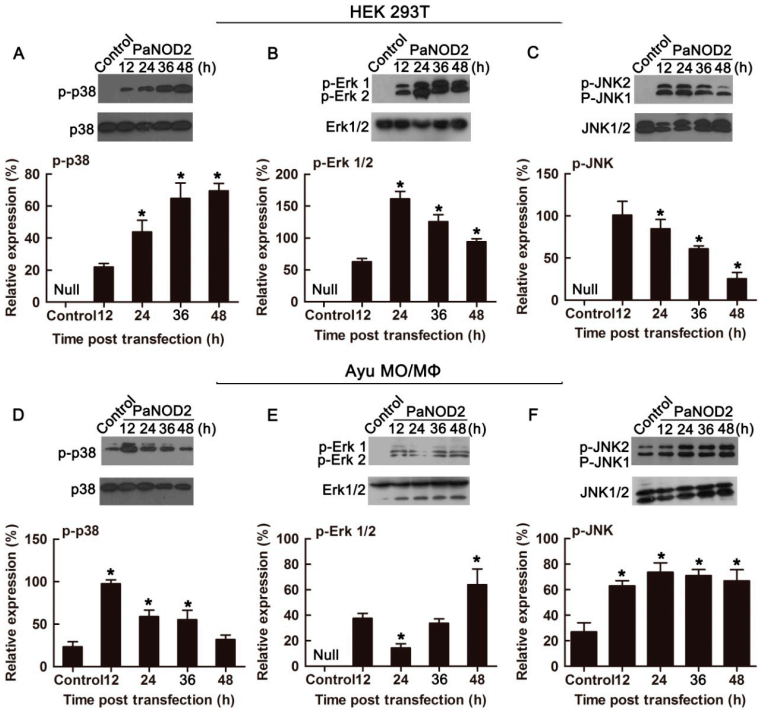

Figure 7 Activation of MAPK signaling by PaNOD2

HEK293T cells (A–C) and ayu MO/MΦ (D–F) were transfected with pcDNA3.1-PaNOD2 or empty plasmid, with cells collected at 12, 24, 36, and 48 hpt and the phosphorylation of p-38 (A and D), Erk1/2 (B and E), and JNK1/2 (C and F) then examined. Histogram shows changes in the relative band intensity of phosphorylated p-38, Erk1/2, and JNK1/2, with their corresponding total proteins (phosphorylated and non-phosphorylated). Values are means±*SEM*; *: $P<0.05$, **: $P<0.01$.

Previous studies in mammals have shown that, in addition to its role in the activation of cytosolic antibacterial signaling, NOD2 also plays an essential role in the prevention of inflammatory bowel disease (IBD). Three mutations of human NOD2 (R702W, G908R, and L1007insC) are also highly associated with susceptibility to Crohn's disease in the intestinal tract (Hugot et al., 2001; Strober et al., 2014). In addition, NOD2 is involved in maintaining the equilibrium between the constant exposure of the intestine to various microorganisms and induced host immune responses (Al Nabhani et al., 2017; Balasubramanian & Gao, 2017). Imbalance of this homeostasis can lead to the prevalence of pathogenic bacteria and the explosion of inflammation as well as damage to the intestinal epithelial barrier (Ramanan et al., 2014). It has been reported that a negative feedback loop exists between NOD2 and intestinal bacteria, whereby the accumulation of pathogenic bacteria promotes the expression of NOD2, which, in turn, prevents bacterial overexpansion (Biswas et al., 2012). Furthermore, spontaneous bacterial peritonitis (SBP), a liver cirrhosis, has been attributed to bacterial translocation from the intestine to liver (Wiest & Garcia-Tsao, 2005). Hence, the involvement of NOD2 in maintaining intestinal equilibrium is also likely essential for liver inflammation, albeit indirectly, as susceptibility to SBP is increased in patients with Crohn's disease (Wiest & Garcia-Tsao, 2005). Furthermore, the upregulation of NOD2 has also been reported during liver injury in mice and humans, and NOD2 may directly contribute to liver injury via a regulatory mechanism affecting immune cells infiltrating the liver and hepatocytes (Appenrodt et al., 2010). As shown in our expression pattern analysis of PaNOD2, the mRNA levels in the liver and intestine were significantly upregulated after *V. anguillarum* infection. Compared to the control group at 24 hpi, the expression of PaNOD2 significantly increased by 111.8- and 241.4-fold in the liver and intestine, respectively, indicating that PaNOD2 may be involved in the maintenance of homeostasis in the liver and intestine. Hence, ayu may also be a potential model for studying IBD and liver injury. However, the detailed mechanisms, signaling pathways, and cells involved still need further elucidation.

Studies in mammals and zebrafish have shown that the LRR motif maintains NOD2 in an autoinhibition state, such that it cannot initiate signaling under physiological state without the stimulation of its ligand MDP (Girardin et al., 2003; Nie et al., 2017). After recognition of MDP by LRR, NOD2 undergoes self-oligomerization and recruits the downstream adaptor receptor-interacting serine/threonine-protein kinase 2 (RIPK2) through CARD-CARD interaction (Park et al., 2007).

The activation of RIPK2 subsequently leads to the activation of the IκB kinase (IKK) complex, followed by the translocation of the NF-κB complex into the nucleus and transcription of proinflammatory genes (Rahighi et al., 2009). In contrast, RIPK2 activates transforming growth factor-β-activated kinase 1 (TAK1), which leads to the activation of MAP kinases (Windheim et al., 2007). In the present study, we found that the LRR motif also maintained PaNOD2 in an autoinhibition state, as overexpression of the LRR-deleted mutant, PaNOD2 (ΔLRR), induced more significant NF-κB activation than in the wildtype group in both HEK293T cells and ayu MO/MΦ (Figure 5A, B). In addition, overexpression of PaNOD2 together with its ligand MDP initiated more intense NF-κB activation (Figure 6). Furthermore, overexpression of PaNOD2 led to activation of the MAP kinases, as shown by the phosphorylation of p-38, Erk1/2, and JNK1/2 in HEK293T cells and ayu MO/MΦ (Figure 7). Therefore, the signaling pathways activated by NOD2 are conserved from teleosts to mammals; however, the network of adaptors and series of regulatory mechanisms involved in teleosts still need further clarification.

Collectively, our data suggested the structural and functional conservation of NOD2 receptors in the NF-κB and MAPK signaling pathways between teleosts and mammals, indicating that NOD2-mediated antibacterial innate immunity may have originated early in teleosts and been conserved throughout vertebrate evolution. This study will hopefully provide valuable insights into our understanding of the NOD2-mediated pathways in teleost fish and the evolutionary history of NLRs and associated signaling networks. Notably, NOD2 has been shown to have biological activities aside from as a pattern recognition receptor, including roles in IBD and liver and lung injuries. Therefore, the functional conservation of NOD2 from ayu to mammals may also make ayu a plausible model for studying NOD2-based diseases and therapeutic applications.

COMPETING INTERESTS

The authors declare that they have no competing interests.

AUTHORS' CONTRIBUTIONS

L.N. and J.C. drafted the experiments; Y.R., S.F.L., L.N., and S.Y.C. performed the experiments, L.N. and J.C. analyzed the data and wrote the paper, all authors read and approved the final version of the manuscript.

REFERENCES

Al Nabhani Z, Dietrich G, Hugot JP, Barreau F. 2017. Nod2: the intestinal gate keeper. *PLoS Pathogens*, **13**(3): e1006177.

Appenrodt B, Grünhage F, Gentemann MG, Thyssen L, Sauerbruch T, Lammert F. 2010. Nucleotide-binding oligomerization domain containing 2 (*NOD2*) variants are genetic risk factors for death and spontaneous bacterial peritonitis in liver cirrhosis. *Hepatology*, **51**(4): 1327–1333.

Balasubramanian I, Gao N. 2017. From sensing to shaping microbiota: insights into the role of NOD2 in intestinal homeostasis and progression of Crohn's disease. *American Journal of Physiology. Gastrointestinal and Liver Physiology*, **313**(1): G7–G13.

Basu M, Paichha M, Lenka SS, Chakrabarty R, Samanta M. 2016. Hypoxic stress: impact on the modulation of TLR2, TLR4, NOD1 and NOD2 receptor and their down-stream signalling genes expression in catla (*Catla catla*). *Molecular Biology Reports*, **43**(1): 1–9.

Biswas A, Petnicki-Ocwieja T, Kobayashi KS. 2012. Nod2: a key regulator linking microbiota to intestinal mucosal immunity. *Journal of Molecular Medicine*, **90**(1): 15–24.

Brubaker SW, Bonham KS, Zanoni I, Kagan JC. 2015. Innate immune pattern recognition: a cell biological perspective. *Annual Review of Immunology*, **33**: 257–290.

Chang MX, Wang TH, Nie P, Zou J, Secombes CJ. 2011. Cloning of two rainbow trout nucleotide-binding oligomerization domain containing 2 (NOD2) splice variants and functional characterization of the NOD2 effector domains. *Fish & Shellfish Immunology*, **30**(1): 118–127.

Chen F, Lu XJ, Nie L, Ning YJ, Chen J. 2018. Molecular characterization of a CC motif chemokine 19-like gene in ayu (*Plecoglossus altivelis*) and its role in leukocyte trafficking. *Fish & Shellfish Immunology*, **72**: 301–308.

Chen WQ, Xu QQ, Chang MX, Nie P, Peng KM. 2010. Molecular characterization and expression analysis of nuclear oligomerization domain proteins NOD1 and NOD2 in grass carp *Ctenopharyngodon idella*. *Fish & Shellfish Immunology*, **28**(1): 18–29.

Fitzgerald KA. 2010. NLR-containing inflammasomes: central mediators of host defense and inflammation. *European Journal of Immunology*, **40**(3): 595–598.

Gao FY, Pang JC, Lu MX, Yang XL, Zhu HP, Ke XL, Liu ZG, Cao JM, Wang M. 2018. Molecular characterization, expression and functional analysis of NOD1, NOD2 and NLRC3 in Nile tilapia (*Oreochromis niloticus*). *Fish & Shellfish Immunology*, **73**: 207–219.

Girardin SE, Boneca IG, Viala J, Chamaillard M, Labigne A, Thomas G, Philpott DJ, Sansonetti PJ. 2003. Nod2 is a general sensor of peptidoglycan through muramyl dipeptide (MDP) detection. *Journal of Biological Chemistry*, **278**(11): 8869–8872.

Harton JA, Linhoff MW, Zhang JH, Ting JPY. 2002. Cutting edge: CATERPILLER: a large family of mammalian genes containing CARD, pyrin, nucleotide-binding, and leucine-rich repeat domains. *The Journal of Immunology*, **169**(8): 4088–4093.

He YQ, Chen J, Lu XJ, Shi YH. 2013. Characterization of P2X7R and its function in the macrophages of ayu, *Plecoglossus altivelis*. *PLoS One*, **8**(2): e57505.

Hou QH, Yi SB, Ding X, Zhang HX, Sun Y, Zhang Y, Liu XC, Lu DQ, Lin HR. 2012. Differential expression analysis of nuclear oligomerization domain proteins NOD1 and NOD2 in orange-spotted grouper (*Epinephelus coioides*). *Fish & Shellfish Immunology*, **33**(5): 1102–1111.

Hugot JP, Chamaillard M, Zouali H, Lesage S, Cézard JP, Belaiche J, Almer S, Tysk C, O'morain CA, Gassull M, Binder V, Finkel Y, Cortot A, Modigliani R, Laurent-Puig P, Gower-Rousseau C, Macry J, Colombel JF, Sahbatou M, Thomas G. 2001. Association of NOD2 leucine-rich repeat variants with susceptibility to Crohn's disease. *Nature*, **411**(6837): 599–603.

Kanneganti TD, Lamkanfi M, Núñez G. 2007. Intracellular NOD-like receptors in host defense and disease. *Immunity*, **27**(4): 549–559.

Keating SE, Baran M, Bowie AG. 2011. Cytosolic DNA sensors regulating type I interferon induction. *Trends in Immunology*, **32**(12): 574–581.

Kufer TA, Banks DJ, Philpott DJ. 2006. Innate immune sensing of microbes by Nod proteins. *Annals of the New York Academy of Sciences*, **1072**(1): 19–27.

Letunic I, Doerks T, Bork P. 2012. SMART 7: recent updates to the protein domain annotation resource. *Nucleic Acids Research*, **40**: D302–D305.

Li JR, Gao YH, Xu TJ. 2015. Comparative genomic and evolution of vertebrate NOD1 and NOD2 genes and their immune response in miiuy croaker. *Fish & Shellfish Immunology*, **46**(2): 387–397.

Maharana J, Swain B, Sahoo BR, Dikhit MR, Basu M, Mahapatra AS, Jayasankar P, Samanta M. 2013. Identification of MDP (muramyl dipeptide)-binding key domains in NOD2 (nucleotide-binding and oligomerization domain-2) receptor of *Labeo rohita*. *Fish Physiology and Biochemistry*, **39**(4): 1007–1023.

Maharana J, Sahoo BR, Bej A, Jena I, Parida A, Sahoo JR, Dehury B, Patra MC, Martha SR, Balabantray S, Pradhan SK, Behera BK. 2015. Structural models of zebrafish (*Danio rerio*) NOD1 and NOD2 NACHT domains suggest differential ATP binding orientations: insights from computational modeling, docking and molecular dynamics simulations. *PLoS One*, **10**(3): e0121415.

Medzhitov R. 2007a. Recognition of microorganisms and activation of the immune response. *Nature*, **449**(7164): 819–826.

Medzhitov R. 2007b. TLR-mediated innate immune recognition. *Seminars in Immunology*, **19**(1): 1–2.

Meissner TB, Li A, Biswas A, Lee KH, Liu YJ, Bayir E, Iliopoulos D, Van Den Elsen PJ, Kobayashi KS. 2010. NLR family member NLRC5 is a transcriptional regulator of MHC class I genes. *Proceedings of the National Academy of Sciences of the United States of America*, **107**(31): 13794–13799.

Nie L, Zhang YS, Dong WR, Xiang LX, Shao JZ. 2015. Involvement of zebrafish RIG-I in NF-κB and IFN signaling pathways: insights into functional conservation of RIG-I in antiviral innate immunity. *Developmental & Comparative Immunology*, **48**(1): 95–101.

Nie L, Xu XX, Xiang LX, Shao JZ, Chen J. 2017. Mutual regulation of NOD2 and RIG-I in zebrafish provides insights into the coordination between innate antibacterial and antiviral signaling pathways. *International Journal of Molecular Sciences*, **18**(6): 1147.

Oehlers SH, Flores MV, Hall CJ, Swift S, Crosier KE, Crosier PS. 2011. The inflammatory bowel disease (IBD) susceptibility genes NOD1 and NOD2 have conserved anti-bacterial roles in zebrafish. *Disease Models & Mechanisms*, **4**(6): 832–841.

Park JH, Kim YG, McDonald C, Kanneganti TD, Hasegawa M, Body-Malapel M, Inohara N, Núñez G. 2007. RICK/RIP2 mediates innate immune responses induced through Nod1 and Nod2 but not TLRs. *The Journal of Immunology*, **178**(4): 2380–2386.

Proell M, Riedl SJ, Fritz JH, Rojas AM, Schwarzenbacher R. 2008. The nod-like receptor (NLR) family: a tale of similarities and differences. *PLoS One*, **3**(4): e2119.

Rahighi S, Ikeda F, Kawasaki M, Akutsu M, Suzuki N, Kato R, Kensche T, Uejima T, Bloor S, Komander D, Randow F, Wakatsuki S, Dikic I. 2009. Specific recognition of linear ubiquitin chains by NEMO is important for NF-κB activation. *Cell*, **136**(6): 1098–1109.

Ramanan D, Tang MS, Bowcutt R, Loke P, Cadwell K. 2014. Bacterial sensor Nod2 prevents inflammation of the small intestine by restricting the expansion of the commensal *Bacteroides vulgatus*. *Immunity*, **41**(2): 311–324.

Sabbah A, Chang TH, Harnack R, Frohlich V, Tominaga K, Dube PH, Xiang Y, Bose S. 2009. Activation of innate immune antiviral responses by Nod2. *Nature Immunology*, **10**(10): 1073–1080.

Shaw MH, Kamada N, Warner N, Kim YG, Nuñez G. 2011. The ever-expanding function of NOD2: autophagy, viral recognition, and T cell activation. *Trends in Immunology*, **32**(2): 73–79.

Strober W, Asano N, Fuss I, Kitani A, Watanabe T. 2014. Cellular and molecular mechanisms underlying NOD2 risk-associated polymorphisms in Crohn's disease. *Immunological Reviews*, **260**(1): 249–260.

Tamura K, Peterson D, Peterson N, Stecher G, Nei M, Kumar S. 2011. MEGA5: molecular evolutionary genetics analysis using maximum likelihood, evolutionary distance, and maximum parsimony methods. *Molecular Biology and Evolution*, **28**(10): 2731–2739.

Tanabe T, Chamaillard M, Ogura Y, Zhu L, Qiu S, Masumoto J, Ghosh P, Moran A, Predergast MM, Tromp G, Williams CJ, Inohara N, Núñez G. 2004. Regulatory regions and critical residues of NOD2 involved in muramyl dipeptide recognition. *The EMBO Journal*, **23**(7): 1587–1597.

Wiest R, Garcia-Tsao G. 2005. Bacterial translocation (BT) in cirrhosis. *Hepatology*, **41**(3): 422–433.

Windheim M, Lang C, Peggie M, Plater LA, Cohen P. 2007. Molecular mechanisms involved in the regulation of cytokine production by muramyl dipeptide. *Biochemical Journal*, **404**(2): 179–190.

Yoneyama M, Kikuchi M, Natsukawa T, Shinobu N, Imaizumi T, Miyagishi M, Taira K, Akira S, Fujita T. 2004. The RNA helicase RIG-I has an essential function in double-stranded RNA-induced innate antiviral responses. *Nature Immunology*, **5**(7): 730–737.

Zhang L, Nie L, Cai SY, Chen J, Chen J. 2018. Role of a macrophage receptor with collagenous structure (MARCO) in regulating monocyte/macrophage functions in ayu, Plecoglossus altivelis. *Fish & Shellfish Immunology*, **74**: 141–151.

Zhang XH, Shi YH, Chen J. 2015. Molecular characterization of a transmembrane C-type lectin receptor gene from ayu (*Plecoglossus altivelis*) and its effect on the recognition of different bacteria by monocytes/macrophages. *Molecular Immunology*, **66**(2): 439–450.

Zou PF, Chang MX, Li Y, Xue NN, Li JH, Chen SN, Nie P. 2016. NOD2 in zebrafish functions in antibacterial and also antiviral responses via NF-κB, and also MDA5, RIG-I and MAVS. *Fish & Shellfish Immunology*, **55**: 173–185.

Metagenomic comparison of the rectal microbiota between rhesus macaques (*Macaca mulatta*) and cynomolgus macaques (*Macaca fascicularis*)

Yan-Fang Cui[1], Feng-Jie Wang[1], Lei Yu[1], Hua-Hu Ye[2], Gui-Bo Yang[1,*]

[1] *National Center for AIDS/STD Control and Prevention, China-CDC, Beijing* 102206*, China*
[2] *Laboratory Animal Center of the Academy of Military Medical Sciences, Beijing* 100071*, China*

ABSTRACT

Rhesus macaques (*Macaca mulatta*) and cynomolgus macaques (*Macaca fascicularis*) are frequently used in establishing animal models for human diseases. To determine the differences in gut microbiota between these species, rectal swabs from 20 rhesus macaques and 21 cynomolgus macaques were collected, and the microbial composition was examined by deep sequencing of the 16S rRNA gene. We found that the rectal microbiota of cynomolgus macaques exhibited significantly higher alpha diversity than that of rhesus macaques, although the observed number of operational taxonomic units (OTUs) was almost the same. The dominant taxa at both the phylum and genus levels were similar between the two species, although the relative abundances of these dominant taxa were significantly different between them. Phylogenetic Investigation of Communities by Reconstruction of Unobserved States (PICRUSt) showed significant differences in the functional components between the microbiota of the two species, in particular the lipopolysaccharide (LPS) synthesis proteins. The above data indicated significant differences in microbial composition and function between these two closely related macaque species, which should be taken into consideration in the future selection of these animals for disease models.

Keywords: Rhesus macaques; Cynomolgus macaques; Gut microbiota; Next generation sequencing

INTRODUCTION

Extensive studies have been conducted on the commensal bacteria in the gastrointestinal tract of mice and humans. The gut microbiota is well established as an integral part of the gut mucosal immune system (Backhed et al., 2005). Commensal bacteria not only affect the development and function of the gut mucosal immune system, but also that of the systemic immune system (Lathrop et al., 2011; Niess & Adler, 2010). Beyond the immune system, the physiologies of other functional systems, such as the nervous system, endocrine system and cardiovascular system, are also under the influence of the commensal microbiota (Rieder et al., 2017; Stilling et al., 2015). Many human diseases are associated with abnormality in gut microbiota or dysbiosis (Manichanh et al., 2006; Tilg & Moschen, 2014). Furthermore, infusion of microbiota from healthy donors has shown effects on gut diseases such as recurrent *Clostridium difficile* infection (van Nood et al., 2013). Therefore, studies on gut microbiota could shed light on our understanding of human health and disease.

Both rhesus macaques (*Macaca mulatta*) and cynomolgus macaques (*Macaca fascicularis*) have long been used in animal models of human diseases such as AIDS and diabetes (Bauer et al., 2011; Feichtinger et al., 1990; Letvin et al., 1985; Li et al., 2017). While the microbiotas of both rhesus and cynomolgus macaques have been reported previously, few comparative studies exist in the literature (Euler et al., 1990; Loftin et al., 1980). To characterize the gut mucosal immune system of macaques, we previously cloned the *MAdCAM-1*, *IL-22* and *DNGR-1* genes and examined their expression in the gut mucosa of rhesus macaques (Wang et al., 2014; Yao et al.,

Received: 12 June 2018; Accepted: 26 July 2018; Online: 8 August 2018
Foundation items: This study was supported by the National Natural Science Foundation of China (81571607), Beijing Natural Science Foundation (7162136) and Ministry of Science and Technology (2017ZX10202102003005, 2015BAI08B03) of China
*Corresponding author, E-mail: guiboyang@chinaaids.cn
DOI: 10.24272/j.issn.2095-8137.2018.061

2017; Yu et al., 2018). In the current study, we examined the rectal microbiota of rhesus and cynomolgus macaques by deep sequencing of the 16S rRNA gene and subsequently analyzed their composition and predicted function.

MATERIALS AND METHODS

Sample collection

Rhesus macaques of Chinese origin and cynomolgus macaques of Indochinese origin (imported into China more than 20 years ago), 2–3 years old, were captive-bred and housed in the same experimental animal center in Beijing and fed the same diet (monkey chow plus seasonal fruit or vegetables). Stool samples were collected with cotton swabs from the rectum of 20 (10 males and 10 females) rhesus macaques and 21 (11 males and 10 females) cynomolgus macaques. All macaques were healthy and had no recent gastrointestinal abnormalities or abnormal weight changes at the time of sample collection. All samples were placed on ice immediately after collection and shipped to the laboratory and stored at −80 ℃ before use. All animals were treated humanely as approved by the Laboratory Animal Welfare & Ethics Committee of the China-CDC.

Extraction of DNA

Total DNA was extracted from the stool samples using the QIAamp DNA Stool Mini Kit (Qiagen, Germany), following the manufacturer's protocols. Briefly, 10–20 mg of each sample was lysed with buffer ASL, digested with protein kinase A, treated with buffer AL and loaded into a QIAamp spin column. After washing with AW1 and AW2, the bound DNA in the column was eluted into 50 μL of buffer AE. Aliquots of the extracted DNA samples were frozen at −80 ℃ before use.

Polymerase chain reaction (PCR) and sequencing

For samples collected from each animal, the 16S rRNA gene was amplified from the extracted DNA using the primers R515F/806R. The PCR products were gel purified and the amplicons were quantified with Nanodrop 2000 (Thermo, USA). Equal amounts of DNA from each sample were mixed to construct the sequencing library and quantified by real-time PCR with the KAPA Library Quantification Kits (Illumina, USA). The DNA library of the 16S rRNA gene with 50% PhiX was sequenced on MiSeq with V3 sequencing reagent kits (Illumina, USA). FASTQ files were generated for each sample.

Bioinformatic analysis

QIIME2 software package (version 2018.4) was used to clean the reads, calculate the alpha and beta diversities, and assign the taxonomy of each representative sequence according to the tutorial on the QIIME2 website (http://qiime2.org/). Greengenes (13_8) was used as a reference and 99% similarity was used for operational taxonomic unit (OTU) picking. The PICRUSt (Langille et al., 2013) and STAMP (Parks et al., 2014) software packages were used to analyze differences in microbial composition and function between the two species.

Statistical analysis

For quantitative comparison of the diversities and compositions of the rectal microbiota between the two species, non-parametric statistical methods (Mann-Whitney *U* test or Wilcoxon sum rank test) were used. *P*-values less than 0.05 were considered statistically significant.

RESULTS

Deep sequencing of the 16S rRNA gene in rectal stool samples from 20 rhesus and 21 cynomolgus macaques resulted in 668 486 clean reads for rhesus macaques (33 424 reads per sample), representing 957 OTUs, and 826 833 clean reads for cynomolgus macaques (39 373 reads per sample), representing 1 216 OTUs. In total 1 411 OTUs were identified in the 41 macaques.

Alpha diversity of rectal microbiota in rhesus and cynomolgus macaques

To determine the microbial diversity differences in the microbiota between the two species, we examined the alpha diversity (level of diversity within individual samples) of the microbiota. As shown in Table 1, there were no differences in the observed OTUs and Chao 1 indexes between the microbiota of the two species. However, the Shannon, Simpson, Faith's phylogenetic diversity (PD) and Good's coverage indexes were significantly different between the two species.

Table 1 Alpha diversity of the rectal microbiota of rhesus and cynomolgus macaques

Evaluation parameters	Diversity index					
	OTUs	Chao1	Shannon	Simpson	Faith's PD	Good's coverage
Rhesus macaques	246±40	264.7±46.8	5.98±0.5	0.1±0.04	15.4±2.1	0.99±0.003
Cynomolgus macaques	266±53	297.7±64.2	5.38±0.6	0.05±0.03	18.2±2.8	0.98±0.004
Mann-Whitney U	0.41	0.18	0.001	<0.0001	0.0028	0.0047

Beta diversity of rectal microbiota in rhesus and cynomolgus macaques

To further reveal the differences between the two species, we examined the beta diversity (level of diversity or dissimilarity between samples) of the microbiota of the two species. As shown in Figure 1, the weighted and un-weighted UniFrac distances (Lozupone et al., 2011) of the microbiota were significantly different between the two species ($P<0.05$, Wilcoxon sum rank test).

Composition of phyla in the rectal microbiota from rhesus and cynomolgus macaques

As shown in Figure 2, Bacteroidetes, Firmicutes and Proteobacteria were the dominant phyla in both rhesus and cynomolgus macaques, representing more than 95% of rectal microbiota. Spirochetes was also present, although relatively rare. Bacteroidetes and Proteobacteria were significantly more abundant in the rectal microbiota of cynomolgus macaques than that of rhesus macaques, whereas Firmicutes was significantly more abundant in rhesus macaques than in cynomolgus macaques ($P<0.05$, Mann-Whitney *U* test).

Composition of genera in the rectal microbiota from rhesus and cynomolgus macaques

The dominant genera of the microbiota of the two species were *Prevotella*, *Ruminococcaceae*, *Oscillospira*, *Faecalibacterium* and *Treponema*, with *Prevotella* being the most abundant (Figure 3). *Prevotella* and *Treponema* were significantly more abundant in cynomolgus macaques than in rhesus macaques, whereas *Ruminococcaceae*, *Oscillospira* and *Faecalibacterium* were significantly more abundant in rhesus macaques than in cynomolgus macaques (P<0.05, Mann-Whitney U test).

Metagenome functional content in the rectal microbiota of rhesus and cynomolgus macaques

As shown in Figure 4, various functional components in the rectal microbiota were significantly different between rhesus and cynomolgus macaques. More transcription factor genes were predicted in the rectal microbiota of rhesus macaques compared with cynomolgus macaques, whereas more genes related to oxidative phosphorylation, lipopolysaccharide (LPS) biosynthesis proteins, lipopolysaccharide biosynthesis and citrate cycle (TCA cycle) were predicted in cynomolgus macaques.

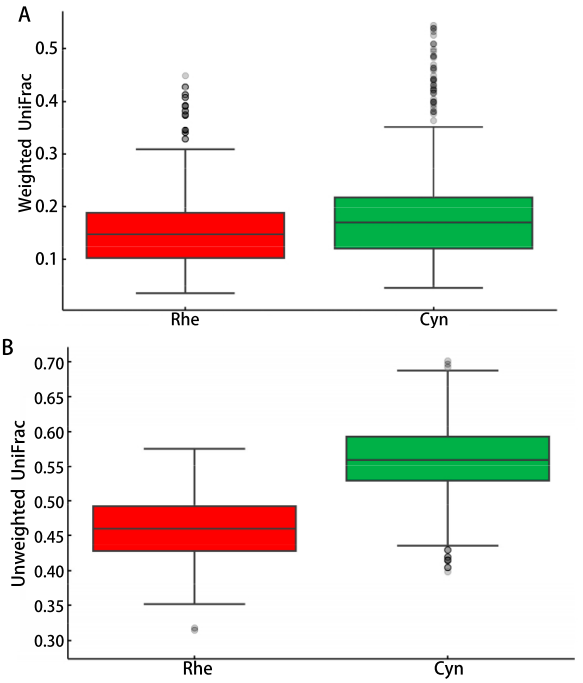

Figure 1 Differences in rectal microbiota beta-diversity between rhesus and cynomolgus macaques

Weighted (A) and unweighted (B) UniFrac distances are shown (Y-axis) for rhesus (Rhe) and cynomolgus (Cyn) macaques.

DISCUSSION

Rhesus and cynomolgus macaques are frequently used in studies of human diseases, in particular those associated with abnormality of gut microbiota such as diabetes and AIDS (Bauer et al., 2011; Dillon et al., 2016; Letvin et al., 1985). However, different results have been reported using the two species; for example, less severe levels of lymphopenia and lower set-point viral loads have been observed in simian immunodeficiency virus (SIV)-infected cynomolgus macaques in comparison to that in SIV-infected rhesus macaques, and cynomolgus macaques survive longer following SIV infection than rhesus macaques (Reimann et al., 2005; ten Haaft et al., 2001). In the current study, we compared the composition and functional components of the rectal microbiota of these two species by deep sequencing of the 16S rRNA gene and bioinformatics analyses. Results indicated that although Bacteroidetes, Firmicutes and Proteobacteria were dominant in both species, their relative abundances were significantly different.

Metagenomics prediction found many differences between the rectal microbiota of the two species, including differences in lipopolysaccharide (LPS) biosynthesis proteins and LPS biosynthesis. These differences in LPS were consistent with the differences in the abundance of bacterial taxa, i.e., more gram-negative phyla (Bacteroidetes and Proteobacteria) were found in cynomolgus macaques. Microbial translocation and attendant immune activation and systemic inflammation can drive rapid disease progression in HIV/AIDS patients. More LPS in the gut lumen generated by microbiota indicates higher basal levels of LPS, which can translocate if the mucosal barrier is damaged. Pig-tailed macaques (*Macaca nemestrina*) have been shown to progress to AIDS more rapidly than rhesus macaques after SIV infection, which may be associated with the higher basal levels of LPS translocation in pig-tailed macaques than rhesus macaques (Klatt et al., 2010). However, whether the differences in rectal microbiota between the two species are linked to the different results observed between SIV infected rhesus and cynomolgus macaques needs further study.

Microbial composition of gut microbiota can be shaped by both the host and environment (Rawls et al., 2006). Complex interacting factors such as diet, hygiene, environmental contact, antibiotic use and breastfeeding can influence microbiota composition in early life (Kaiko & Stappenbeck, 2014). The two closely related species used in this study were fed the same monkey chow and housed in the same experimental animal center. Although microbial species richness was not significantly different, as shown by the Chao 1 index and the number of observed OTUs, the alpha diversity of the rectal microbiota was significantly different between the two macaque species when the evenness and phylogenetic relationships of the microbial species were considered (Table 1). Furthermore, the beta diversity, taxon composition and functional content of the rectal microbiota were also significantly different between the two species (Figures 1–4). Therefore, our data demonstrated significant differences in the microbial composition and function between the two species. It seems informative to dissect the factors that may have caused these microbiome differences, both host and environmental factors using these animals.

Although we analyzed taxa at the species level, only a small proportion of OTUs could be assigned to species. Among the top 10 dominant OTUs, *Prevotella copri*, *Faecalibacterium prausnitzii*, *Prevotella stercorea* and *Streptococcus luteciae* were the first, sixth, seventh and tenth most dominant species. Further studies are needed to identify the other OTUs to the species level. However, intestinal *Prevotella copri* is correlated

with enhanced susceptibility to arthritis (Bernard, 2014) and *Faecalibacterium prausnitzii* is identified as an anti-inflammatory commensal bacterial in Crohn's disease patients (Sokol et al., 2008). Thus, the presence of these commensals qualifies rhesus and cynomolgus macaques as suitable animal models for studies related to these bacteria.

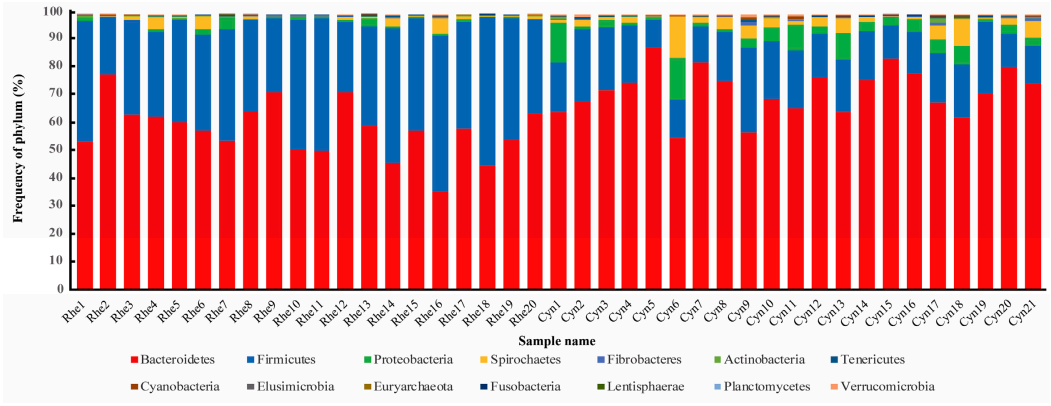

Figure 2 Phylum level taxon composition of the rectal microbiota of rhesus and cynomolgus macaques
Frequency of microbial phyla (Y-axis) is shown for rhesus (Rhe1-Rhe20) and cynomolgus (Cyn1-Cyn21) macaques. Color code for each phylum is shown at the bottom of the image.

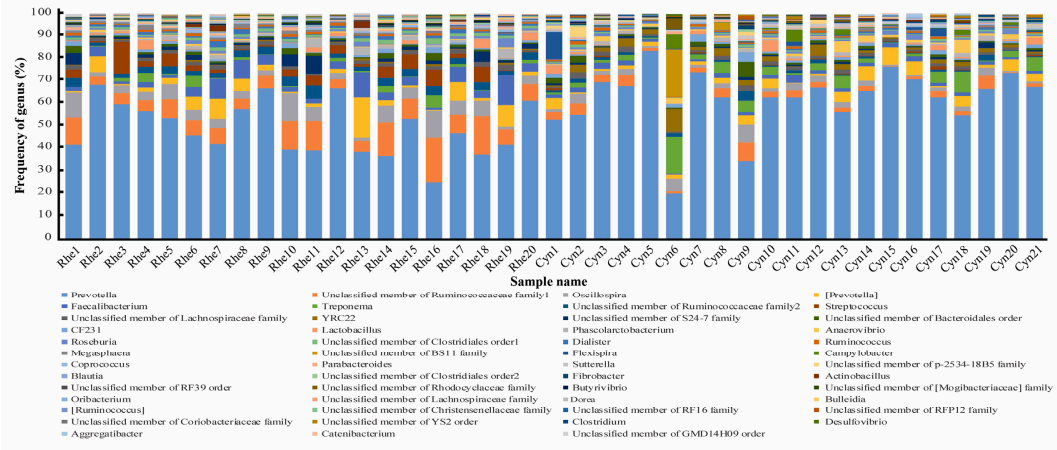

Figure 3 Genus level taxon composition of the rectal microbiota of rhesus and cynomolgus macaques
Frequency of microbial genera (Y-axis) is shown for rhesus (Rhe1-Rhe20) and cynomolgus (Cyn1-Cyn21) macaques. Color code for each genus was shown at the bottom of the image.

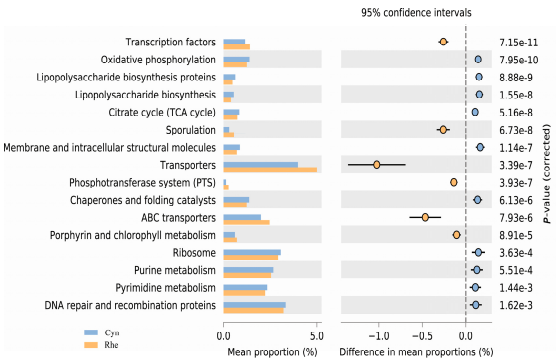

Figure 4 Functional contents predicted in the rectal microbiota of rhesus (Rhe) and cynomolgus (Cyn) macaques
Proportion of functional components in the rectal microbiota is shown for rhesus (blue bar) and cynomolgus (orange bar) macaques. Image was generated with STAMP software using data from PICRUSt analyses.

COMPETING INTERESTS

The authors declare that they have no competing interests.

AUTHORS' CONTRIBUTIONS

Y.F.C. performed the experiments, analyzed the data and partially prepared the manuscript. F.J.W. and L.Y. provided technical assistance in the experiments. H.H.Y. handled the animals and collected the samples. G.B.Y. designed the study, supervised the experiments, performed bioinformatics analyses and finished the manuscript. All authors read and approved the final version of the manuscript.

REFERENCES

Backhed F, Ley RE, Sonnenburg JL, Peterson DA, Gordon JI. 2005. Host-bacterial mutualism in the human intestine. *Science*, **307**(5717): 1915–1920.

Bauer SA, Arndt TP, Leslie KE, Pearl DL, Turner PY. 2011. Obesity in rhesus and cynomolgus macaques: a comparative review of the condition and its implications for research. *Comparative Medicine*, **61**(6): 514–526.

Bernard NJ. 2014. Rheumatoid arthritis: *Prevotella copri* associated with new-onset untreated RA. *Nature Reviews Rheumatology*, **10**(1): 2.

Dillon SM, Lee EJ, Kotter CV, Austin GL, Gianella S, Siewe B, Smith DM, Landay AL, Mcmanus MC, Robertson CE, Frank DN, Mccarter MD, Wilson CC. 2016. Gut dendritic cell activation links an altered colonic microbiome to mucosal and systemic T-cell activation in untreated HIV-1 infection. *Mucosal Immunology*, **9**(1): 24–37.

Euler AR, Zurenko GE, Moe JB, Ulrich RG, Yagi Y. 1990. Evaluation of two monkey species (*Macaca mulatta* and *Macaca fascicularis*) as possible models for human Helicobacter pylori disease. *Journal of Clinical Microbiology*, **28**(10): 2285–2290.

Feichtinger H, Putkonen P, Parravicini C, Li SL, Kaaya EE, Bottiger D, Biberfeld G, Biberfeld P. 1990. Malignant lymphomas in cynomolgus monkeys infected with simian immunodeficiency virus. *American Journal of Pathology*, **137**(6): 1311–1315.

Kaiko GE, Stappenbeck TS. 2014. Host-microbe interactions shaping the gastrointestinal environment. *Trends in Immunology*, **35**(11): 538–548.

Klatt NR, Harris LD, Vinton CL, Sung H, Briant JA, Tabb B, Morcock D, Mcginty JW, Lifson JD, Lafont BA, Martin MA, Levine AD, Estes JD, Brenchley JM. 2010. Compromised gastrointestinal integrity in pigtail macaques is associated with increased microbial translocation, immune activation, and IL-17 production in the absence of SIV infection. *Mucosal Immunology*, **3**(4): 387–398.

Langille MG, Zaneveld J, Caporaso JG, Mcdonald D, Knights D, Reyes JA, Clemente JC, Burkepile DE, Vega Thurber RL, Knight R, Beiko RG, Huttenhower C. 2013. Predictive functional profiling of microbial communities using 16S rRNA marker gene sequences. *Nature Biotechnology*, **31**(9): 814–821.

Lathrop SK, Bloom SM, Rao SM, Nutsch K, Lio CW, Santacruz N, Peterson DA, Stappenbeck TS, Hsieh CS. 2011. Peripheral education of the immune system by colonic commensal microbiota. *Nature*, **478**(7368): 250–254.

Letvin NL, Daniel MD, Sehgal PK, Desrosiers RC, Hunt RD, Waldron LM, Mackey JJ, Schmidt DK, Chalifoux LV, King NW. 1985. Induction of AIDS-like disease in macaque monkeys with T-cell tropic retrovirus STLV-III. *Science*, **230**(4721): 71–73.

Li D, Wang FJ, Yu L, Yao WR, Cui YF, Yang GB. 2017. Expression of pIgR in the tracheal mucosa of SHIV/SIV-infected rhesus macaques. *Zoological Research*, **38**(1): 44–48.

Loftin KC, Brown LR, Levy BM. 1980. Comparison of the predominant cultivable microflora in the dental plaque of *Macaca mulatta* (rhesus) and *Macaca fascicularis* (cynomolgus). *Journal of Dental Research*, **59**(10): 1606–1612.

Lozupone C, Lladser ME, Knights D, Stombaugh J, Knight R. 2011. UniFrac: an effective distance metric for microbial community comparison. *The ISME Journal*, **5**(2): 169–172.

Manichanh C, Rigottier-Gois L, Bonnaud E, Gloux K, Pelletier E, Frangeul L, Nalin R, Jarrin C, Chardon P, Marteau P, Roca J, Dore J. 2006. Reduced diversity of faecal microbiota in Crohn's disease revealed by a metagenomic approach. *Gut*, **55**(2): 205–211.

Niess JH, Adler G. 2010. Enteric flora expands gut lamina propria CX3CR1+ dendritic cells supporting inflammatory immune responses under normal and inflammatory conditions. *Journal of Immunology*, **184**(4): 2026–2037.

Parks DH, Tyson GW, Hugenholtz P, Beiko RG. 2014. STAMP: statistical analysis of taxonomic and functional profiles. *Bioinformatics*, **30**(21): 3123–3124.

Rawls JF, Mahowald MA, Ley RE, Gordon JI. 2006. Reciprocal gut microbiota transplants from zebrafish and mice to germ-free recipients reveal host habitat selection. *Cell*, **127**(2): 423–433.

Reimann KA, Parker RA, Seaman MS, Beaudry K, Beddall M, Peterson L, Williams KE, Veazey RS, Montefiori DC, Mascola JR, Nabel GJ, Letvin NL. 2005. Pathogenicity of simian-human immunodeficiency virus SHIV-89.6P and SIVmac is attenuated in cynomolgus macaques and associated with early T-lymphocyte responses. *Journal of Virology*, **79**(14): 8878–8885.

Rieder R, Wisniewski PJ, Alderman BL, Campbell SC. 2017. Microbes and mental health: A review. *Brain, Behavior, and Immunity*, **66**: 9–17.

Sokol H, Pigneur B, Watterlot L, Lakhdari O, Bermudez-Humaran LG, Gratadoux JJ, Blugeon S, Bridonneau C, Furet JP, Corthier G, Grangette C, Vasquez N, Pochart P, Trugnan G, Thomas G, Blottiere HM, Dore J, Marteau P, Seksik P, Langella P. 2008. *Faecalibacterium prausnitzii* is an anti-inflammatory commensal bacterium identified by gut microbiota analysis of Crohn disease patients. *Proceedings of the National Academy of Sciences of the United States of America*, **105**(43): 16731–16736.

Stilling RM, Ryan FJ, Hoban AE, Shanahan F, Clarke G, Claesson MJ, Dinan TG, Cryan JF. 2015. Microbes & neurodevelopment–Absence of microbiota during early life increases activity-related transcriptional pathways in the amygdala. *Brain, Behavior, and Immunity*, **50**: 209–220.

ten Haaft P, Almond N, Biberfeld G, Cafaro A, Cranage M, Ensoli B, Hunsmann G, Polyanskaya N, Stahl-Hennig C, Thortensson R, Titti F, Heeney J. 2001. Comparison of early plasma RNA loads in different macaque species and the impact of different routes of exposure on SIV/SHIV infection. *Journal of Medical Primatology*, **30**(4): 207–214.

Tilg H, Moschen AR. 2014. Microbiota and diabetes: an evolving relationship. *Gut*, **63**(9): 1513–1521.

van Nood E, Vrieze A, Nieuwdorp M, Fuentes S, Zoetendal EG, de Vos WM, Visser CE, Kuijper EJ, Bartelsman JF, Tijssen JG, Speelman P, Dijkgraaf MG, Keller JJ. 2013. Duodenal infusion of donor feces for recurrent Clostridium difficile. *The New England Journal of Medicine*, **368**(5): 407–415.

Wang Y, Yao WR, Duan JZ, Xu W, Yang GB. 2014. Mucosal addressin cell adhesion molecule-1 of rhesus macaques: molecular cloning, expression, and alteration after viral infection. *Digestive Diseases and Sciences*, **59**(10): 2433–2443.

Yao WR, Yu L, Li D, Yang GB. 2017. Molecular cloning and characterization of DNGR-1 in rhesus macaques. *Molecular Immunology*, **87**: 217–226.

Yu L, Wang FJ, Cui YF, Li D, Yao WR, Yang GB. 2018. Molecular characteristics of rhesus macaque interleukin-22: cloning, in vitro expression and biological activities. *Immunology*, **154**(4): 651–662.

Identification and characterization of two novel cathelicidins from the frog *Odorrana livida*

Ruo-Han Qi[1,#], Yan Chen[1,#], Zhi-Lai Guo[1], Fen Zhang[1], Zheng Fang[1], Kai Huang[3], Hai-Ning Yu[2,*], Yi-Peng Wang[1,*]

[1] *College of Pharmaceutical Sciences, Soochow University, Suzhou Jiangsu* 215123*, China*
[2] *Department of Bioscience and Biotechnology, Dalian University of Technology, Dalian Liaoning* 116023*, China*
[3] *School of Biology & Basic Medical Sciences, Medical College, Soochow University, Suzhou Jiangsu* 215123*, China*

ABSTRACT

Antimicrobial peptides (AMPs) are a group of gene-encoded small peptides that play pivotal roles in the host immune system of multicellular organisms. Cathelicidins are an important family of AMPs that exclusively exist in vertebrates. Many cathelicidins have been identified from mammals, birds, reptiles and fish. To date, however, cathelicidins from amphibians are poorly understood. In the present study, two novel cathelicidins (OL-CATH1 and 2) were identified and studied from the odorous frog *Odorrana livida*. Firstly, the cDNAs encoding the OL-CATHs (780 and 735 bp in length, respectively) were successfully cloned from a lung cDNA library constructed for the frog. Multi-sequence alignment was carried out to analyze differences between the precursors of the OL-CATHs and other representative cathelicidins. Mature peptide sequences of OL-CATH1 and 2 were predicted (33 amino acid residues) and their secondary structures were determined (OL-CATH1 showed a random-coil conformation and OL-CATH2 demonstrated α-helical conformation). Furthermore, OL-CATH1 and 2 were chemically synthesized and their *in vitro* functions were determined. Antimicrobial and bacterial killing kinetic analyses indicated that OL-CATH2 demonstrated relatively moderate and rapid antimicrobial potency and exhibited strong anti-inflammatory activity. At very low concentrations (10 μg/mL), OL-CATH2 significantly inhibited the lipopolysaccharide (LPS)-induced transcription and production of pro-inflammatory cytokines TNF-α, IL-1β and IL-6 in mouse peritoneal macrophages. In contrast, OL-CATH1 did not exhibit any detectable antimicrobial or anti-inflammatory activities. Overall, identification of these OL-CATHs from *O. livida* enriches our understanding of the functions of cathelicidins in the amphibian immune system. The potent antimicrobial and anti-inflammatory activities of OL-CATH2 highlight its potential as a novel candidate in anti-infective drug development.

Keywords: Antimicrobial peptides (AMPs); Cathelicidins; *Odorrana livida*; OL-CATHs; Antimicrobial activity; Anti-inflammatory activity

INTRODUCTION

Antimicrobial peptides (AMPs) are small gene-encoded peptides that possess direct antimicrobial activities against diverse microorganisms (Boman, 1998). AMPs are evolutionarily ancient weapons found widely in living organisms, from prokaryotic bacteria to eukaryotic mammals (Radek & Gallo, 2007; Zasloff, 2002; Zhang, 2015). According to their structures, AMPs can be divided into many different families. Generally, most are rich in basic amino acids and are cationic in the physiological environment (Nguyen et al., 2011;

Received: 13 June 2018; Accepted: 18 July 2018; Online: 31 July 2018
Foundation items: This work was supported by grants from the Jiangsu Students' Innovation and Entrepreneurship Training Program (2017suda098), the National Natural Science Foundation of China (31772455), Natural Science Foundation of Jiangsu Province (BK20160336 and BK20171214), Natural Science Foundation of College in Jiangsu Province (16KJB350004), and Suzhou Science and Technology Development Project (SYN201504 and SNG2017045)
[#]Authors contributed equally to this work
[*]Corresponding authors, E-mail: yipengwang@suda.edu.cn; yuhaining@dlut.edu.cn
DOI: 10.24272/j.issn.2095-8137.2018.062

Radek & Gallo, 2007). AMPs can exhibit direct antimicrobial activity against microorganisms, including bacteria, fungi, viruses, and even parasites (Nguyen et al., 2011), though these activities and spectra differ among different peptides. Unlike conventional antibiotics, most AMPs target the microbial membrane by electrostatic adsorption, subsequently resulting in cell rupture. As this action occurs rapidly, it is unlikely to induce resistance in microorganisms.

Cathelicidins are a family of important AMPs found exclusively in vertebrates. Since their first discovery (Gennaro et al., 1989), hundreds of cathelicidins have been identified from diverse vertebrates, including mammals (Zaiou & Gallo, 2002), birds (Feng et al., 2011; Wang et al., 2011; Xiao et al., 2006), reptiles (Chen et al., 2017; Wang et al., 2008; Wei et al., 2015; Zhao et al., 2018; Zhao et al., 2008), amphibians (Hao et al., 2012; Wei et al., 2013), and fish (Chang et al., 2005; Maier et al., 2008). Cathelicidin precursors possess a conserved structural organization, including a N-terminal signal peptide (30 residues), highly conserved cathelin domain (99–114 residues), and heterogenic C-terminal mature peptide (12–100 residues) (Zanetti et al., 2000). Upon stimulation, these precursors are proteolytically processed and the mature peptides are released (Zanetti, 2004). Cathelicidins are multifunctional AMPs, many of which possess potent and broad-spectrum antimicrobial activities against a wide range of microorganisms (Zanetti, 2004; Zanetti et al., 2000). Some also possess additional functions and are actively involved in host immune modulation and disease resistance, such as chemoattraction and activation of immune cells and promotion of angiogenesis and wound healing (Kahlenberg & Kaplan, 2013; Wong et al., 2013).

Cathelicidins from mammals, especially human cathelicidin LL-37, have been studied extensively. However, cathelicidins from amphibians remain poorly understood, with only 10 cathelicidins identified to date. In the present study, we reported on the identification and characterization of two novel amphibian cathelicidins, named OL-CATH1 and 2, from the odorous frog *Odorrana livida*. The cDNAs encoding OL-CATH1 and 2 were cloned, peptides were chemically synthesized, and their structures and functions were determined.

MATERIALS AND METHODS

Frog collection and tissue preparation

Two adult *O. livida* specimens (female, weight=150–200 g) were captured from Tongren, Guizhou Province, China (N27.94°, E108.62°). No specific permissions were required for the sampling location/activity, and the present study did not involve endangered or protected species. After collection, the frogs were euthanized, and the tissues were removed quickly and stored in liquid nitrogen for later use. All animal experimental protocols were approved by the Animal Care and Use Ethics Committee of Soochow University.

cDNA library construction and screening of cDNA encoding cathelicidins

The lung tissue of *O. livida* was ground into powder in liquid nitrogen and total RNA was extracted using Trizol reagent (Life Technologies, CA, USA). A cDNA library of the frog lung tissue was constructed using an In-Fusion SMARTer^{TM} Directional cDNA Library Construction Kit (Clotech, Palo Alto, CA, USA). The experiment was conducted strictly according to the kit manual. The synthesized second-strand cDNA was used as the template for the following PCR screening.

According to the highly conserved cathelin domain sequence of previously characterized cathelicidins, an antisense degenerate primer (5′-WSCRCAGRYCTTCACCTCC-3′) was designed and coupled with a 5′ sense primer (5′-AAGCAGTG GTATCAACGCAGAGT-3′) supplied by the kit to amplify the 5′ fragments of the cathelicidin encoded cDNA. The PCR procedure was: 5 min of denaturation at 94 °C; 30 cycles: denaturation at 94 °C for 30 s, primer annealing at 57 °C for 30 s, and an extension at 72 °C for 1 min. The last cycle was followed by an extension step at 72 °C for 10 min. The PCR product was purified by gel electrophoresis and cloned into the pMD19-T vector (Takara, Japan) for sequencing.

According to the acquired sequences of the 5′ fragments, a sense primer (5′-ATGGAGATCTGGCAGTGTGTGATAT-3′) was designed and coupled with a 3′ antisense primer (5′-TACGCGACGCGATACGCGAAT-3′) supplied by the kit to amplify the full-length sequence of the cDNA encoding cathelicidins. The PCR procedure was: 5 min of denaturation at 94 °C; 30 cycles: denaturation at 94 °C for 30 s, primer annealing at 58 °C for 30 s, and an extension at 72 °C for 1 min. The last cycle was followed by an extension step at 72 °C for 10 min. The PCR product was finally cloned into the pMD19-T vector and sequenced.

Multi-sequence alignment

The cathelicidins used for multi-sequence alignment were obtained from the protein database at the National Center for Biotechnology Information (NCBI, https://www.ncbi.nlm.nih.gov/protein/?term=cathelicidin). To ensure the result was as accurate as possible, representative cathelicidins from mammals, birds, reptiles and fish were selected. All cathelicidins from amphibians identified so far were also included. ClustalX (v2.1) and GeneDoc (v2.7.0) software were used for multi-sequence alignment.

Bioinformatic analysis and structure prediction of OL-CATHs

The physical and chemical parameters of the OL-CATHs were analyzed using the ExPASy Bioinformatics Resource Portal (http://www.expasy.org/tools/). Secondary structures of the OL-CATHs were predicted by a novel online computational framework PEP-FOLD3.5 (http://bioserv.rpbs.univ-paris-diderot.fr/services/PEP-FOLD3/) (Lamiable et al., 2016). Secondary structure components of the OL-CATHs were calculated by an online SOPMA secondary structure prediction method (https://npsa-prabi.ibcp.fr/cgi-bin/npsa_automat.pl?page=npsa_sopma.html).

Peptide synthesis

The OL-CATHs were synthesized by a peptide synthesizer (GL Biochem Shanghai Ltd., China). The crude peptides were

purified by RP-HPLC and analyzed by MALDI-TOF MS to confirm purity higher than 95%.

Antimicrobial assay

A standard two-fold broth microdilution method was used to determine the antimicrobial activity of OL-CATHs, as described previously (Chen et al., 2017; Wei et al., 2015). Briefly, microorganisms were incubated in Mueller-Hinton broth (MH broth) at 37 °C to exponential phase and diluted to 1×10^6 colony forming units (CFUs)/mL. Two-fold dilutions of OL-CATHs (50 μL) were prepared with MH broth in 96-well microtiter plates and mixed with equal volumes of microorganism dilutions. The plates were slowly shaken (100 r/min) at 37 °C for 18 h and the minimum concentrations (MIC) at which no visible microbial growth occurred were recorded. The conventional antibiotic ampicillin was used as a positive control. The antimicrobial activity of the OL-CATHs against *Helicobacter pylori* was determined using CFU counting, as described previously (Makobongo et al., 2009), with minor modification. The *H. pylori* 26695 and 11637 strains were incubated with MH broth (Oxoid, UK) containing 10% fetal bovine serum (FBS) at 37 °C in microaerophilic conditions produced using a 2.5-L AnaeroJar atmosphere generation system (Oxoid, UK) and AnaeroPack-MicroAero (Mitsubishi Gas Chemical Company, Japan). After growth, the bacteria were diluted with fresh MH broth (containing 10% FBS) to 1×10^4 CFU/mL. Serial concentrations of the OL-CATHs were added to the bacteria and the samples were coated on MH plates (containing 10% FBS). The plates were incubated at 37 °C in microaerophilic conditions for 3 d and the colonies on the plates were determined. The MIC values at which no bacterial colony growth occurred were recorded.

Bacterial killing kinetics assay

The bacterial killing kinetics of OL-CATH2 against *H. pylori* 11637 were determined according to previously described methods (Chen et al., 2017), with minor modification. Briefly, *H. pylori* 11637 was incubated in MH broth (containing 10% FBS) at 37 °C in microaerophilic conditions and diluted to 1×10^6 CFU/mL with fresh medium. OL-CATH2 was added to the bacterial suspension to a final concentration of 5×MIC, and the mixture was incubated at 37 °C in microaerophilic conditions for 0, 10, 20, 30, 45, 60, 90, 120 and 180 min. At each time point, aliquots (50 μL) were removed and diluted 1 000 times with fresh MH broth (containing 10% FBS). We coated 50 μL of each dilution on MH agar plates (containing 10% FBS), which were then incubated at 37 °C in microaerophilic conditions for 3 d, after which the number of viable colonies were counted. Ampicillin was used as the positive control and sterile deionized water was used as the negative control.

Quantitative real-time PCR

The experiment was performed according to previous methods (Wei et al., 2015). Briefly, Brewer thioglycollate medium (Sigma-Aldrich, USA) was injected into the peritoneal cavity of C57BL/6 mice. The mice were euthanized 3 d later, and the mouse peritoneal macrophages (MPMs) were harvested. The MPMs were cultured in RPMI-1640 (containing 10% FBS, 100 U/mL penicillin and 100 μg/mL streptomycin, Gibco, USA) and plated in 96-well culture plates (1×10^4 cells/well). After adhesion, the medium was replaced with fresh RPMI-1640 (containing 2% FBS, 100 U/mL penicillin, and 100 μg/mL streptomycin). The OL-CATHs (10 μg/mL) and lipopolysaccharide (LPS, 100 ng/mL, from *E. coli* 055:B5, Sigma-Aldrich, USA) were added to the wells and the cells were incubated for 6 h. At the end of incubation, the cells were collected for quantitative real-time PCR (qRT-PCR) to examine the gene expression levels of pro-inflammatory cytokines TNF-α, IL-1β and IL-6. Trizol reagent (Life Tech, USA) was used to extract total RNA. A PrimeScript First-Strand cDNA Synthesis Kit (Takara, Japan) was used to synthesize the first-strand cDNA. A SYBR Premix Ex Taq™ II (Tli RNaseH Plus) two-step qRT-PCR kit (Takara, Japan) was used to perform the qRT-PCR experiment on an ABI Prism 7000 Real-Time PCR System (Applied Biosystems, Carlsbad, CA, USA). Cycle counts of the target genes were normalized to the GAPDH gene, and their fold changes were calculated. The primers used for qRT-PCR are listed in Table 1.

Table 1 Primers used for quantitative real-time PCR

Name	Forward (5′–3′)	Reverse (3′–5′)
TNF-α	CGGTGCCTATGTCTCAGCCT	GAGGGTCTGGGCCATAGAAC
IL-1β	ATGGCAACTGTTCCTGAACTC	GCCCATACTTTAGGAAGACA
IL-6	AGTTGCCTTCTTGGGACTGA	TCCACGATTTCCCAGAGAAC
GAPDH	GTGAAGGTCGGTGTGAACGGATT	GGAGATGATGACCCTTTTGGCTC

Pro-inflammatory cytokine determination

The MPMs were cultured in RPMI-1640 (containing 10% FBS, 100 U/mL penicillin, and 100 μg/mL streptomycin, Gibco, USA) and plated in 96-well culture plates (1×10^4 cells/well). After adhesion, the medium was replaced with fresh RPMI-1640 (containing 2% FBS, 100 U/mL penicillin, and 100 μg/mL streptomycin). The OL-CATHs (10 μg/mL) and LPS (100 ng/mL) were added to the wells and the plates were incubated at 37 °C for 6 h, after which the cell culture supernatants were collected to determine TNF-α, IL-1β and IL-6 levels by enzyme-linked immunosorbent assay (ELISA, eBiosciences, USA).

RESULTS

Identification and characterization of OL-CATHs

A *O. livida* lung cDNA library was successfully constructed using a cDNA library construction kit. From the library, two cDNA sequences encoding two novel cathelicidins were cloned (GenBank accession Nos.: MH282906–MH282907). The complete nucleotide sequences and translated amino acid sequences of the two cathelicidin precursors are shown in Figure 1. The two cDNAs encoding the OL-CATH1 and 2 precursors were 780 and 735 bp in length, respectively. The translated peptide precursors comprised 162 and 156 amino acid residues, respectively. Consistent with representative cathelicidins from other animals, the precursors of OL-CATH1 and 2 possessed an N-terminal signal peptide sequence, followed by a middle cathelin domain and a C-terminal mature

peptide sequence (Figure 2). The signal peptide sequences and cathelin domains of the OL-CATHs shared high similarity with other cathelicidins. In particular, the four cysteine residues at the end of the cathelin domain were highly conserved within most of the cathelicidins, except for AdCath from salamander and Ss-CATH from salmon, in which the position of the fourth cysteine residue was different from that of other cathelicidins (Figure 2). Among the cathelicidins from frogs (including cathelicidin-PP from the tree-frog), there was a short acidic residue-rich fragment (D/E-rich) between the third and fourth cysteine residue of the cathelin domain. These frog cathelicidins also exhibited a high degree of similarity throughout the entire sequence (Figure 2).

Previously, Wei et al. (2013) reported on the purification and characterization of a native cathelicidin (cathelicidin-PY) from the skin secretions of *Paa yunnanensis* and successfully cloned the cathelicidin from the skin cDNA library of the frog. The precursors of the OL-CATHs and cathelicidin-PY shared a highly conserved cleavage site for maturation (Figure 2), and accordingly the mature peptides of OL-CATH1 and 2 in the present study were predicted (Figure 1). OL-CATH1 was composed of 33 amino acid residues, including seven basic residues (three Lys, four Arg) and two acid residues (one Asp, one Glu), with an amino acid sequence of KKCKGYRCRPVGFSSPISRRINDSENIYLPFGV. OL-CATH2 was also comprised of 33 amino acid residues, including eight basic residues (six Lys and two Arg), with an amino acid sequence of RKCNFLCKVKNKLKSVGSKSLIGSATHHGIYRV. Consistent with cathelicidin-PY, the two cysteines in the sequences of OL-CATH1 and OL-CATH2 formed an intramolecular disulfide bridge. Sequence BLAST searching the NCBI protein database indicted that OL-CATH1 did not show significant sequence similarity with any known cathelicidins, whereas OL-CATH2 showed 61% similarity with cathelicidin-RC2 from *Rana catesbeiana*.

Secondary structure modeling of OL-CATHs

The physical and chemical parameters of OL-CATH1 and 2 were analyzed by the ExPASy Bioinformatics Resource Portal (http://www.expasy.org/tools/) (Table 2). Both OL-CATH1 and 2 were found to be rich in basic amino acid residues (five and eight residues, respectively), with theoretical pI values of >9, implying that they are positively charged under physiological conditions.

As shown in Figure 3, OL-CATH1 demonstrated a random coil secondary conformation, whereas the N-terminal of OL-CATH2 mainly adopted an α-helical conformation (Asn-4-Ser-15), as predicted by the online PEP-FOLD3 method. The predicted secondary structure components of the OL-CATHs using the SOPMA online prediction method indicated similar results. The predicted α-helix percentages for OL-CATH1 and 2 were 3.03% and 39.39%, respectively.

Antimicrobial activity of OL-CATHs

The *in vitro* antimicrobial activities of the OL-CATHs were examined using a standard two-fold broth microdilution method. As shown in Table 3, OL-CATH1 did not show any detectable antimicrobial activity against the eight tested bacterial strains. In contrast, OL-CATH2 exhibited relatively moderate antimicrobial potency and was active against five of the eight tested bacterial strains, with MICs ranging from 9.38 to 75 μg/mL. In addition, OL-CATH2 appeared to be more potent against gram-negative bacteria than gram-positive bacteria and showed the most potent activity against the two *H. pylori* strains (MIC=9.38 μg/mL).

OL-CATH1

```
attgagacggaagggaagatggagatctggcagtgtgtgatatggctctgtgcaatcaca      60
                    M  E  I  W  Q  C  V  I  W  L  C  A  I  T      14
ttggaggtggctcactctcaatctccagatcaggaggaacagatcagagctgctctgggt     120
 L  E  V  A  H  S  Q  S  P  D  Q  E  E  Q  I  R  A  A  L  G      34
ctctacaaccagaaggaaggtggagagtttttattcaagctcctgtctgatctcccagcc     180
 L  Y  N  Q  K  E  G  G  E  F  L  F  K  L  L  S  D  L  P  A    54
ccccttctgcaggacggggaagactctccagcggtctctttcctaataaaggagacagaa     240
 P  L  L  Q  D  G  E  D  S  P  A  V  S  F  L  I  K  E  T  E    74
tgtctcaaatctgaagataataatttggcccaatgtgactacaagaaggacggggaggtg     300
 C  L  K  S  E  D  N  N  L  A  Q  C  D  Y  K  K  D  G  E  V    94
aagatctgtggattgtacacggaggaggaggaggaggagacctcagagattctgaaatgc     360
 K  I  C  G  L  Y  T  E  E  E  E  E  E  T  S  E  I  L  K  C   114
gtcagcctgaccgagaactcacggggcgagcgatcaaaaaaaaagaagaaatgtaaaggt     420
 V  S  L  T  E  N  S  R  G  E  R  S  K  K  K [K  K  C  K  G]  134
tatcgctgcagaccagttggattcagtagtccaatttctcggcgtattaacgacagcgag     480
[Y  R  C  R  P  V  G  F  S  S  P  I  S  R  R  I  N  D  S  E]  154
aacatatatctacccttcggtgtctaaaaatgagccccgtgtatctgatcgcaccacgcc     540
[N  I  Y  L  P  F  G  V] *                                     162
gctgaccactgccccagcttgccttatcacatcggcttatagccaatctactctcacatg     600
tgcatttccatgtactgtgacatcttgctttgcacatccccctatggaaaataaatgttat     660
tgtttgtatcagtttttatactctgttacaatttagccaaaaacactttgcgctggatac     720
aaagatgggaataaaatgattggctcaggccaaaaaaaaaaaaaaaaaaaaaaaaaaaa     780
```

OL-CATH2

```
tcaccttcaccatacaccacccatcgagggaagatggagatctggcagtgtgtgatatgg      60
                                M  E  I  W  Q  C  V  I  W           9
ctctgcgcagtcacattggaggtggctcactctcagtctccagttcaggaaggacggatc     120
 L  C  A  V  T  L  E  V  A  H  S  Q  S  P  V  Q  E  G  R  I      29
agagaagctctggatctctacaaccagagagaagatggagagttccttttttaaactcctg     180
 R  E  A  L  D  L  Y  N  Q  R  E  D  G  E  F  L  F  K  L  L      49
tctgagctcccgcctcgctcctggaggaggagggagactcttcagcaatcactttcttg     240
 S  E  L  P  A  S  L  L  E  E  E  G  D  S  S  A  I  T  F  L      69
ataaaggagacggactgccccaaatctgaggacaatgacttggagagatgtgactacaag     300
 I  K  E  T  D  C  P  K  S  E  D  N  D  L  E  R  C  D  Y  K      89
gaggacggggaggtgaaggtctgcgctctgcaccgggaggacgaggatgtgaaatgcatc     360
 E  D  G  E  V  K  V  C  A  L  H  R  E  D  E  D  V  K  C  I     109
agcctgtctgagaattcacgtaccaagcgatccaataaaaagagaaagtgcaacttcctc     420
 S  L  S  E  N  S  R  T  K  R  S  N  K  K [R  K  C  N  F  L]  129
tgcaaagtgaaaaacaagctcaaatctgtcggctccaagagccttatcgggtcagcgact     480
[C  K  V  K  N  K  L  K  S  V  G  S  K  S  L  I  G  S  A  T]  149
catcatggaatttatcgcgtataaatgatacatcaccgcgccatcagtgcaataagagca     540
[H  H  G  I  Y  R  V] *                                        156
ccaatcgccaacgctcacctgggtacaccgtgcaacctctgcttcatcagacatcttttc     600
tatcatggatacattgtatgtgtaattctatcagacgatctgcagatggcgttttattt     660
gcttccaacatttctgcaaattgatccaaataaaattatattacaaaaaaaaaaaaaaaa     720
aaaaaaaaaaaaaa                                                 735
```

Figure 1 cDNA sequences encoding the OL-CATHs and predicted prepropeptide sequences

5′-noncoding sequences are marked in italics. Putative mature peptides of OL-CATHs are boxed. Stop codon is indicated by an asterisk (*).

Table 2 Physical and chemical parameters of OL-CATH1 and OL-CATH2

Peptide	Grand average of hydropathicity	Number of amino acids (*n*)	Net charge	Theoretical pI	Molecular weight
OL-CATH1	−0.582	33	5+	9.89	3 788.4
OL-CATH2	−0.291	33	8+	10.41	3 673.4

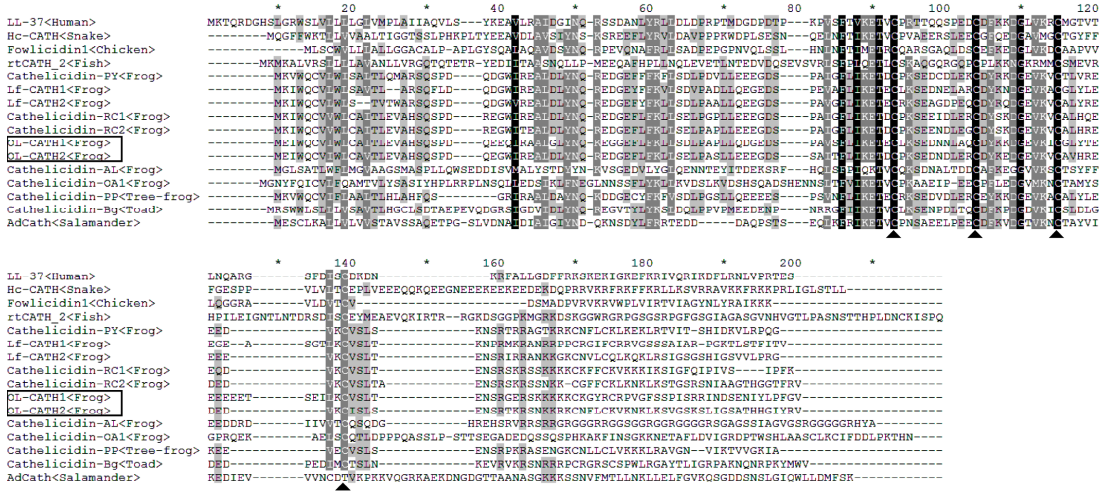

Figure 2 Multi-sequence alignment of the OL-CATHs with other representative cathelicidins
Identical residues are indicated in black and highly conserved residues are shaded. OL-CATHs are boxed and four highly conserved cysteines are indicated by a triangle (▲).

Table 3 Physical and chemical parameters of OL-CATH1 and OL-CATH2

Microorganisms	MIC (μg/mL)		
	OL-CATH1	OL-CATH2	Ampicillin
Gram-negative bacteria			
Escherichia coli ATCC25922	>200	37.5 (10.21 μmol/L)	4.69 (12.62 μmol/L)
Helicobacter pylori 26695	>200	9.38 (2.55 μmol/L)	18.75 (50.48 μmol/L)
Helicobacter pylori 11637	>200	9.38 (2.55 μmol/L)	9.38 (25.24 μmol/L)
Pseudomonas aeruginosa ATCC27853	>200	37.5 (10.21 μmol/L)	>200
Gram-positive bacteria			
Staphylococcus aureus ATCC25923	>200	75 (20.42 μmol/L)	9.38 (25.24 μmol/L)
Bacillus subtilis clinical strain	>200	>200	75 (201.9 μmol/L)
Enterococcus faecalis clinical strain	>200	>200	37.5 (100.9 μmol/L)
Staphylococcus epidermidis clinical strain	>200	>200	>200

MIC: Minimal inhibitory concentration. These concentrations represent mean values of three independent experiments performed in duplicates.

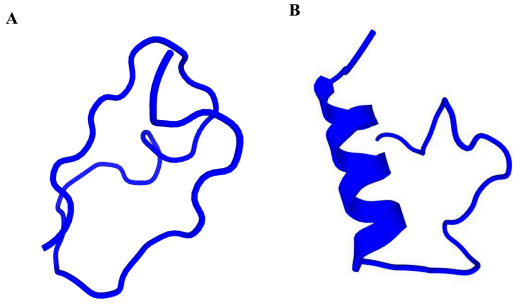

Figure 3 Secondary structure prediction of the OL-CATHs
Structures of OL-CATHs were predicted by a novel online computational framework PEP-FOLD3.5 (http://bioserv.rpbs.univ-paris-diderot.fr/services/PEP-FOLD3/). A: OL-CATH1; B: OL-CATH2.

Bacterial killing kinetics of OL-CATH2

According to the antimicrobial assay, OL-CATH2 showed the most potent activity against the two tested *H. pylori* strains. Therefore, we used *H. pylori* 11637 in the following bacterial killing kinetics assay. As illustrated in Table 4, at a concentration of 5×MIC, OL-CATH2 rapidly eradicated *H. pylori* 11637 cells within 45 min. In contrast, the positive control ampicillin needed at least 120 min to kill all bacterial cells. More importantly, the CFUs in the OL-CATH2-treated group remained unchanged at zero when the incubation time was extended to 180 min, implying that the effect of OL-CATH2 on bacteria was bactericidal rather than bacteriostatic.

Anti-inflammatory activity of OL-CATHs

To study their anti-inflammatory activity, qRT-PCR was carried out to examine the effect of OL-CATHs on LPS-induced pro-inflammatory cytokine gene expression in MPM cells. As shown in Figure 4, compared with the untreated cells, 100 ng/mL of LPS significantly induced the transcription of TNF-α, IL-1β and IL-6 genes by 294-, 1 381-, and 2 110-fold, respectively. Furthermore, OL-CATH2 (10 μg/mL) significantly inhibited the LPS-induced gene expression of TNF-α (38%), IL-1β (37%) and IL-6 (31%), respectively. However, OL-CATH2 alone did not alter the transcriptional level of the pro-inflammatory cytokine genes. In addition, OL-CATH1 did not show any inhibitory effect on LPS-induced pro-inflammatory cytokine gene expression.

Furthermore, ELISA was carried out to study the inhibitory effect of OL-CATHs on LPS-induced pro-inflammatory cytokine production in MPMs. As shown in Figure 4, 100 ng/mL of LPS significantly induced the production of TNF-α, IL-1β and IL-6 to 1 294, 1 147, and 647 pg/mL, respectively. Consistent with the qRT-PCR results, OL-CATH2 significantly reduced the LPS-induced production of TNF-α, IL-1β and IL-6 to 691, 730 and 378 pg/mL, respectively. However,

OL-CATH2 alone did not affect the production of the three pro-inflammatory cytokines. Furthermore, OL-CATH1 did not show significant inhibition of LPS-induced pro-inflammatory cytokine production. Overall, the above results indicate that only OL-CATH2 possessed potent anti-inflammatory activity.

DISCUSSION

Amphibians are the first group of animals to bridge the evolutionary water-land gap. They are directly exposed to and interact with diverse ecological and physical factors, such as microorganisms, parasites, predators and environments (He et al., 2012; Xu & Lai, 2015). As the outermost organ, amphibian skin is directly exposed to harsh environments (Clarke, 1997), and is therefore endowed with an excellent chemical defense system comprised of many gene-encoded bioactive peptides (Clarke, 1997; He et al., 2012; Zhang et al., 2012). Over the past several decades, bioactive peptides from amphibian skin have been studied extensively (Li et al., 2007; Xu & Lai, 2015; Yang et al., 2009). In total, more than 100 families of peptides have been identified from diverse species of amphibians (Xu & Lai, 2015), with frogs belonging to the family Ranidae possessing the largest number of bioactive peptides in their skin. For instance, Li et al. (2007) identified 107 novel AMPs from an individual skin of *Odorrana grahami*. However, most previously detected AMPs are specifically expressed in the skin, and AMPs from other organs of frogs have not been studied extensively. Cathelicidins, an important AMP family expressed in many different organs of vertebrates, have also not been well studied in amphibians. To date, only 10 cathelicidins have been identified from amphibians, including cathelicidin-PY from the skin secretions of *Paa yunnanensis* (Wei et al., 2013), Lf-CATH1 and 2 from the spleen of *Limnonectes fragilis* (Yu et al., 2013), cathelicidin-RC1 and 2 from the lungs of *Rana catesbeiana* (Ling et al., 2014), cathelicidin-OA1 from skin secretions of *Odorrana andersonii* (Cao et al., 2018), cathelicidin-AL from the skin secretions of *Amolops loloensis* (Hao et al., 2012), cathelicidin-Bg from the ear-side glands of *Bufo gargarizans* (Gao et al., 2016; Sun et al., 2015), cathelicidin-PP from the skin secretions of *Polypedates puerensis* (Mu et al., 2017), and AdCath from the skin of *Andrias davidianus* (Yang et al., 2017).

Table 4 Killing kinetics of OL-CATH2 against *Helicobacter pylori* 11637

Time (min)	Colony forming units ($\times 10^3$, CFUs/mL)								
	0	10	20	30	45	60	90	120	180
OL-CATH2	55	54.7	39	13.7	0	0	0	0	0
Ampicillin	58.3	56.3	70	64.3	60	39.3	16.7	0	0
Control	58.7	64	58.3	58.3	67.7	68.7	65.3	62.7	69.3

Helicobacter pylori 11637 was mixed with samples at concentration of 5×MIC for 0, 10, 20, 30, 45, 60, 90, 120 and 160 mins. The results represent mean values of three independent experiments performed in duplicates.

In the present study, two novel cathelicidins (OL-CATH1 and 2) were identified from the lungs of the frog *O. livida*. The cloned cDNAs encoding OL-CATH1 and 2 were 780 and 735 bp in length, respectively (Figure 1) and the translated precursors were comprised of 162 and 156 amino acid residues, respectively. The precursors of the OL-CATHs possessed an identical structural organization to that of other representative cathelicidins, including an N-terminal signal peptide, highly conserved cathelin domain and C-terminal mature peptide (Figure 2). Of note, the position of the four cysteines at the C-terminus of the cathelin domain were highly conserved, which is a typical characteristic of the cathelicidin family of AMPs (Figure 2). The precursors of the OL-CATHs shared a highly conserved cleavage site for maturation with cathelicidin-PY, a novel cathelicidin isolated from the skin secretions of *Paa yunnanensis* (Figure 2), and accordingly the mature peptides of OL-CATH1 and 2 were determined (Figure 1). Protein BLAST searching indicted that OL-CATH1 did not show significant sequence similarity with any known cathelicidins, but OL-CATH2 showed 61% similarity with cathelicidin-RC2 from *Rana catesbeiana* (Ling et al., 2014).

Furthermore, the secondary structures of OL-CATHs were determined using bioinformatics prediction. According to the results, OL-CATH1 adopted a random coil secondary conformation, whereas the N-terminal of OL-CATH2 mainly adopted an α-helical conformation (Asn-4-Ser-15) (Figure 3). The α-helix percentages of OL-CATH1 and 2 calculated by the SOPMA online prediction method were 3.03% and 39.39%, respectively.

The OL-CATHs were chemically synthesized for further functional study. The *in vitro* antimicrobial assay results indicated that OL-CATH1 did not possess direct antimicrobial activity, whereas OL-CATH2 exhibited relatively moderate antimicrobial potency. Of note, OL-CATH2 showed strong activity against *H. pylori* bacteria (Table 3). As a result, *H. pylori* was selected for the further bacterial killing kinetics assay. Results demonstrated that OL-CATH2 exhibited efficient bactericidal effects against *H. pylori* cells within 45 min, which was more rapid than the effects of the positive control ampicillin (Table 4). The above results imply that OL-CATH2 plays an important role in host anti-infective responses by directly killing bacteria.

In addition to direct antimicrobial activity, some cathelicidins execute anti-infective functions in other ways, such as anti-inflammation, LPS neutralization, chemoattraction and activation of immune cells, and promotion of angiogenesis and wound healing (Chen et al., 2017; Kahlenberg & Kaplan, 2013; Steinstraesser et al., 2011; Wong et al., 2013). In the present study, we constructed an LPS-induced inflammatory cell model and studied the anti-inflammatory activities of the OL-CATHs. Consistent with the antimicrobial assay results, OL-CATH2 exhibited potent anti-inflammatory activity, though OL-CATH1 did not show any detectable effect. At a low concentration of 10 μg/mL, OL-CATH2 significantly inhibited the LPS-induced gene transcription and protein synthesis of several pro-inflammatory cytokines in MPMs (Figure 4). Thus, although OL-CATH2 could not kill the invading bacteria by direct antimicrobial activity at concentrations below the MIC, it still exhibited anti-infective functions by inhibiting excessive inflammation, which ultimately protected the host from pathogenic invasions.

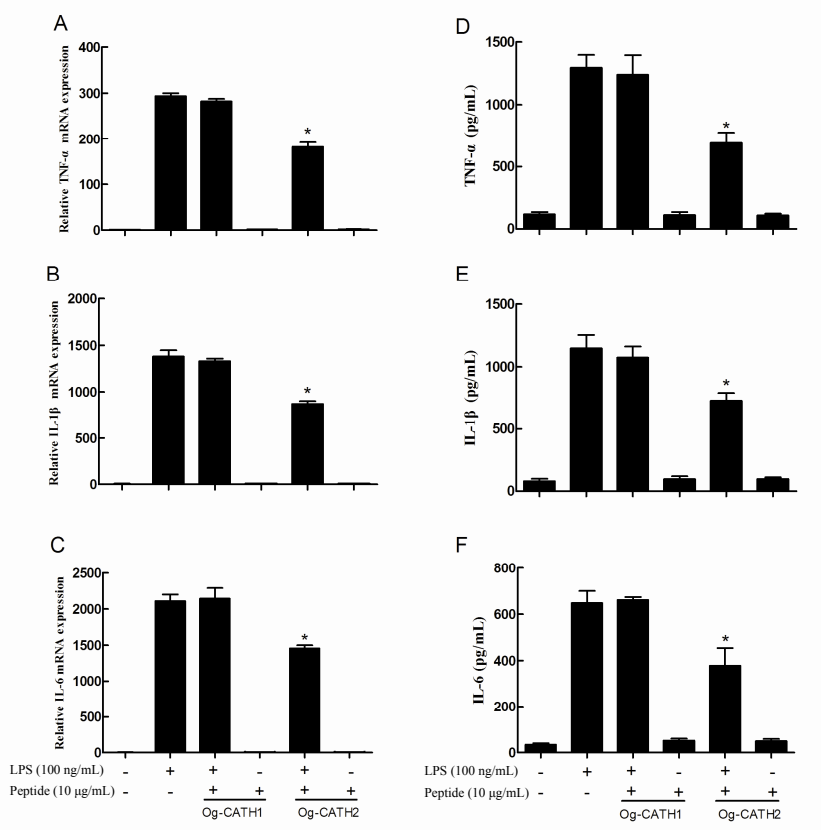

Figure 4 Anti-inflammatory activity of the OL-CATHs
A: TNF-α mRNA. B: IL-1β mRNA. C: IL-6 mRNA. D: TNF-α production. E: IL-1β production. F: IL-6 production. Data are means±*SEM* of three separate experiments. *: $P<0.05$ significantly different to LPS-only group.

In the present study, we reported on the identification and characterization of two novel cathelicidin family AMPs, i.e., OL-CATH1 and 2, from the odorous frog *O. livida*. Both peptides possessed conserved precursor construction but exhibited low sequence similarity of mature peptides with other known cathelicidins. OL-CATH2 exhibited moderate but rapid antimicrobial activity, and also possessed potent anti-inflammatory activity. Although the function of OL-CATH1 remains unclear, the identification of these OL-CATHs from *O. livida* has enriched our understanding of the functions of cathelicidins in the amphibian immune system. Furthermore, the potent antimicrobial and anti-inflammatory activities of OL-CATH2 make it a potential candidate in anti-infective drug development.

COMPETING INTERESTS

The authors declare that they have no competing interests.

AUTHORS' CONTRIBUTIONS

R.H.Q. and Y.C. performed the gene cloning experiments. Z.L.G. performed the structure analysis. F.Z., Z.F., and H.K. performed the functional study experiments. H.N.Y. and Y.P.W. designed the study and analyzed the data. Y.P.W. wrote and revised the paper. All authors read and approved the final version of the manuscript.

REFERENCES

Boman HG. 1998. Gene-encoded peptide antibiotics and the concept of innate immunity: an update review. *Scandinavian Journal of Immunology*, **48**(1): 15–25.

Cao XQ, Wang Y, Wu CY, Li XJ, Fu Z, Yang MF, Bian WX, Wang SY, Song YL, Tang J, Yang XW. 2018. Cathelicidin-OA1, a novel antioxidant peptide identified from an amphibian, accelerates skin wound healing. *Scientific Reports*, **8**: 943.

Chang CI, Pleguezuelos O, Zhang YA, Zou J, Secombes CJ. 2005. Identification of a novel cathelicidin gene in the rainbow trout, *Oncorhynchus mykiss*. *Infection and Immunity*, **73**(8): 5053–5064.

Chen Y, Cai SS, Qiao X, Wu ML, Guo ZL, Wang RP, Kuang YQ, Yu HN, Wang YP. 2017. As-CATH1-6, novel cathelicidins with potent antimicrobial and immunomodulatory properties from *Alligator sinensis*, play pivotal roles in host antimicrobial immune responses. *The Biochemical Journal*, **474**(16): 2861–2885.

Clarke BT. 1997. The natural history of amphibian skin secretions, their normal functioning and potential medical applications. *Biological Reviews of the Cambridge Philosophical Society,* **72**(3): 365–379.

Feng FF, Chen C, Zhu WJ, He WY, Guang HJ, Li Z, Wang D, Liu JZ, Chen M, Wang YP, Yu HN. 2011. Gene cloning, expression and characterization of

avian cathelicidin orthologs, Cc-CATHs, from *Coturnix coturnix*. *The FEBS Journal*, **278**(9): 1573–1584.

Gao F, Xu WF, Tang LP, Wang MM, Wang XJ, Qian YC. 2016. Characteristics of cathelicidin-Bg, a novel gene expressed in the ear-side gland of *Bufo gargarizans*. *Genetics and Molecular Research*, **15**(3). doi: 10.4238/gmr.15038481.

Gennaro R, Skerlavaj B, Romeo D. 1989. Purification, composition, and activity of two bactenecins, antibacterial peptides of bovine neutrophils. *Infection and Immunity*, **57**(10): 3142–3146.

Hao X, Yang HL, Wei L, Yang SL, Zhu WJ, Ma DY, Yu HN, Lai R. 2012. Amphibian cathelicidin fills the evolutionary gap of cathelicidin in vertebrate. *Amino Acids*, **43**(2): 677–685.

He WY, Feng FF, Huang Y, Guo HH, Zhang SY, Li Z, Liu JZ, Wang YP, Yu HN. 2012. Host defense peptides in skin secretions of *Odorrana tiannanensis*: Proof for other survival strategy of the frog than merely anti-microbial. *Biochimie*, **94**(3): 649–655.

Kahlenberg JM, Kaplan MJ. 2013. Little peptide, big effects: the role of LL-37 in inflammation and autoimmune disease. *Journal of Immunology*, **191**(10): 4895–4901.

Lamiable A, Thévenet P, Rey J, Vavrusa M, Derreumaux P, Tufféry P. 2016. PEP-FOLD3: faster de novo structure prediction for linear peptides in solution and in complex. *Nucleic Acids Research*, **44**(W1): W449–454.

Li JX, Xu XQ, Xu CH, Zhou WP, Zhang KY, Yu HN, Zhang YP, Zheng YT, Rees HH, Lai R, Yang DM, Wu J. 2007. Anti-infection peptidomics of amphibian skin. *Molecular and Cellular Proteomics*, **6**(5): 882–894.

Ling GY, Gao JX, Zhang SM, Xie ZP, Wei L, Yu HN, Wang YP. 2014. Cathelicidins from the bullfrog *Rana catesbeiana* provides novel template for peptide antibiotic design. *PLoS One*, **9**(3): e93216.

Maier VH, Dorn KV, Gudmundsdottir BK, Gudmundsson GH. 2008. Characterisation of cathelicidin gene family members in divergent fish species. *Molecular Immunology*, **45**(14): 3723–3730.

Makobongo MO, Kovachi T, Gancz H, Mor A, Merrell DS. 2009. *In vitro* antibacterial activity of acyl-lysyl oligomers against *Helicobacter pylori*. *Antimicrobial Agents and Chemotherapy*, **53**(10): 4231–4239.

Mu LX, Zhou L, Yang JJ, Zhuang L, Tang J, Liu T, Wu J, Yang HL. 2017. The first identified cathelicidin from tree frogs possesses anti-inflammatory and partial LPS neutralization activities. *Amino Acids*, **49**(9): 1571–1585.

Nguyen LT, Haney EF, Vogel HJ. 2011. The expanding scope of antimicrobial peptide structures and their modes of action. *Trends in Biotechnology*, **29**(9): 464–472.

Radek K, Gallo R. 2007. Antimicrobial peptides: natural effectors of the innate immune system. *Seminars in Immunopathology*, **29**(1): 27–43.

Steinstraesser L, Kraneburg U, Jacobsen F, Al-Benna S. 2011. Host defense peptides and their antimicrobial-immunomodulatory duality. *Immunobiology*, **216**(3): 322–333.

Sun T, Zhan B, Gao Y. 2015. A novel cathelicidin from *Bufo bufo gargarizans* Cantor showed specific activity to its habitat bacteria. *Gene,* **571**(2): 172–177.

Wang YP, Hong J, Liu XH, Yang HL, Liu R, Wu J, Wang AL, Lin DH, Lai R. 2008. Snake cathelicidin from *Bungarus fasciatus* is a potent peptide antibiotics. *PLoS One*, **3**(9): e3217.

Wang YP, Lu ZK, Feng FF, Zhu W, Guang HJ, Liu JZ, He WY, Chi LL, Li Z, Yu HN. 2011. Molecular cloning and characterization of novel cathelicidin-derived myeloid antimicrobial peptide from *Phasianus colchicus*. *Developmental and Comparative Immunology*, **35**(3): 314–322.

Wei L, Gao JX, Zhang SM, Wu SJ, Xie ZP, Ling GY, Kuang YQ, Yang YL, Yu HN, Wang YP. 2015. Identification and characterization of the first cathelicidin from sea snakes with potent antimicrobial and anti-inflammatory activity and special mechanism. *Journal of Biological Chemistry*, **290**(27): 16633–16652.

Wei L, Yang JJ, He XQ, Mo GX, Hong J, Yan XW, Lin DH, Lai R. 2013. Structure and function of a potent lipopolysaccharide-binding antimicrobial and anti-inflammatory peptide. *Journal of Medicinal Chemistry*, **56**(9): 3546–3556.

Wong JH, Ye XJ, Ng TB. 2013. Cathelicidins: peptides with antimicrobial, immunomodulatory, anti-inflammatory, angiogenic, anticancer and procancer activities. *Current Protein & Peptide Science*, **14**(6): 504–514.

Xiao Y, Cai Y, Bommineni YR, Fernando SC, Prakash O, Gilliland SE, Zhang G. 2006. Identification and functional characterization of three chicken cathelicidins with potent antimicrobial activity. *Journal of Biological Chemistry*, **281**(5): 2858–2867.

Xu XQ, Lai R. 2015. The chemistry and biological activities of peptides from amphibian skin secretions. *Chemical Reviews*, **115**(4): 1760–1846.

Yang H, Lu BY, Zhou DD, Zhao L, Song WJ, Wang LX. 2017. Identification of the first cathelicidin gene from skin of Chinese giant salamanders *Andrias davidianus* with its potent antimicrobial activity. *Developmental and Comparative Immunology*, **77**: 141–149.

Yang HL, Wang X, Liu XH, Wu J, Liu CB, Gong, WM, Zhao ZQ, Hong J, Lin DH, Wang YZ, Lai R. 2009. Antioxidant peptidomics reveals novel skin antioxidant system. *Molecular and Cellular Proteomics*, **8**(3): 571–583.

Yu HN, Cai SS, Gao JX, Zhang SY, Lu YL, Qiao X, Yang HL, Wang YP. 2013. Identification and polymorphism discovery of the cathelicidins, Lf-CATHs in ranid amphibian (*Limnonectes fragilis*). *The FEBS Journal*, **280**(23): 6022–6032.

Zaiou M, Gallo RL. 2002. Cathelicidins, essential gene-encoded mammalian antibiotics. *Journal of Molecular Medicine (Berlin, Germany)*, **80**(9): 549–561.

Zanetti M. 2004. Cathelicidins, multifunctional peptides of the innate immunity. *Journal of Leukocyte Biology*, **75**(1): 39–48.

Zanetti M, Gennaro R, Scocchi M, Skerlavaj B. 2000. Structure and biology of cathelicidins. *Advances in Experimental Medicine and Biology*, **479**: 203–218.

Zasloff M. 2002. Antimicrobial peptides of multicellular organisms. *Nature*, **415**(6870): 389–395

Zhang Y. 2015. Why do we study animal toxins? *Zoological Research*, **36**(4): 183–222.

Zhang SY, Guo HH, Shi F, Wang H, Li LL, Jiao XD, Wang YP, Yu HN. 2012. Hainanenins: a novel family of antimicrobial peptides with strong activity from Hainan cascade-frog, *Amolops hainanensis*. *Peptides*, **33**(2): 251–257.

Zhao F, Lan XQ, Du Y, Chen PY, Zhao J, Zhao F, Lee WH, Zhang Y. 2018. King cobra peptide OH-CATH30 as a potential candidate drug through clinic drug-resistant isolates. *Zoological Research*, **39**(2): 87–96.

Zhao H, Gan TX, Liu XD, Jin Y, Lee WH, Shen JH, Zhang Y. 2008. Identification and characterization of novel reptile cathelicidins from elapid snakes. *Peptides*, **29**(10): 1685–1691.

Developmental expression of three *prmt* genes in *Xenopus*

DEAR EDITOR,

Protein arginine methyltransferases (PRMTs) are involved in many cellular processes via the arginine methylation of histone or non-histone proteins. We examined the expression patterns of *prmt4*, *prmt7*, and *prmt9* during embryogenesis in *Xenopus* using whole-mount *in situ* hybridization and quantitative reverse transcription polymerase chain reaction (RT-PCR). *Xenopus prmt4* and *prmt7* were expressed in the neural crest, brain, and spinal cord, and also detected in the eye, branchial arches, and heart at the tailbud stage. Specific *prmt9* signals were not detected in *Xenopus* embryos until the late tailbud stage when weak expression was observed in the branchial arches. Quantitative RT-PCR indicated that the expression of *prmt4* and *prmt7* was up-regulated during the neurula stage, whereas *prmt9* maintained its low expression until the late tailbud stage, consistent with the whole-mount *in situ* hybridization results. Thus, the developmental expression patterns of these three *prmt* genes in *Xenopus* embryos provide a basis for further functional study of such genes.

Post-translational modification plays an essential role in modulating the structure and function of a protein (Walsh & Jefferis, 2006). Arginine methylation is a common post-translational modification in vertebrates, and is mediated by protein arginine methyltransferases (PRMTs) (Biggar & Li, 2015; Carr et al., 2015). PRMTs can catalyze the transfer of a methyl group from S-adenosylmethionine (SAM) to the guanidine nitrogen atoms of arginine to form methylarginine (Herrmann et al., 2009). Based on the number and symmetry of the methyl group in methylarginine, PRMTs can be divided into three categories. PRMT4 (type I PRMT) and PRMT9 (type II PRMT) catalyze the formation of asymmetric and symmetric dimethylarginine, respectively (Cook et al., 2006; Yang & Bedford, 2013), whereas PRMT7 (type III PRMT) catalyzes the formation of monomethylarginine (Feng et al., 2013; Feng et al., 2014).

The PRMT-mediated arginine methylation of histone or non-histone proteins is involved in many cellular processes, including transcriptional regulation, signal transduction, and RNA splicing (Biggar & Li, 2015; Carr et al., 2015; Yang et al., 2015). PRMT4, also known as coactivator associated arginine methyltransferase 1 (CARM1), can regulate the cell cycle through arginine methylation of the retinoblastoma protein tumor suppressor (Kim et al., 2015). PRMT9 can methylate SAP145, a component of the U2 snRNP involved in the early stages of splicing, with attenuation of PRMT9 also known to cause gross changes in RNA splicing (Yang et al., 2015).

PRMT7 is required for the maintenance of the regeneration capacity of muscle stem cells by regulating the DNMT3b/p21 axis (Blanc et al., 2016). Specific knockout of *PRMT7* in muscle stem cells can cause elevated expression of CDK inhibitor p21CIP1 and reduced expression of its repressor, DNMT3b, leading to cell-cycle arrest and premature cellular senescence, which can be rescued by restoration of DNMT3b (Blanc et al., 2016). Both *prmt4* and *prmt5* play a combinatorial role during zebrafish myogenesis by controlling fast and slow muscle fiber formation (Batut et al., 2011). Furthermore, *prmt4* is also suggested to regulate the expression of myogenic microRNAs directly (Mallappa et al., 2011).

Although PRMTs are widely involved in various cellular processes via catalyzing the methylation of target proteins, their roles in embryonic development are not yet well understood. Limited studies have shown that PRMT4 and PRMT7 are involved in myogenesis (Batut et al., 2011; Blanc et al., 2016; Mallappa et al., 2011). *Xenopus* is an excellent model in developmental biology (Harland & Grainger, 2011), and all *prmt* genes (*prmt1–9*) have been identified in the *Xenopus tropicalis* genome. In this study, we selected three *prmt* genes, that is, *prmt4*, *prmt7,* and *prmt9*, and studied their spatial and temporal expression patterns during the embryonic development of *Xenopus*. Our study will provide a basis for further investigations on the functions of *prmt* genes in *Xenopus*.

We searched *prmt* genes of *Xenopus tropicalis* and other species in the NCBI database (Supplementary Table S1, available online). Protein sequence alignments were performed using Geneious v4.8.5 (www.geneious.com/previous-versions/#geneious-4-dot-8), with a dendrogram tree then constructed using neighbor-joining in the same program.

Received: 08 May 2018; Accepted: 15 June 2018; Online: 20 August 2018
Foundation items: This work was supported by grants from the Research Grants Council of Hong Kong CUHK14167017, CUHK24100414 to H.Z., and the Shenzhen Innovation Committee of Science and Technology grants (JCYJ20150331101823691) and Guangdong Provincial Key Laboratory of Cell Microenvironment and Disease Research (2017B030301018) to Y.D.
DOI: 10.24272/j.issn.2095-8137.2018.064

Xenopus laevis prmt4 (NM_001094676), *prmt7* (NM_001086541), and *prmt9* (NM_001096961) sequences were obtained by searching the NCBI database. The open reading frames (ORFs) of *prmt4*, *prmt7*, and *prmt9* were amplified using reverse transcription polymerase chain reaction (RT-PCR). The PCR products were subcloned into the pBluescript II KS (+) vector and verified by sequencing. To prepare probes for *in situ* hybridizations, plasmids were linearized by cutting with *Xho*1 and used as templates for the synthesis of digoxigenin-labeled anti-sense probes with T7 RNA polymerase (Roche, Indianapolis, USA).

Xenopus laevis embryos were collected, cultured, and fixed as described previously (Wang et al., 2011). Whole-mount *in situ* hybridization was performed according to standard methods (Harland, 1991). After *in situ* hybridization, the embryos were embedded and sectioned at a thickness of 50 μm. Detailed information on the vibratome sections is described in our previous study (Kam et al., 2010).

Total RNA was extracted from *Xenopus tropicalis* embryos using TRIzol reagent (Molecular Research Center Inc., USA). The cDNA was synthesized using the ReverTra Ace® qPCR RT Kit (Toyobo, Japan). Quantitative PCR was performed using the SYBR® Green real-time PCR master mix (Toyobo, Japan). The primer sequences used are listed in Table 1. *Ornithine decarboxylase* (*odc*) was used as the internal control.

Table 1 Primers for quantitative RT-PCR

Gene	Sequence (5′–3′)
prmt1	Fw: CAAACATGGCTGAAGCGAGC
	Re: ACATCTCCTCATGGATGCCAAAG
prmt2	Fw: ACAGCCTGCATTCACTTGGT
	Re: TAATCAGGCTTGGGTCTGGC
prmt3	Fw: AAGATGTGGATCTGCCCGTG
	Re: CAGGTATCGGGGTACACTGC
prmt4	Fw: GGAGATCCAGAGACACGCTG
	Re: TGCATTTGAACACGCAGACG
prmt6	Fw: GGCCAGTAGTATGTCCCAGC
	Re: GCGTACCCCATCCATTCACT
prmt7	Fw: TGCGTGTGGTACAGCCTAAC
	Re: AATGACATGCAGGACGCTCT
prmt9	Fw: TTGATGCAGGCTTGTTTGGC
	Re: TCTGGGCACTCTACTGCCAT
odc	Fw: GGGCAAAAGAGCTTAATGTGG
	Re: TGCCAACATGGAAACTTACA

We performed whole-mount *in situ* hybridization to examine the spatial expression of *prmt* genes in *Xenopus* embryos. No evident signals were detected before gastrulation. In the early gastrula stage, the *prmt4* signal was mainly expressed in the dorsal ectoderm, which gives rise to the neural ectoderm (Figure 1A). At the early neurula stage, the *prmt4* signal was enriched in the anterior region of the neural plate as well as the posterior region around the blastopore (Figure 1B). After this, *prmt4* was strongly expressed in the neural plate and neural crest (Figure 1C, D). This expression pattern persisted when neural crest migration began in the later neurula stage (Figure 1E, F). During the tailbud stage, *prmt4* was detected throughout the central nervous system, including the brain and spinal cord (Figure 1G, H). Strong expression was also observed in the branchial arches and eye vesicles (Figure 1G, H). In stage 35, *prmt4* expression was enriched in the head region, including the forebrain, midbrain, hindbrain, eye, and branchial arches (Figure 1I, J). In stage 40, *prmt4* was expressed in the olfactory placode, jaw, and heart, and weak expression in the paraxial mesoderm was also observed (Figure 1K–R). Weak signals were also detected in the eye, brain, dorsal region of the endoderm, and spinal cord (Figure 1N–R).

No apparent expression of *prmt7* was detected in the embryos at the early gastrula stage (data not shown). In the early neurula stage, *prmt7* was weakly expressed in the neural plate (Figure 2A). The expression of *prmt7* intensified and expanded to the migrating neural crest, anterior neural tube, and somites (Figure 2B, C), and then showed strong expression in the branchial arches during the tailbud stage (Figure 2D, E). At stage 25, *prmt7* expression was also detected in the intermediate mesoderm (Figure 2D). At stage 29, *prmt7* signals were detected in the brain, eye, and somites (Figure 2E–H). Weak expression was also observed in the pronephric tubule (Figure 2I). At stage 40, *prmt7* was strongly expressed in the branchial arches, with weak signals in the heart, eye, brain, and olfactory placode (Figure 2J–L).

Whole-mount *in situ* hybridization could not detect specific signals of *prmt9* in *Xenopus* embryos at almost every stage, though a weak signal was observed in the branchial arches at the late tailbud stage (data not shown).

We studied the temporal expression patterns of *Xenopus prmt* genes using quantitative RT-PCR. Different from pseudotetraploid *Xenopus laevis*, the diploid *Xenopus tropicalis* species has two sets of chromosomes. Thus, we collected *Xenopus tropicalis* embryos at different stages and measured the mRNA expression levels of *prmt1–4*, *prmt6*, *prmt7*, and *prmt9* (Figure 3). Maternal expression of *prmt6* and *prmt7* was detected, which decreased during the cleavage stage (Figure 3E, F). Apart from *prmt7,* the expression levels of the detected *prmt* genes were low during the gastrula stage (Figure 3F). The expression of *prmt4*, *prmt6*, and *prmt7* were gradually up-regulated from the neurula stage (Figure 3D–F). However, the expression levels of *prmt2*, *prmt3*, and *prmt9* increased from the tailbud stage (Figure 3B, C, G). During the late tailbud stage, most of the *prmt* genes maintained their high expression levels, except for *prmt2* and *prmt9*, whose expression continued to increase (Figure 3B, G). The expression of *prmt9* remained low before the late tailbud stage (Figure 3G). In contrast, *prmt1* expression reached a high level at the early neurula stage (Figure 3A). The up-regulation in the expression of *prmt4* and *prmt7* during neurulation (Figure 3D, F) accords with their enhanced staining of embryos, as revealed by whole-mount *in situ* hybridization (Figure 1B–F; Figure 2A–C). The low expression level of *prmt9* before the late tailbud stage (Figure 3G) is consistent with the slight staining of embryos after *in situ* hybridization.

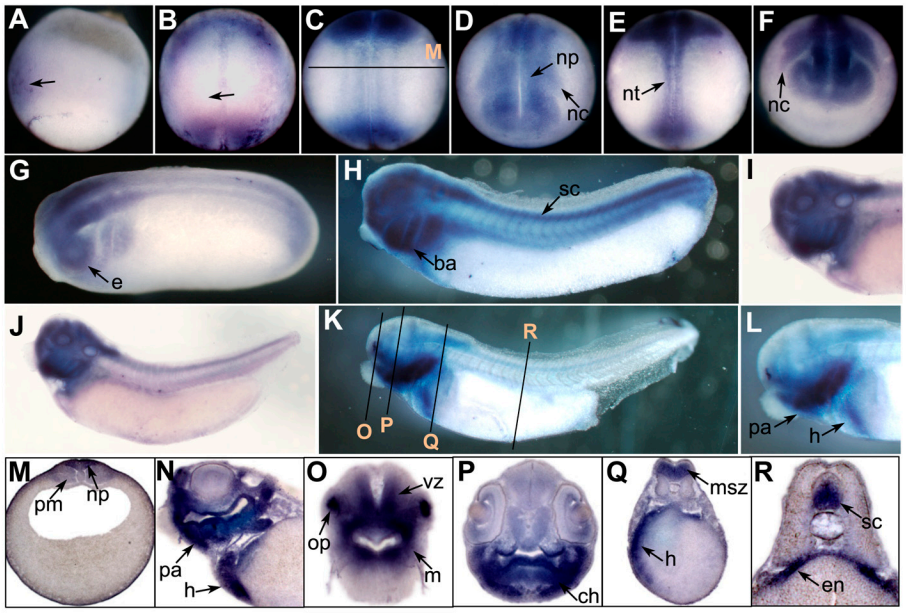

Figure 1 Spatial expression of *prmt4* in *Xenopus* embryos

A: Lateral view of a stage 10 embryo with dorsal toward the left showing differential expression of *prmt4* along the dorsoventral axis. Arrow indicates signal on the dorsal side. B–F: *prmt4* signal detected in the neural crest and neural plate during the neurula stage. B: Stage 15 embryo; C, D: Stage 18 embryos; E, F: Stage 20 embryos. B, C, E: Dorsal view with anterior toward the top. D, F: Anterior view with dorsal toward the top. G–L: Expression of *prmt4* detected in the brain, spinal cord, branchial arches, and heart anlage. G, H, J, K: Lateral view of stage 25 (G), stage 28 (H), stage 35 (J), and stage 40 (K) embryos. Enlarged head regions of embryos in J and K are shown in I and L, respectively. M: Transverse section of embryo at the level illustrated by the black line in C. N: Longitudinal section of a stage 40 embryo. O–R: Transverse sections of embryo at the levels illustrated by the black lines in K. ba: branchial arches; e: eye; en: endoderm; ch: second pharyngeal arch; h: heart; m: first pharyngeal (maxillary) arch; msz: marginal and subventricular zones of midbrain and neural tube; nc: neural crest; np: neural plate; nt: neural tube; op: olfactory placode; pa: pharyngeal arch; pm: paraxial mesoderm; sc: spinal cord; vz: ventricular zone of neural tube.

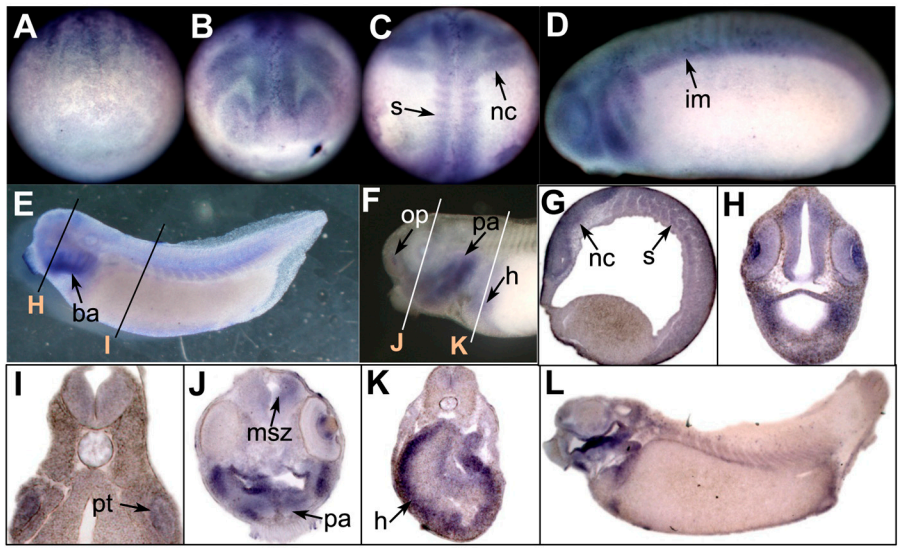

Figure 2 Expression of *prmt7* in *Xenopus* embryos

A: Weak signal of *prmt7* detected on the neural fold of stage 15 embryo. Anterior view with dorsal toward the top. B, C: *prmt7* expressed in migrating neural crest, neural tube, and somites in a stage 20 embryo. B: Anterior view with dorsal toward the top; C: Dorsal view. D, E: Expression of *prmt7* in branchial arches, intermediate mesoderm, brain, and eye in a stage 25 embryo (D). At later stage (stage 29, E), strong *prmt7* signals remained at branchial arches. Faint *prmt7* expression detected in pronephric tubule and in somites. F: *prmt7* signals detected in the eye, pharyngeal arches, and heart at stage 40. G: Longitudinal section of a stage 20 embryo showing *prmt7* signals the in neural crest and somites. H, I: Transverse sections of a stage 29 embryo at the levels illustrated by the black lines in E. J, K: Transverse sections from a stage 40 embryo at the levels illustrated by the white lines shown in F. L: Longitudinal section of a stage 40 embryo. ba: branchial arches; h: heart; im: intermediate mesoderm; msz: marginal and subventricular zones of midbrain and neural tube; nc: neural crest; op: olfactory placode; pa: pharyngeal arch; pt: pronephric tubule; s: somite.

Searching the NCBI database we found that all *prmt* genes, including *prmt1–9*, have been identified in *Xenopus tropicalis*. A phylogenetic tree based on their protein sequence alignments was generated (Figure 4A). Results showed that type I PRMTs (prmt1, prmt2, prmt3, prmt4, prmt6, and prmt8) exhibited fewer genetic changes, whereas prmt5 and prmt7 demonstrated more significant genetic variation (Figure 4A). We conducted phylogenetic analysis of the *Xenopus* prmt4, prmt7, and prmt9 proteins to illustrate their evolutionary distances to humans, mice, chickens, frogs, and zebrafish (Figure 4B).

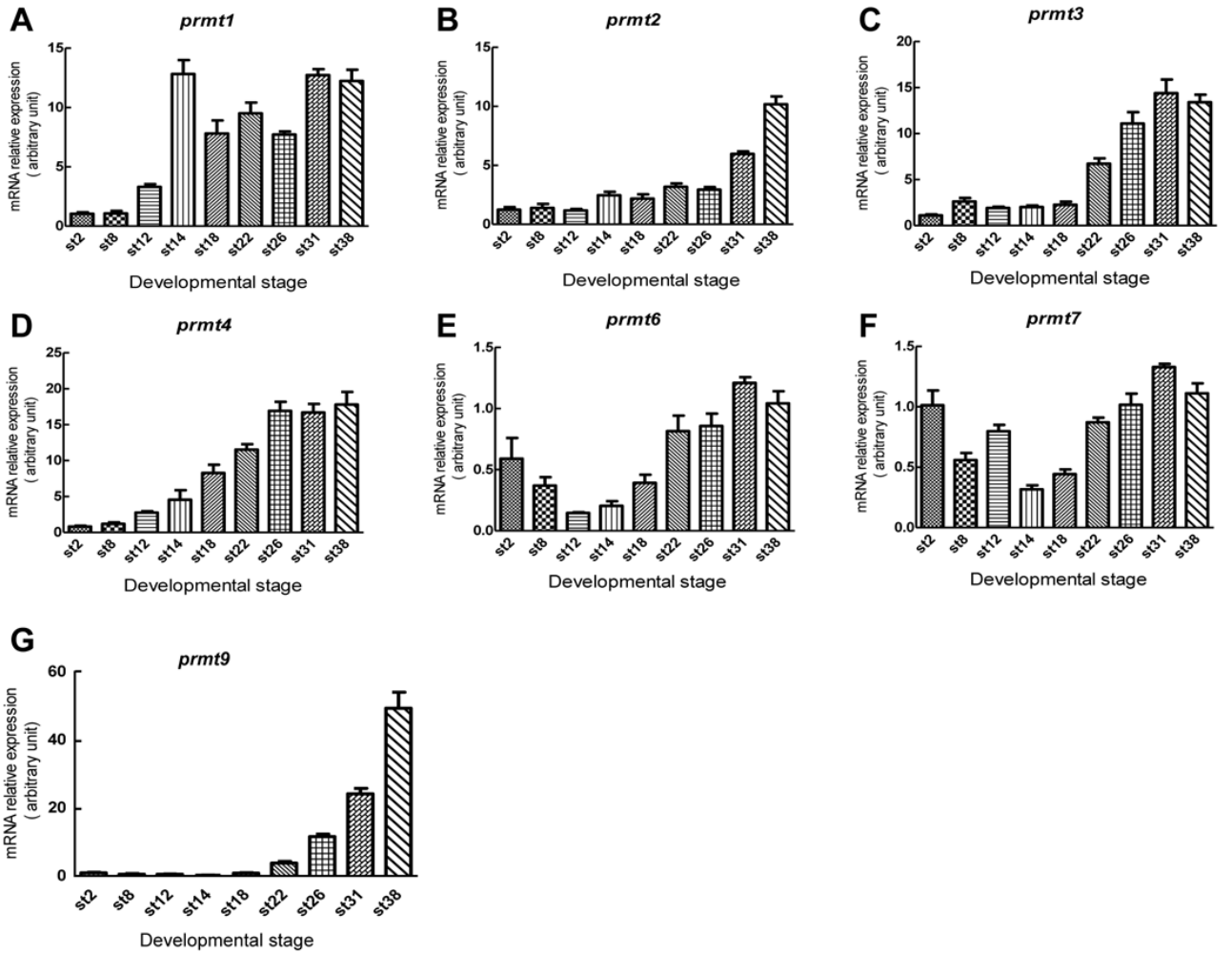

Figure 3 Quantitative RT-PCR analysis of *prmt* gene expression in *Xenopus tropicalis* embryos

mRNA expression levels of *Xenopus prmt1–4* (A–D), *prmt6* (E), *prmt7* (F), and *prmt9* (G) were measured in different embryonic stages, including cleavage (stage 2), blastula (stage 8), gastrula (stage 12), neurula (stages 14, 18), early tailbud (stages 22, 26), and late tailbud (stages 31, 38), *ornithine decarboxylase* (*odc*) was used as an internal control.

We examined the expression patterns of three *prmt* genes during embryonic development. Our results indicated that *prmt4* and *prmt7* showed similar expression patterns. Both were expressed in the neural plate during neurulation and were then detected in the brain and spinal cord (Figure 1 and Figure 2). These data suggest that *prmt4* and *prmt7* function in neural development, similar to that found in other PRMT members (Batut et al., 2005; Hashimoto et al., 2016; Honda et al., 2017; Lee et al., 2005; Lee et al., 2017; Lin et al., 2013). Furthermore, *prmt4* and *prmt7* were both expressed in the neural crest, which has not been reported previously. Apart from the brain, *prmt4* and *prmt7* were also expressed in other regions of the head, including the eye and branchial arches. At the late tailbud stage, both were detected in the olfactory placode, pharyngeal arches, and heart regions (Figure 1K, N–R; Figure 2F, J–L). In zebrafish, the expression of *prmt8* has also been detected in the heart at the later stages (Lin et al., 2013). Here, weak *prmt4* signals were detected in the paraxial mesoderm (Figure 1M), whereas *prmt7* was evidently expressed in the somites (Figure 2C, G). These results are in agreement with their potential roles in myogenesis,

which have been studied to some extent in zebrafish (Batut et al., 2011). In addition, *prmt4* and *prmt7* also shared similar temporal expression patterns at the neurula and tailbud stages when their expression levels were gradually up-regulated (Figure 3D, F). The high similarity in expression patterns between *prmt4* and *prmt7* implies that different members of the PRMT family may have redundant roles in regulating early embryonic development. Compared with other examined *prmt* genes, *prmt9* exhibited a distinct temporal expression pattern. Its expression level was very low before the early tailbud stage but was dramatically elevated from the late tailbud stage (Figure 3G). This is in line with the *in situ* hybridization results, in which specific *prmt9* signals were not detected until the late tailbud stage. Although prmt9 is a non-histone methyltransferase involved in regulating RNA splicing (Yang et al., 2015), whether the special expression pattern of *prmt9* is related to its role in RNA splicing remains to be illustrated. This study will facilitate further functional study of *prmt* genes during embryonic development.

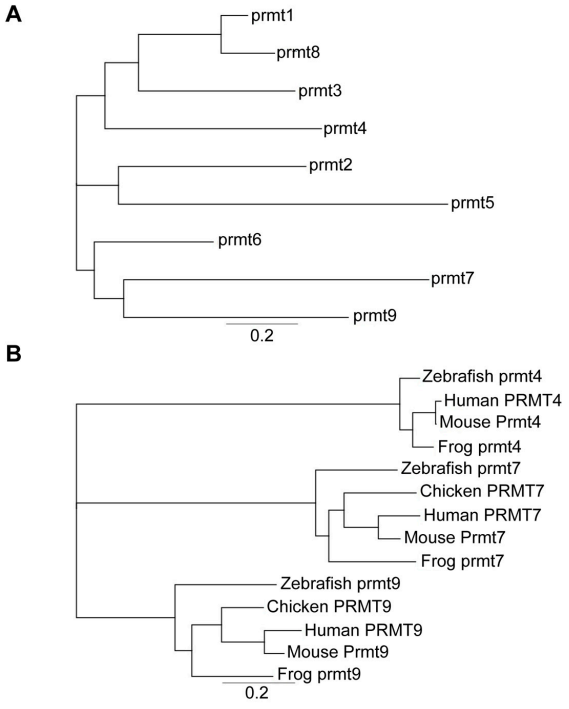

Figure 4 Phylogenetic analysis of prmt proteins
A: prmt1–9 proteins of *Xenopus tropicalis*. B: prmt4, prmt7, and prmt9 proteins from humans (*Homo sapiens*), mice (*Mus musculus*), chickens (*Gallus gallus*), frogs (*Xenopus tropicalis*), and zebrafish *(Danio rerio*).

COMPETING INTERESTS

The authors declare that they have no competing interests.

AUTHORS' CONTRIBUTIONS

H.Z. designed the study and supervised the project. C.D.W., X.F.G., T.C.B.W. and H.W. performed the whole-mount *in situ* hybridization. T.C.B.W. did vibratome sectioning on the stained embryos. C.D.W. made phylogenic analysis on prmt members. X.F.G did quantitative RT-PCR to analyze expression of prmt genes. C.D.W., X.F.G and H.Z. analyzed the results. C.D.W and X.F.G wrote the manuscript with input from all authors. X.F.Q., D.Q.C., Y.D., and H.Z. revised the manuscript. All authors read and approved the final version of the manuscript.

ACKNOWLEDGEMENTS

We thank our laboratory colleagues for helpful discussion on this project.

Cheng-Dong Wang[1,#], Xiao-Fang Guo[2,5,#], Thomas Chi Bun Wong[1], Hui Wang[1], Xu-Feng Qi[2,5], Dong-Qing Cai[2,5], Yi Deng[3], Hui Zhao[1,4,*]

[1] *Key Laboratory for Regenerative Medicine, Ministry of Education, School of Biomedical Sciences, Faculty of Medicine, The Chinese University of Hong Kong, Hong Kong SAR, China*
[2] *Key Laboratory for Regenerative Medicine of Ministry of Education, Jinan University, Guangzhou Guangdong* 510632, *China*
[3] *Guangdong Provincial Key Laboratory of Cell Microenvironment, Department of Biology, South University of Science and Technology of China, Shenzhen Guangdong* 518055, *China*
[4] *Kunming Institute of Zoology, Chinese Academy of Sciences-The Chinese University of Hong Kong Joint Laboratory of Bioresources and Molecular Research of Common Diseases, Hong Kong SAR, China*
[5] *Department of Developmental & Regenerative Biology, College of Life Science and Technology, Jinan University, Guangzhou Guangdong* 510632, *China*
[#]Authors contributed equally to this work
[*]Corresponding author, E-mail: zhaohui@cuhk.edu.hk

REFERENCES

Batut J, Duboé C, Vandel L. 2011. The methyltransferases PRMT4/CARM1 and PRMT5 control differentially myogenesis in zebrafish. *PLoS One*, **6**(10): e25427.

Batut J, Vandel L, Leclerc C, Daguzan C, Moreau M, Néant I. 2005. The Ca^{2+}-induced methyltransferase xPRMT1b controls neural fate in amphibian embryo. *Proceedings of the National Academy of Sciences of the United States of America*, **102**(42): 15128–15133.

Biggar KK, Li SS. 2015. Non-histone protein methylation as a regulator of cellular signalling and function. *Nature Reviews, Molecular Cell Biology*, **16**(1): 5–17.

Blanc RS, Vogel G, Chen T, Crist C, Richard S. 2016. PRMT7 preserves satellite cell regenerative capacity. *Cell Reports*, **14**(6): 1528–1539.

Carr SM, Poppy Roworth A, Chan C, La Thangue NB. 2015. Post-translational control of transcription factors: Methylation ranks highly. *The FEBS Journal*, **282**(23): 4450–4465.

Cook JR, Lee JH, Yang ZH, Krause CD, Herth N, Hoffmann R, Pestka S. 2006. FBXO11/PRMT9, a new protein arginine methyltransferase, symmetrically dimethylates arginine residues. *Biochemical and Biophysical Research Communications*, **342**(2): 472–481.

Feng Y, Hadjikyriacou A, Clarke SG. 2014. Substrate specificity of human protein arginine methyltransferase 7(PRMT7): The importance of acidic

residues in the double E loop. *The Journal of Biological Chemistry*, **289**(47): 32604–32616.

Feng Y, Maity R, Whitelegge JP, Hadjikyriacou A, Li Z, Zurita-Lopez C, Al-Hadid Q, Clark AT, Bedford MT, Masson JY, Clarke SG. 2013. Mammalian protein arginine methyltransferase 7(PRMT7) specifically targets RXR sites in lysine- and arginine-rich regions. *The Journal of Biological Chemistry*, **288**(52): 37010–37025.

Harland RM. 1991. In situ hybridization: an improved whole-mount method for *Xenopus* embryos. *Methods in Cell Biology*, **36**: 685–695.

Harland RM, Grainger RM. 2011. *Xenopus* research: Metamorphosed by genetics and genomics. *Trends in Genetics*, **27**(12): 507–515.

Hashimoto M, Murata K, Ishida J, Kanou A, Kasuya Y, Fukamizu A. 2016. Severe hypomyelination and developmental defects are caused in mice lacking protein arginine methyltransferase 1(PRMT1) in the central nervous system. *The Journal of Biological Chemistry*, **291**(5): 2237–2245.

Herrmann F, Pably P, Eckerich C, Bedford MT, Fackelmayer FO. 2009. Human protein arginine methyltransferases in vivo–distinct properties of eight canonical members of the PRMT family. *Journal of Cell Science*, **122**(Pt 5): 667–677.

Honda M, Nakashima K, Katada S. 2017. PRMT1 regulates astrocytic differentiation of embryonic neural stem/precursor cells. *Journal of Neurochemistry*, **142**(6): 901–908.

Kam RK, Chen Y, Chan SO, Chan WY, Dawid IB, Zhao H. 2010. Developmental expression of *Xenopus* short-chain dehydrogenase/reductase 3. *The International Journal of Developmental Biology*, **54**(8–9): 1355–1360.

Kim KY, Wang DH, Campbell M, Huerta SB, Shevchenko B, Izumiya C, Izumiya Y. 2015. PRMT4-mediated arginine methylation negatively regulates retinoblastoma tumor suppressor protein and promotes E2F-1 dissociation. *Molecular and Cellular Biology*, **35**(1): 238–248.

Lee J, Sayegh J, Daniel J, Clarke S, Bedford MT. 2005. PRMT8, a new membrane-bound tissue-specific member of the protein arginine methyltransferase family. *The Journal of Biological Chemistry*, **280**(38): 32890–32896.

Lee PK, Goh WW, Sng JC. 2017. Network-based characterization of the synaptic proteome reveals that removal of epigenetic regulator Prmt8 restricts proteins associated with synaptic maturation. *Journal of Neurochemistry*, **140**(4): 613–628.

Lin YL, Tsai YJ, Liu YF, Cheng YC, Hung CM, Lee YJ, Pan H, Li C. 2013. The critical role of protein arginine methyltransferase *prmt8* in zebrafish embryonic and neural development is non-redundant with its paralogue prmt1. *PLoS One*, **8**(3): e55221.

Mallappa C, Hu YJ, Shamulailatpam P, Tae S, Sif S, Imbalzano AN. 2011. The expression of myogenic microRNAs indirectly requires protein arginine methyltransferase(Prmt)5 but directly requires *Prmt4*. *Nucleic Acids Research*, **39**(4): 1243–1255.

Walsh G, Jefferis R. 2006. Post-translational modifications in the context of therapeutic proteins. *Nature Biotechnology*, **24**(10): 1241–1252.

Wang C, Liu Y, Chan WY, Chan SO, Grunz H, Zhao H. 2011. Characterization of three synuclein genes in *Xenopus laevis*. *Developmental Dynamics* , **240**(8): 2028–2033.

Yang Y, Bedford MT. 2013. Protein arginine methyltransferases and cancer. *Nature Reviews, Cancer*, **13**(1): 37–50.

Yang Y, Hadjikyriacou A, Xia Z, Gayatri S, Kim D, Zurita-Lopez C, Kelly R, Guo A, Li W, Clarke SG, Bedford MT. 2015. PRMT9 is a type II methyltransferase that methylates the splicing factor SAP145. *Nature Communications*, **6**: 6428.

Marker-assisted selection of YY supermales from a genetically improved farmed tilapia-derived strain

DEAR EDITOR,

Genetically improved farmed tilapia (GIFT) and GIFT-derived strains account for the majority of farmed tilapia worldwide. As male tilapias grow much faster than females, they are often considered more desirable in the aquacultural industry. Sex reversal of females to males using the male sex hormone 17-α-methyltestosterone (MT) is generally used to induce phenotypic males during large-scale production of all male fingerlings. However, the widespread use of large quantities of sex reversal hormone in hatcheries may pose a health risk to workers and ecological threats to surrounding environments. Breeding procedures to produce genetically all-male tilapia with limited or no use of sex hormones are therefore urgently needed. In this study, by applying marker-assisted selection (MAS) for the selection of YY supermales from a GIFT-derived strain, we identified 24 XY pseudofemale and 431 YY supermale tilapias. Further performance evaluation on the progenies of the YY supermales resulted in male rates of 94.1%, 99.5% and 99.6%, respectively, in three populations, and a daily increase in body weight of 1.4 g at 3 months (n=997). Our study established a highly effective MAS procedure in the selection of YY supermales from a GIFT-derived strain. Furthermore, the development of MAS-selected YY supermales will help reduce the utilization of hormones for controlling sex in the tilapia aquaculture.

Tilapia is the second most important fish species in the global aquaculture industry after carp (FAO, 2010). China is the world's largest tilapia producer, with total production of 1.87 million metric tons (MMT) in 2016, and is expected to exceed 1.9 MMT in 2017 (Bureau of Fisheries of the Ministry of Agriculture, 2018). Total tilapia exports could reach 875 000 tons, accounting for 45% of total tilapia production in 2017 (Bureau of Fisheries of the Ministry of Agriculture, 2018).

Several species of tilapia (such as Nile tilapia, *Oreochromis niloticus*, blue tilapia, *Oreochromis aureus* and Mozambique tilapia, *Oreochromis mossambicus*) are cultured commercially. Genetically improved farmed tilapia (GIFT) and GIFT-derived strains are the predominant cultured tilapia strains worldwide due to their faster growth rates, higher survival rates, shorter harvest time, and dramatically increased yields (ADB, 2005; Van Bers et al., 2012).

Male GIFT grow much faster than females. In mixed-sexed populations, uncontrolled reproduction leads to excessive recruitment of fingerlings, competition for food, and stunting of the original stock. Therefore, sex reversal of females to males is desirable in tilapia aquaculture. The male sex hormone 17-α-methyltestosterone (MT) is often used to induce phenotypic males. However, widespread use of large quantities of sex reversal hormone in hatcheries may pose a health risk to workers (Mair, 1997) and an ecological threat to the surrounding environment. Therefore, breeding procedures to produce genetically all-male tilapia with lower or no use of sex hormone are urgently needed.

Tilapia mossambica YY supermales were originally produced by crossing sex-reversed XY pseudofemales obtained by hormone treatment with normal XY males (Mair, 1988, 1997), with the supermales then identified by progeny testing. However, this breeding process was highly time-consuming. In contrast, marker-assisted selection (MAS) can greatly improve selection efficiency compared with traditional methods using markers closely linked to economic traits (Rishell, 1997). Sex-linked markers in tilapia have been identified on LG1 (Palaiokostas et al., 2013), LG3 (Cnaani & Kocher, 2008), LG8 (Lee et al., 2003), LG22 (Liu et al., 2013) and LG23 (Eshel et al., 2011; Sun et al., 2014), thus providing a solid basis for applying MAS in the sex control of tilapia (Chen et al., 2018). YY supermales from Nile tilapia have been identified using sex-linked markers, with the YY progeny reported to be 100% male (Li & Wang, 2017). These suggests it is possible to produce YY supermales by MAS in tilapia breeding.

GIFT and GIFT-derived strains are the most commonly farmed tilapia in the world, with much higher market value than unselected Nile tilapia (Bureau of Fisheries of the Ministry of Agriculture, 2018; ADB, 2005). However, no GIFT-derived strain fingerlings selected using MAS are currently available in the seed market. In this study, we reported on the selection of more than 400 YY supermales from a GIFT-derived strain using MAS. The new GIFT-derived YY supermale populations

Received: 20 June 2018; Accepted: 30 August 2018; Online: 6 September 2018

Foundation items: This work was supported by the Special Fund for Marine Fisheries-Scientific Research of Guangdong Province (A201501A04), Science and Technology Program of Guangzhou, China (201803020043), National Natural Science Foundation of China (31572612), and Science and Technology Planning Project of Guangdong Province, China (2017A030303008)

DOI: 10.24272/j.issn.2095-8137.2018.071

with high male offspring rates will be helpful in controlling or limiting the use of sex hormones in tilapia aquaculture.

This study was approved by the Animal Care and Use Committee from the School of Life Science at Sun Yat-Sen University.

In the hatchery, we first selected 20 large males and 20 large females from the broodstock population of nearly 500 individuals from Wulonggang Aquaculture Ltd., Guangzhou, Guangdong Province, China. One male (with red flush to head, lower body, dorsal and caudal fins) and one female (ready to spawn, showing pink to red and protruding genital papilla, fully opened genital pore, and distended abdomen) were then selected based on body size, body shape and reproductive status. One full-sib family (named WLG-Fam1-F1) was established by crossing these two individuals. The swim-up fry were divided into three experimental groups of ~500 individuals and reared in independent nursery tanks (5 m×5 m×1 m). The fry from one tank were fed normal food. The fry from the other two tanks (for sex-reversal treatment) were provided with feed treated with diethylstilbestrol (DES, Aladdin, China) at 0.5 g or 1 g per kg of feed. The DES was first dissolved with ethanol to prepare a stock solution, which was then thoroughly mixed with the feed. The dried pellets were provided to the fry twice a day from 3 d post hatchery (dph) for three weeks.

At 30 dph, the fingerlings from each group were transferred to a pond (around 1 000 m^2), respectively. The fish were fed twice daily with commercial pellets. At 120 dph, the sex phenotype and body weight of each fish was recorded, and fin samples from each fish were also collected and kept in absolute ethanol for DNA extraction and genotyping.

We used the SD marker closely linked to sex trait located on chrLG23 (forward primer: 5′-TCCCATTTAGACC ACCACACCTCAACAACA-3′; reverse primer: 5′-GTCAGAAT GCACTTTAACACAGAGATACCA-3′; patent application no.: 2016107162044) to genotype each individual. This marker was determined to be family-specific as it was not significantly associated with sex traits in another full-sib tilapia family in our pilot study. PCR amplifications were performed as per previous research (Gu et al., 2018) and were carried out in a 20-μL volume using 2× PCR mastermix, 1 ng genomic DNA, and 0.5 μmol/L forward and reverse primers (Dongsheng, China) in a BioRad cycler. The following program was applied (one cycle of 3 min at 94 ℃, 38 cycles of 30 s at 94 ℃, 30 s at 55 ℃ and 30 s at 72 ℃, followed by a final extension of 5 min at 72 ℃). The resulting PCR products were detected by electrophoresis with 6% polyacrylamide gels and silver staining. The pseudofemales (XY genotype), XX females and XY males were identified based on phenotypic sex traits and genotypic data.

We generated F2 families by crossing six pseudofemales (XY genotype) with three genetic males (XY genotype). At 120 dph, the sex of each fish was recorded, and fin samples were collected and kept in absolute ethanol for DNA extraction and genotyping. The supermales (YY genotype) were identified based on phenotypic sex traits and genotypic data of the SD marker.

Two YY supermales were randomly selected for crossing with three XX GIFT-derived females collected from the same farm. At 21 dph, around 2 000 fingerlings (0.7 g) were transferred into a pond (1 000 m^2) for maturation. The fish were fed twice daily with commercial pellets. At 89 dph, the sex of each fish was recorded, and fin samples were collected and kept in absolute ethanol for DNA extraction and genotyping. We also recorded the body weights of 61 randomly selected individuals with a weighing machine.

To test the rate of male offspring, two other populations were also generated by crossing two randomly selected YY supermales with three GIFT-derived females collected from other farms or with three GIFT-derived females collected from the same family that generated YY supermales. The sex of each fish was manually checked at 240 dph.

We harvested 1 356 F1 generation individuals (WLG-Fam1-F1) from the three groups (Table 1). In group 1 (treated with 1 g DES/kg feed), all individuals (n=330) were female (100%). In group 2 (treated with 0.5 g DES/kg feed), we found 371 of the 390 individuals were phenotypically female (95%). In contrast, the female rate (n=636) was only 30% in the control group (no DES treatment). These data suggest the DES treatment was highly effective for sex reversal in this study.

Table 1 Summary information on sex reversal of the F1 generation

Group	DES (g)/feed (kg)	Individual number (n)	Female	Male	Intersex	Female rate (%)
Group1	1	330	330	0	0	100
Group2	0.5	390	371	6	13	95
Control	No DES	636	190	446	0	30
Total	N/A	1 356	891	452	13	N/A

N/A: Not available.

Based on the sex phenotype and body weight (data not provided), 73 faster-growing females from WLG-Fam1-F1 were selected for genotyping using the SD marker closely linked to sex trait previously developed in our lab. From this female population, 24 XY pseudofemales were finally identified. Genotyping of the female population is shown in Figure 1A.

Six XY pseudofemales were then crossed with three XY males to generate the F2 generation (WLG-F1-F2). At 120 dph, we harvested 1 770 adult male tilapias from the WLG-Fam1-F2 population. Genotypic analysis using the SD marker indicated that 431 males had the YY genotype and the remaining males had the XY genotype. Genotyping of the WLG-F1-F2 population is shown in Figure 1B. Surprisingly, the YY rate in the male population was around 25%, which is lower than the expected rate (~33%). In addition, we randomly measured the body weights of 40 individuals with the YY, XY and XX genotypes, respectively. The average body weight for the YY supermales was the lowest (average 69.5±23.89 g), followed by the XX females (77.1±38.07 g) and normal XY males (94.6±28.24 g). These data indicate that several unknown factors have affected the survivability and growth of

YY supermales in this study. However, additional data from different families and populations are required to clarify this in future research.

Two randomly selected YY supermales were crossed with five normal XX females collected from local farms to generate the F3 generation (WLG-Fam1-F3). At 89 dph, 994 of the 997 harvested individuals were phenotypically male and three were phenotypically female. Thus, the male rate was 99.6% in the progeny population of the YY supermales.

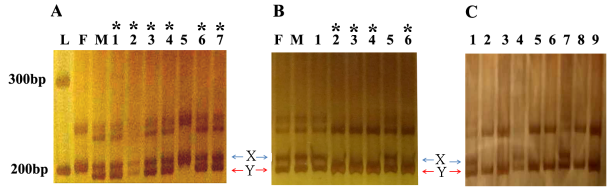

Figure 1 Genotyping of individuals during marker-assisted selection using the sex-linked marker SD

A: Screening of pseudofemales. L: ladder; "F" and "M" indicate female and male parents, respectively; lanes 1 to 7 indicate seven randomly selected female individuals from WLG-F1-F1; band "Y" is the male-specific band and band "X" is the female band. A symbol "*" indicates pseudofemale detected in the F1 population. B: Screening of YY supermales. "F" and "M" indicate XY pseudofemale and XY male parents, respectively; lanes 1 to 6 indicate six randomly selected male individuals from WLG-F1-F2; band "Y" is male-specific band and band "X" is female band. A symbol "*" indicates YY supermales identified in the F2 population. C: Genotyping analysis of all-male offspring produced using YY supermales with XX females. Lanes 1 to 9 indicate nine randomly selected all-male offspring from WLG-F1-F3; band "Y" is male-specific band.

We randomly collected fin samples from 61 phenotypic males for genotyping with the SD marker. Results demonstrated that all phenotypic male progenies possessed a male-specific band 'Y' (Figure 1C), thus indicating the reliability of the GIFT-derived strain YY supermales in this study. The average body weight for the 61 individuals was 117±14.9 g (Figure 2) and the daily increase in body weight was around 1.4 g. These data are comparable to the values reported in previous studies; for example, the daily increase in body weight at 3 months for a GIFT strain in Guangxi Province, China was reported to be 1.4–1.6 g (Tand et al., 2011). Thus, in the current study, the F3 all-male offspring grew as quickly as the normal GIFT strain and the differences among individual body weights were small, which would be advantageous for tilapia aquaculture.

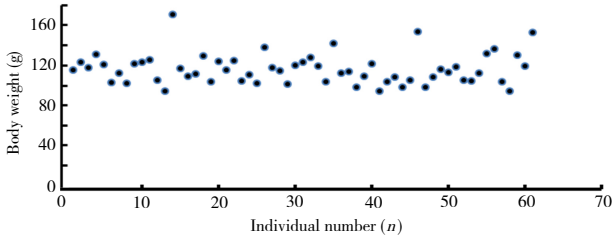

Figure 2 Distribution of body weight (g) among 61 all-male offspring from WLG-Fam1-F3 at 89 dph

To test the reliability of the YY supermales, two other populations were constructed by crossing YY supermales with females collected from other farms or from the same family generating YY supermales. We observed a male rate of 99.5% for the population (n=200) generated using females from other farms and 94.1% for the population (n=187) generated using females from the same family as YY supermales. Thus, these results again show that the offspring developed here are highly suitable for tilapia aquaculture.

The threat of environmental hormones has emerged as a worldwide concern, and can disrupt the central nervous system, pituitary integration of hormonal and sexual behavior, female and male reproductive system development and function, and thyroid function (Crisp et al., 1998). MT is a synthetic male hormone widely used in animal products to promote weight gain. There are no reports showing that MT treatment of tilapia affects human health, provided it is applied only during the early fry stage at the recommended dosage. However, widespread use of large quantities of sex reversal hormones in hatcheries may pose a health risk to workers (Mair, 1997) and cause potential hormone contamination to surrounding environments due to the release of wastewater from tilapia production facilities that utilize MT treatment. Sex control for the production of all-male tilapia in breeding procedures is considered to be a potential solution to the problem.

The GIFT program successfully resulted in an accumulated response of 85% after six generations of selection (Eknath et al., 1998). Currently, more than 100 countries now farm tilapia (FAO, 2013), with GIFT or GIFT-derived strains the major cultured tilapia strains worldwide. For example, in the Philippines, 70% of farmed tilapia are either GIFT or of GIFT-derived origin (ADB, 2005).

Previous studies have shown that GIFT or GIFT-derived strains possess diverse genetic sources that are different from the Nile tilapia. Founders of GIFT strains are composed of eight different populations of Nile tilapia (four wild tilapia populations from Egypt, Ghana, Kenya, and Senegal and four farmed populations from Israel, Singapore, Taiwan, and Thailand) (Van Bers et al., 2012). Genetic analysis has shown that the development of many GIFT or GIFT-derived strains has led to the coexistence of different varieties and levels of hybridization among stocks (McKinna et al., 2010; Xia et al., 2014). Previous mtDNA analysis of a Fijian GIFT strain and WorldFish Centre strain revealed introgression of two *Oreochromis* species (*O. mossambicus* and *O. aureus*) to the GIFT strain, which is considered to be an improved line to the Nile tilapia (McKinna et al., 2010). Our previous study also suggested slight introgression from Mozambique tilapia to the GIFT strain, with GIFT and Nile tilapia significantly and genetically differentiated from red tilapia and Mozambique tilapia (Xia et al., 2014). These findings provide good explanation for their differences in economic traits.

Efforts to select YY supermale tilapia have been conducted previously (Li & Wang, 2017; Yang et al., 1980). However, the commercial production of MAS-selected all-male tilapia is not available currently in China. In our study, we focused on the MAS of YY supermales from a GIFT-derived strain.

Using a sex-linked marker, we selected 24 pseudofemales (XY genotype) from 73 females and 431 supermales (YY genotype) from 1 770 adult males from the WLG-F1-F2 population. From the three offspring populations of the YY supermales, male offspring rates were 94.1%, 99.5% and 99.6%, respectively. Previous studies on tilapia have shown that the mean percentage of males obtained by MT treatment is 68% to 99% (Kohinoor et al., 2003; Shamsuddin et al., 2012), whereas YY progenies are 100% male in MAS selection (Li & Wang, 2017). Therefore, the male rates observed in our study are comparable to the results of former studies. Furthermore, we observed a daily increase in body weight of around 1.4 g, which is also comparable to the values reported in previous studies. For example, the daily increase in body weight at 3 months for a GIFT strain from Guangxi Province, China, was reported to be 1.4–1.6 g (Tand et al., 2011). Thus, our study indicates the YY supermales are suitable for production of aquaculture seeds.

However, in the control group identifying pseudofemales, we observed that ~30% of the progeny were females. Thus, the sex segregation ratio of female:male was ~3:7. This suggests a male priority for sex determination/differentiation under the environmental conditions. Temperature is one of the most important environmental factors that influence sexual determination in tilapia. Although low temperature treatment (18 ℃) is not generally effective at influencing sex ratios (Tessema et al., 2006), previous research has shown that at high temperatures, 91.2% of progeny exhibited an excess of males in three populations of Nile tilapia (Bezault et al., 2007). Another study further indicated that when the water temperature increased from 25 ℃ to 35 ℃, the male ratio significantly increased from 52.47% to 75.91% after one week of rearing (Khater et al., 2017). In the current study, progenies were raised in outdoor tanks and ponds during early development, without water temperature control. Therefore, in the field test of YY progenies, the male rates of 94%–99.6% were likely to be overestimated due to the temperature effect on the sex determination. Nevertheless, it has been suggested that thermal effects are secondary to genetics in zebrafish, as sex ratio only changes at extreme water temperatures (Ospina-Álvarez & Piferrer, 2008). To clearly address the environmental effects on the male offspring rate, a control group under the same environmental conditions should be established in the future.

MAS has only been applied in very limited aquaculture species, such as selection of resistance to lymphocystis disease in Japanese flounders and resistance to infectious pancreatic necrosis (IPN) in salmon (Yue, 2014). Our study, as well as that of Li & Wang (2017), indicate that MAS can be highly valuable for sex control in tilapia. Currently, in addition to sex determination traits (Eshel et al., 2011; Lee et al., 2003, 2004; Shirak et al., 2006), many quantitative trait loci controlling other economically beneficial traits have been mapped for tilapia, e.g., body size (Cnaani et al., 2004), temperature tolerance (Cnaani et al., 2003), general disease resistance and immune response (Cnaani et al., 2004), body color (Lee et al., 2005), salinity tolerance (Gu et al., 2018; Rengmark et al., 2007) and hypoxia stress (Li et al., 2017). These data provide a cost-effective starting point to search for markers closely linked to economic traits within breeding populations. Therefore, we would expect greater application of MAS in commercial breeding programs in the tilapia aquaculture industry in the future.

By applying MAS for the selection of supermale GIFT-derived strains, we established a set of MAS procedures and obtained more than 400 YY supermales. Analysis of the progeny rates indicated the reliability of the YY supermales. Further systematic evaluation of the mating strategies with different sources of females will help speed up the commercial production of all-male seeds.

COMPETING INTERESTS

The authors declare that they have no competing interests.

AUTHORS' CONTRIBUTIONS

J.H.X. and H.R.L. contributed to project conception. Experimental and data analyses were conducted by J.H.X., C.H.C., B.J.L. and X.H.G. The manuscript was prepared by J.H.X. and C.H.C. All authors read and approved the final version of the manuscript.

Chao-Hao Chen[1], Bi-Jun Li[1], Xiao-Hui Gu[1], Hao-Ran Lin[1], Jun-Hong Xia[1,*]

[1] *State Key Laboratory of Biocontrol, Institute of Aquatic Economic Animals and Guangdong Provincial Key Laboratory for Aquatic Economic Animals, College of Life Sciences, Sun Yat-Sen University, Guangzhou Guangdong* 510275, *China*

[*]Corresponding author, E-mail: xiajunh3@mail.sysu.edu.cn

REFERENCES

Asian Development Bank (ADB). 2005. An Impact Evaluation of the Development of Genetically Improved Farmed Tilapia and Their Dissemination in Selected Countries. Manila, Philippines, 124.

Bezault E, Clota F, Derivaz M, Chevassus B, Baroiller JF. 2007. Sex determination and temperature-induced sex differentiation in three natural populations of Nile tilapia (*Oreochromis niloticus*) adapted to extreme temperature conditions. *Aquaculture,* **272**(1): S3–S16.

Chen J, Tan D, Wang D, Jiang D, Fan Z. 2018. A review of genetic advances related to sex control and manipulation in tilapia. *Journal of the World Aquaculture Society,* **49**(2): 277–291.

Bureau of Fisheries of the Ministry of Agriculture. 2018. China's Fishery Annual 2017. Beijing: China Agricultural Press, China, 25.

Cnaani A, Hallerman EM, Ron M, Weller J, Indelman M, Kashi Y, Gall G, Hulata G. 2003. Detection of a chromosomal region with two quantitative trait loci, affecting cold tolerance and fish size, in an F_2 tilapia hybrid. *Aquaculture,* **223**(1–4): 117–128.

Cnaani A, Kocher TD. 2008. Sex-linkedmarkers and microsatellite locus duplication in the cichlid species *Oreochromis tanganicae*. *Biology Letters,* **4**(6): 700–703.

Cnaani A, Zilberman N, Tinman S, Hulata G, Ron M. 2004. Genome-scan analysis for quantitative trait loci in an F_2 tilapia hybrid. *Molecular Genetics and Genomics* **272**(2): 162–172.

Crisp TM, Clegg ED, Cooper RL, Wood WP, Anderson DG, Baetcke KP, Hoffmann JL, Morrow MS, Rodier DJ, Schaeffer JE, Touart LW, Zeeman MG, Patel YM. 1998. Environmental endocrine disruption: an effects assessment and analysis. *Environmental Health Perspectives,* **106**(Suppl 1): 11–56.

Eknath AE, Dey MM, Rye M, Gjerde B, Abella TA, Sevilleja R, Tayamen MM, Reyes RA, Bentsen HB. 1998. Selective breeding of Nile tilapia for Asia. Proceedings of the 6th World Congress on Genetics Applied to Livestock Production (vol. 27). University of New England, Armidale, Australia, 89–96.

Eshel O, Shirak A, Weller JI, Hulata G, Ron M. 2012. Linkage and physical mapping of sex region on LG23 of Nile tilapia (*Oreochromis niloticus*). *Genes, Genomes, Genetics,* **2**(1): 35–42.

Eshel O, Shirak A, Weller JI, Slossman T, Hulata G, Cnaani A, Ron M. 2011. Fine-mapping of a locus on linkage group 23 for sex determination in Nile tilapia (*Oreochromis niloticus*). *Animal Genetics,* **42**(2): 222–224.

Food and Agriculture Organization of the United Nations (FAO). 2010. Cultured aquatic species information programme, *Oreochromis niloticus* (Linnaeus,1758). http://www.fao.org/fishery/culturedspecies/*Oreochromis_niloticus*/en.

Food and Agriculture Organization of the United Nations (FAO). 2013. FAO FishStatJ: a tool for Fishery Statistics Analysis. Available at: http://www.fao.org/fishery/statistics.

Gu XH, Jiang DL, Huang Y, Li BJ, Chen CH, Lin HR, Xia JH. 2018. Identifying a major QTL associated with salinity tolerance in Nile tilapia using QTL-Seq. *Marine Biotechnology,* **20**(1): 98–107.

Khater EG, Ali SA, Mohamed WE. 2017. Effect of water temperature on masculinization and growth of Nile tilapia fish. *Journal of Aquaculture Research and Development,* **8**(9): 507.

Kohinoor AHM, Islam MS, Mazid MA, Hussain MG. 2003. Breeding biology and monosex male seed production of Genetically Improved Farmed Tilapia (GIFT) strain of *Oreochromis niloticus* L. in Bangladesh. *Bangladesh Journal of Fisheries Research,* **7**(2): 105–114.

Lee BY, Hulata G, Kocher TD. 2004. Two unlinked loci controlling the sex of blue tilapia (*Oreochromis aureus*). *Heredity,* **92**(6): 543–549.

Lee BY, Lee WJ, Streelman JT, Carleton KL, Howe AE, Hulata G, Slettan A, Stern JE, Terai Y, Kocher TD. 2005. A second-generation genetic linkage map of tilapia (*Oreochromis* spp.). *Genetics,* **170**(1): 237–244.

Lee BY, Penman D, Kocher TD. 2003. Identification of a sex-determining region in Nile tilapia (*Oreochromis niloticus*) using bulked segregant analysis. *Animal Genetics,* **34**(5): 379–383.

Li HL, Gu XH, Li BJ, Chen CH, Lin HR, Xia JH. 2017. Genome-wide QTL analysis identified significant associations between hypoxia tolerance and mutations in the GPR132 and ABCG4 genes in Nile tilapia. *Marine Biotechnology (New York, N.Y.),* **19**(5): 441–453.

Li MH, Wang DS. 2017. Gene editing nuclease and its application in tilapia. *Science Bulletin,* **62**(3): 165–173.

Liu F, Sun F, Li J, Xia JH, Lin G, Tu RJ, Yue GH. 2013. A microsatellite-based linkage map of salt tolerant tilapia (*Oreochromis mossambicus* × *Oreochromis* spp.) and mapping of sex-determining loci. *BMC Genomics,* **14**: 58.

Mair GC. 1988. Studies on sex determining mechanisms in *Oreochromis* species. Ph.D. dissertation, University of Wales, Swansea, UK, 326.

Mair GC. 1997. The problem of sexual maturity in tilapia culture, 6–13. *In*: Mair GC, Abella TA. Technoguide on the Production of Genetically Male Tilapia (GMT). Freshwater Aquaculture Center, Central Luzon State University, Nueva Ecija, Philippines.

McKinna EM, Nandlal S, Mather PB, Hurwood DA. 2010. An investigation of the possible causes for the loss of productivity in genetically improved farmed tilapia strain in Fiji: inbreeding versus wild stock introgression. *Aquaculture Research,* **41**(11): e730–e742.

Ospina-Álvarez N, Piferrer F. 2008. Temperature-dependent sex determination in fish revisited: prevalence, a single sex ratio response pattern, and possible effects of climate change. *PLoS One,* **3**(7): e2837.

Palaiokostas CM, Bekaert MGQ, Khan JB, Taggart K, Gharbi BJ, McAndrew JP, Penman DJ. 2013. Mapping and validation of the major sex-determining region in Nile tilapia (*Oreochromis niloticus* L.) using RAD sequencing. *PLoS One,* **8**(7): e68389.

Rengmark AH, Slettan A, Lee WJ, Lie Ø, Lingaas F. 2007. Identification and mapping of genes associated with salt tolerance in tilapia. *Journal of Fish Biology,* **71**(sc): 409–422.

Rishell WA. 1997. Symposium: Genetic selection – Strategies for the future breeding and genetics – Historical perspective. *Poultry Science,* **76**(8): 1057–1061.

Shamsuddin M, Hossain MB, Rahman MM, Asadujjaman M, Ali MY. 2012. Performance of monosex fry production of two Nile tilapia strains: GIFT and NEW GIPU. *World Journal of Fish and Marine Sciences,* **4**(1): 68–72.

Shirak A, Seroussi E, Cnaani A, Howe AE, Domokhovsky R, Zilberman N, Kocher TD, Hulata G, Ron M. 2006. Amh and Dmrta2 genes map to tilapia (*Oreochromis* spp.) linkage group 23 within quantitative trait locus regions for sex determination. *Genetics,* **174**(3): 1573–1581.

Sun YL, Jiang DN, Zeng S, Hu CJ, Ye K, Yang C, Yang SJ, Li MH, Wang DS. 2014. Screening and characterization of sex-linked DNA markers and marker-assisted selection in the Nile tilapia (*Oreochromis niloticus*). *Aquaculture,* **433**: 19–27.

Tand ZS, Lin Y, Yang HZ, Zhang YD, Chen Z, Huang Y, Peng T, Zhang Y. 2011. Growth model of GIFT strain tilapia (*Oreochromis niloticus*). *Guangdong Agricultural Sciences,* **38**(18): 104–107.

Tessema M, Muller-Belecke A, Horstgen-Schwark G. 2006. Effect of rearing temperatures on the sex ratios of *Oreochromis niloticus* populations. *Aquaculture,* **258**(1–4): 270–277.

Van Bers NE, Crooijmans RP, Groenen MA, Dibbits BW, Komen J. 2012. SNP marker detection and genotyping in tilapia. *Molecular Ecology Resources,* **12**(5): 932–941.

Xia JH, Wan ZY, NG ZL, Wang L, Fu GH, Lin G, Liu F, Yue GH. 2014. Genome-wide discovery and in silico mapping of gene-associated SNPs in Nile tilapia. *Aquaculture,* **432**: 67–73.

Yang YQ, Zhang ZY, Lin KH, Wei Y, Huang EC, Gao ZH, Xu Z, Ke SH, Wei JG. 1980. Use of three line combination for production of genetic all-male tilapia mossambica. *Acta Genetica Sinica*, **7**(3): 241–246.

Yue GH. 2014. Recent advances of genome mapping and marker-assisted selection in aquaculture. *Fish and fisheries,* **15**(3): 376–396.

Social functions of relaxed open-mouth display in golden snub-nosed monkeys (*Rhinopithecus roxellana*)

You-Ji Zhang[1,2,#], Yi-Xin Chen[1,#], Hao-Chun Chen[1], Yuan Chen[1], Hui Yao[3], Wan-Ji Yang[1,3], Xiang-Dong Ruan[4], Zuo-Fu Xiang[1,2,*]

[1] *Institute of Evolutionary Ecology and Conservation Biology, Central South University of Forestry & Technology, Changsha Hunan* 410004*, China*
[2] *College of Life Science and Technology, Central South University of Forestry and Technology, Changsha Hunan* 410004*, China*
[3] *Shennongjia National Park, Shennongjia Forest District, Shennongjia Hubei* 442411*, China*
[4] *National Forest Inventory and Design Institute, Beijing* 100714*, China*

ABSTRACT

Relaxed open-mouth display serves important social functions in relation to submission, reconciliation, affiliation and reassurance among non-human primate societies; however, quantitative evidence on this behavior remains insufficient among multi-level social groups. From July to November 2016, we examined four potential functions of the relaxed open-mouth display during pairwise, intra-unit social interactions among 18 free-ranging adult and sub-adult golden snub-nosed monkeys (*Rhinopithecus roxellana*) who belonged to three one-male, multi-female units (OMU) at Dalongtan, Shennongjia National Park, China. Results showed that: compared with no relaxed open-mouth display, (1) the occurrence of displacement by a dominant individual approaching a subordinate was lower and the distance of the subordinate to the approaching dominant was shorter when the subordinate showed open-mouth display; (2) relaxed open-mouth display reduced the probability of continued attack for victims of aggression and allowed victims to achieve closer proximity to the aggressor during post-conflict periods; (3) relaxed open-mouth display by dominant individuals allowed them to achieve closer proximity to subordinates; and (4) the exchange of relaxed open-mouth display had a greater impact on the outcome of interactions than one individual alone giving this signal. These findings suggest that relaxed open-mouth display serves important functions regarding submission, reconciliation, affiliation and reassurance in coordinating social interactions within OMUs in golden snub-nosed monkeys.

Keywords: Golden snub-nosed monkey; Open-mouth; Submission; Reconciliation; Affiliation; Reassurance

INTRODUCTION

Open-mouth display is a common social behavior in non-human primates. It comprises individuals opening their mouths and presenting their teeth or canines and can be associated with different body postures and behaviors in either hostile or relaxed scenarios (Altmann, 1962; Hinde & Rowell, 1962; Yang et al., 2013). There are diverse patterns and functions of open-mouth display among primates. In hostile scenarios, open-mouth displays are aggressive. As observed in *Macaca mulatta* and *Macaca arctoides*, open-mouth display by dominant individuals involves the slight opening of mouths and presentation of mandibles, followed by teeth chattering, pulling back of lips and orienting their heads towards subordinates while making threatening calls; if subordinates do not respond submissively, the aggression can escalate to ritualized fighting or physical attack, resulting in subordinate displacement (Altmann, 1962; Hinde & Rowell, 1962; Ren et al., 1990a).

Received: 08 April 2018; Accepted: 30 July 2018; Online: 13 August 2018

Foundation items: This study was supported by the National Natural Science Foundation of China (31670397, 31870509) and Science Foundation of the State Forestry Administration of China

[#]Authors contributed equally to this work

[*]Corresponding author, E-mail: xiangzf@csuft.edu.cn

DOI: 10.24272/j.issn.2095-8137.2018.043

In addition to the functions of aggression in hostile scenarios, researchers have noted that relaxed open-mouth displays in normal, calm or post-conflict periods are crucial in many primate species for submission, reconciliation and reassurance to coordinate social interactions, increase social tolerance and maintain group stability (Aureli, 1997; de Waal, 1986; de Waal & Luttrell, 1989; de Waal & Ren, 1988).

Until now, only a handful of studies have quantitatively tested functional hypotheses of relaxed open-mouth display in behavioral interactions among non-human primate societies. For example, within social groups of *Trachypithecus francoisi*, lower-ranked members exhibit submissive behavior when being attacked by dominant individuals, including opening mouths and showing teeth, shaking heads slightly, and keeping the body and limbs slack, to ease tension and decrease the possibility of continuous attack (Wang, 2009). In groups of *Mandrillus sphinx*, frequencies of relaxed open-mouth display and teeth chattering during post-conflict periods between two individuals are significantly higher than during pre-conflict periods, suggesting that relaxed open-mouth display may have important reconciliatory effects (Bout & Thierry, 2005). In groups of *Macaca sylvanus*, the exchange of relaxed open-mouth display (i.e., presented by both subordinate and dominant individuals) has greater impact than when one individual alone displays the signal (Wiper & Semple, 2007). Relaxed open-mouth display may also function as reassurance, a kind of affiliative signal exhibited by dominant individuals opening their mouths slightly and approaching subordinates under normal, relaxed scenarios (van Hooff, 1967; Wiper & Semple, 2007), as observed in groups of *Mandrillus sphinx* and *Macaca sylvanus* (Bout & Thierry, 2005; Wiper & Semple, 2007).

The golden snub-nosed monkey (*Rhinopithecus roxellana*) is endemic to China, inhabiting the Sichuan, Gansu, Shaanxi and Hubei provinces (Guo et al., 2007; Yao et al., 2011). This species is characterized by a multi-level society consisting of several one-male, multi-female units (OMUs), at least one all male unit (AMU), and satellite solitary males forming a large and cohesive group (Qi et al., 2014). In addition to the common function of aggression, researchers have suggested that relaxed open-mouth display in *R. roxellana* may also function in submission, reconciliation, affiliation or reassurance during normal, calm or post-conflict periods (Li et al., 2006; Ren et al., 1990b; Yan et al., 2006; Yang et al., 2013). However, these conclusions are primarily based on qualitative observations, with no current research providing quantitative evidence regarding the functions of relaxed open-mouth display in golden snub-nosed monkeys during normal, relaxed or post-conflict periods.

Here, we studied pairwise, relaxed open-mouth display in a free-ranging group of *R. roxellana* and quantitatively tested four potential functional hypotheses–i.e., submission, reconciliation, affiliation and reassurance–during normal, relaxed and post-conflict periods. We predicted that: (1) for submission, the occurrence of displacement by a dominant individual approaching a subordinate should be less frequent when the subordinate shows relaxed open-mouth display; and the risk of continued aggression by an aggressor should be reduced if the victim shows relaxed open-mouth display; (2) for affiliation, the distance from the subordinate to the approaching dominant individual should be shorter when the subordinate shows relaxed open-mouth display; (3) for reconciliation, the distance between the aggressor and victim should be closer if the victim shows relaxed open-mouth display; and (4) for reassurance, a dominant individual should be able to approach a subordinate more closely when showing relaxed open-mouth display.

MATERIALS AND METHODS

Study site and study group

We conducted the study at Dalongtan, Shennongjia National Park, Hubei, China (N31°29′65″, E110°17′93″; 2 170 m a.s.l.). The study site is comprised of highly seasonal deciduous broadleaf and conifer forest. The monthly average temperature ranges from 17.11 °C in July to –3.51 °C in January (Yao et al., 2011).

During the study period, the study group consisted of 76 individuals belonging to five OMUs and one AMU. Reserve staff have successfully habituated and provisioned this group since 2006, making close observation and individual identification possible (Yao et al., 2011). We were able to identify and name each individual based on distinct physical features of the body and face, e.g., body size, fur color, shape of nipples in females, shape of granulomatous flanges on sides of upper lip in males, and body deformities. We named each OMU based on the male leader's name (Xiang et al., 2014; Yao et al., 2011; Yu et al., 2013). Reserve staff provisioned the monkeys twice daily (1130–1200 h and 1800–1830 h, UTC+8) with lichen, pine seeds, apples, carrots, peaches and peanuts. When not provisioned, the monkeys ranged freely across an area with a radius of approximately 1 km (Xiang et al., 2014). To maximize sampling efforts due to the limited period and OMUs containing insufficient adults, we chose 18 adults and sub-adults as focal individuals (4–19 years old) from the three OMUs with the greatest number of adult females (HH, XZ, and XB, Table 1) and recorded relaxed open-mouth displays during intra-unit social interactions.

Data collection

Dominance rank

Our study was divided into two successive periods. In the first period (22 July–31 August 2016) before systematic sampling, we used an "aggression-submission" index to calculate the dominance rank of each individual within an OMU (Martin & Bateson, 1993). We observed the study group from distances of 3–20 m from 0830 h to 1130 h and 1430 h to 1730 h (UTC+8). Using all-occurrence sampling (Altmann, 1974), we recorded every incidence of "aggression-submission" as well as the initiators, recipients, and all social behaviors related to conflict (e.g., grasping, chasing, displacing, threatening, avoiding, crouching and fleeing) involving the 18 focal individuals. Due to our focus on intra-OMU pairwise interactions and to avoid biases from multi-individual alliances within or among OMUs, we only recorded intra-OMU aggressive-submissive behaviors involving two individuals.

Table 1 Aggressive and submissive behavior sampling number and rank of each individual in three focal units

Social Unit	Individual	Sex	Age	Aggressive behavior/acts	Submissive behavior/acts	Sum	Dominance index	Ranking order
HH	HH	M	Adult	37	9	46	0.94±0.03	1
	HH_2	F	Adult	33	15	48	0.79±0.16	2
	HHE	F	Adult	12	6	18	0.56±0.18	3
	YY_1	F	Adult	10	5	15	0.48±0.20	4
	DWB	F	Adult	4	3	7	0.36±0.20	5
	TJ	F	Adult	14	2	16	0.32±0.13	6
	AL	F	Sub-adult	3	0	3	0.06±0.04	7
XZ	XZ	M	Adult	38	24	62	0.92±0.04	1
	XB_2	F	Adult	36	18	54	0.80±0.15	2
	XE	F	Adult	26	12	38	0.50±0.19	3
	YB	F	Adult	24	9	33	0.41±0.15	4
	XH	F	Adult	12	8	20	0.29±0.16	5
	SB	F	Sub-adult	7	0	7	0.08±0.03	6
XB	XB	M	Adult	23	13	36	0.91±0.03	1
	GG	F	Adult	17	5	22	0.67±0.20	2
	LN	F	Adult	23	5	28	0.50±0.20	3
	SS	F	Adult	15	4	19	0.34±0.22	4
	YY_2	F	Adult	3	1	4	0.08±0.03	5
Sum				337	139	476		

M: Male; F: Female.

We defined an individual of higher rank to be dominant in each pairwise social interaction (involving two individuals only) and the lower-ranked individual to be subordinate. Similarly, when aggression occurred, we defined the one who threatened or attacked another individual to be the aggressor and the other party to be the victim. In most cases, aggressors were dominant, and victims were subordinate (Ren et al., 1990b).

During the study period, we also provisioned the 18 focal individuals with peanuts on four occasions per month to ascertain whether intra-OMU hierarchy remaining unchanged, i.e., the "nut test" (Prud'Homme, 1991; Wiper & Semple, 2007). In the test, we positioned peanuts, a highly favored food item, at a point equidistant from two individuals to invoke a dominance-based interaction and assumed the individual who approached and ate the peanut to be the dominant of the two (Prud'Homme, 1991; Wiper & Semple, 2007). To minimize bias, we repeated the nut test three times on each occasion when we were unsure of the intra-OMU hierarchy.

Relaxed open-mouth display and related behavior definitions

Based on the dominance rank data obtained in the first period, during the second period (1 September–4 November 2016) we used focal animal sampling (Altmann, 1974) to record relaxed open-mouth displays of each focal individual for 30 min between 0830–1130 h and 1430–1730 h per day (UTC+8).

Focal animal sampling began when one individual approached the focal individual to within 5 m or the focal individual moved toward another individual within 5 m with eye contact (Wiper & Semple, 2007). We simultaneously recorded the identities of the two individuals who approached each other, whether displacement, aggression or continued aggression occurred, the presence or absence of relaxed open-mouth display, and the closest distance between the two individuals.

We defined relaxed open-mouth display as an instance when an individual slightly opened mouth without presenting canines, with an associated relaxation of limbs, head, neck and shoulders (Ren et al., 1990b) (Figure 1A, B). Furthermore, during such action, the individual could approach another OMU member with only slight communicative calls rather than threatening sounds (Li et al., 1993). We considered both individuals exhibiting these actions as an "exchange of relaxed open-mouth display" (Wiper & Semple, 2007).

Additionally, we defined the related behavioral patterns and hypothesized functions as follows:

Aggression: aggressors threatened and attacked victims by opening their mouths aggressively and staring, while tightening their head, neck, shoulder and limb muscles and initiating warning calls (Figure 2A, B). Ritualized fighting or physical attack could occur if victims did not respond submissively (Cui et al., 2014; Li et al., 2013).

Post-conflict period: a period lasting up to 10 min after aggressors completely ceased threatening or attacking victims. During this period, relaxed open-mouth display and submissive behaviors, especially exhibited by victims, eased tension and individuals gradually returned to a relaxed or normal status (Ren et al., 1991).

Figure 1 Relaxed open-mouth display in golden snub-nosed monkeys (*Rhinopithecus roxellana*) during normal, relaxed or post-conflict periods

Canines are not presented. A: Male; B: Female. Photo by You-Ji Zhang.

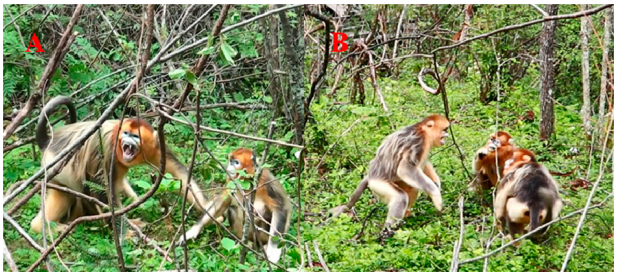

Figure 2 Aggressive open-mouth display in golden snub-nosed monkeys (*Rhinopithecus roxellana*) during hostile scenarios

Canines are presented, facial expressions and body postures are aggressive. A: Male; B: Female. Photo by You-Ji Zhang.

Continued aggression: aggressors continued to threaten or attack victims after the initial aggression occurred, even if victims exhibited relaxed open-mouth display and submissive behaviors. Continued aggression could occur subsequently after the initial aggression or could erupt anytime within 10 min of the post-conflict period (Ren et al., 1991). It could be relentless aggressive behavior or the escalation of aggression from threat to ritualized fight, even physical attack.

Displacement: a higher-ranking individual displaced a lower-ranking individual to occupy a superior position (such as a cool, warm or feeding place). During displacement, the subordinate typically showed evasive behavior and surrendered a food resource or favored site when the dominant individual approached (Yan et al., 2006).

Submission: a series of behaviors performed by victims to prevent continued aggression, including opening their mouths and showing teeth, slightly shaking their heads, and keeping their body and limbs slack (Li et al., 2013; Wang, 2009).

Affiliation: friendly contact between individuals to maintain group balance (Ren et al., 1990b). Subordinates slightly opened their mouths or both subordinates and dominants exchanged relaxed open-mouth display to attain a closer distance and ease tension in the OMU.

Reconciliation: any affiliative contact between former opponents within 10 min after a conflict ceased (Ren et al., 1991). The function of reconciliation behavior is thought to be a recovery mechanism of the social relationship between the two opponents (de Waal & van Roosmalen, 1979).

Reassurance: dominant individuals actively and firstly opened their mouths without presenting canines to reduce the risk of aggression perceived by subordinates in post-conflict or relaxed periods. Reassurance is a form of affiliation but is considered separately as the dominant individual, rather than the subordinate, is the key signaler (Wiper & Semple, 2007).

Finally, relaxed open-mouth display in this study (Figure 1A, B) was quite different from "aggressive open-mouth display" in behavioral patterns (Figure 2A, B), although the latter is ubiquitous among *Rhinopithecus* species (*R. roxellana*: Ren et al., 1991; Yang et al., 2013; *R. bieti*: Li et al., 2013; *R. brelichi*: Cui et al., 2014).

Data analysis

Analysis of dominance rank

We adopted the dominance index to explore the intra-OMU dominance rank of the 18 focal individuals using four steps (Ren et al., 1990c; Zumpe & Michael, 1986).

(1) Percentage of aggressive behaviors given: for each pair of individuals, we calculated the percentage of the total number of aggressive behaviors given by each participant to the other.

(2) Percentage of submissive behaviors received: for each pair of individuals, we calculated the percentage of submissive behaviors received by each participant from the other.

(3) Percentage of aggression given and submission received per pair: we combined the percentage scores of aggression given and submission received for each individual in the pair.

(4) Dominance index: we evaluated the dominance index by averaging, for each individual, the percentage scores of aggression given and submission received with all other individuals in the group.

Finally, we produced the dominance rank by sequencing the intra-OMU dominance index values from high to low.

Analysis of relaxed open-mouth display

We divided all behavioral data into the following categories: "absence of relaxed open-mouth display" vs. "presence of relaxed open-mouth display" and "single individual showing open-mouth display" vs. "both individuals showing open-mouth display". We then respectively summed the occurrences of displacement and continued aggression, and distances between dominant individuals and subordinates or aggressors and victims.

We adopted the *Chi*-square test to detect differences in the occurrences of displacement and continued aggression under different relaxed open-mouth display patterns. We used one-way analysis of variance (ANOVA) for overall comparison followed by *t*-tests (SPSS v17.0) to identify differences in distances between subordinates, dominants, and/or aggressors and victims. Each sample showed normal distribution. Statistical tests were two-tailed, and significance was set at 0.05.

Ethical statement

Prior to conducting this study, we obtained approval from the Shennongjia National Park and the Institutional Animal Care and Use Committee of Central South University of Forestry and Technology.

RESULTS

Dominance rank

We observed aggressive behavior 337 times and submissive behavior 139 times. Based on our calculation of dominance index, we ranked the 18 focal individuals within their OMUs as follows: HH unit, HH>HH_2>HHE>YY_2>DWB>TJ>AL; XZ unit, XZ>XB_2>XE>YB>XH>SB; XB unit, XB>GG>LN>SS>YY (Table 1). The intra-OMU hierarchy remained stable throughout the entire study period (22 July–4 November 2016) based on the results from the random nut tests.

Relaxed open-mouth display

We observed relaxed open-mouth display 212 times out of 322 total approaches within the OMUs. The occurrence of relaxed open-mouth display was related with displacement 29 times (13.68%, n=212), with aggression 24 times (11.32%, n=212), with friendliness 59 times (27.83%, n=212), with post-conflict period 53 times (25%, n=212) and with reassurance 47 times (22.17%, n=212). We obtained 154 h of observation on the focal group, and the average occurrence of relaxed open-mouth display for the 18 focal individuals was 1.38 times/h. The displacement occurrence of subordinates by approaching dominant individuals is shown in Table 2. There was a higher risk of being displaced by a dominant individual if the subordinate did not exhibit relaxed open-mouth display (χ^2=25.259, P<0.001) (Table 2).

Table 2 Displacement occurrence of subordinates by approaching dominant individuals

	Occurrence of displacement event (n)	No. displacement event (n)	Statistical tests (*Chi*-square test)
Neither dominant nor subordinate showed relaxed open-mouth display	21	2	χ^2=25.259, P<0.001
Subordinates alone showed relaxed open-mouth display*	5	24	

*: There were no "Dominants alone exhibited relaxed open-mouth display".

Table 3 shows the occurrence of continued aggression during the post-conflict period. The occurrence of continued aggression was lower when victims alone exhibited relaxed open-mouth display towards aggressors (χ^2=14.368, P<0.001) (Table 3).

We recorded three different relaxed open-mouth display patterns when subordinates approached dominant individuals, i.e., subordinates did not show open-mouth display (40 times), only subordinates showed open-mouth display (31 times) and both subordinates and dominants showed open-mouth display (28 times). The average minimum distance achieved by subordinates approaching dominant individuals without becoming the target of aggression is shown in Figure 3. Relaxed open-mouth display had a significant effect on distance (F=37.062, P<0.001). Subordinates were able to get closer to dominant individuals if they exhibited relaxed open-mouth display than if they did not (t=4.796, P<0.001). Furthermore, exchange of relaxed open-mouth display from both participants facilitated the closest distances between them (t=5.068, P<0.001).

Table 3 Times of continued aggression

	Occurrence of continued aggression (n)	No. continued aggression (n)	Statistical tests (Chi-square test)
Neither victim nor aggressor showed relaxed open-mouth display	10	1	χ^2=14.368, P<0.001
Victims alone showed relaxed open-mouth display*	4	20	

*: There were no "Aggressors alone exhibited relaxed open-mouth display".

Figure 3 Closest distance achieved by a subordinate approaching a dominant individual (n=99)

***: P<0.001.

After aggressive events ceased, we recorded three different relaxed open-mouth display patterns, i.e., victims did not show open-mouth display (11 times), victims showed open-mouth display toward aggressors (24 times) and both participants showed open-mouth display (29 times). Relaxed open-mouth display had a significant effect on distance (F=34.907, P<0.001). By exhibiting a relaxed open-mouth display, victims were able to get closer to aggressors (t=3.759, P<0.01), and exchange of relaxed open-mouth display allowed victims and aggressors to get much closer than when only victims exhibited the behavior alone (t=2.828, P<0.01) (Figure 4).

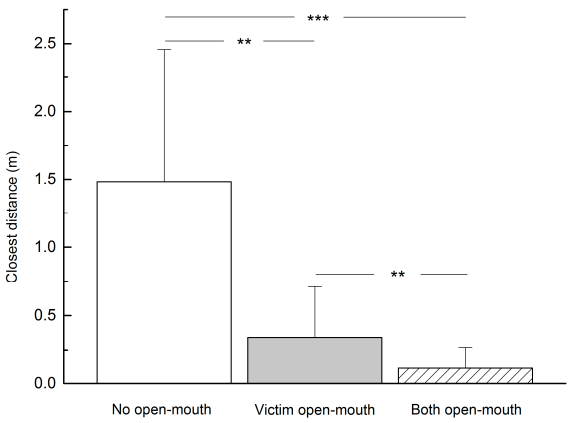

Figure 4 Closest distance between victim and aggressor after aggression (*n*=64)

***: P<0.001; **: P<0.01.

Dominant individuals showed and did not show relaxed open-mouth behavior when approaching subordinates 47 times and 25 times, respectively. Dominant individuals were able to get closer to subordinates when they exhibited this display behavior (t=7.924, P<0.001) (Figure 5).

Figure 5 Distance achieved by a dominant individual approaching a subordinate when showing relaxed open-mouth display (*n*=72)

***: P<0.001.

DISCUSSION

We explored four hypotheses related to relaxed open-mouth display within the OMUs of free-ranging *R. roxellana*. Results suggested that relaxed open-mouth display served four social functions in *R. roxellana* societies: that is, submission, reconciliation, affiliation and reassurance. Furthermore, an exchange of relaxed open-mouth display facilitated more significant outcomes than when one individual exhibited the behavior alone.

In our study group, relaxed open-mouth display usually functioned as a sign of submission. For subordinates, relaxed open-mouth display significantly reduced the probability of being displaced when dominant individuals approached (Table 2). For victims, relaxed open-mouth display significantly reduced the occurrence of continued aggression (Table 3). These outcomes are similar to those reported in previous study on *R. roxellana* populations in the Qinling Mountains of China, where adult females and juveniles were observed to open their mouths to exhibit submission, prevent aggression and maintain OMU stability (Yang et al., 2013).

Relaxed open-mouth display also served as a clear signal of reconciliation as aggression was unlikely to continue while aggressors and victims could reengage in social interactions in close proximity (Figure 4). These results are in agreement with those reported from a captive group of *R. roxellana* (Ren et al., 1991), as well as another colobine species such as *Trachypithecus francoisi* (Wang, 2009). This behavioral pattern can be explained as a mechanism of reconciliation, thus supporting the hypothesis of "increasing social tolerance" to pacify tension within groups (Aureli & van Schaik, 1991; de Waal & Ren, 1988), ease anxiety (Cords, 1992; Das et al., 1998), reduce continued aggression (Call et al., 1999; Cords, 1992; de Waal, 1993) and decrease heart rates (Smucny et al., 1996).

Similar to earlier descriptions (Ren et al., 1990b), relaxed open-mouth display in *R. roxellana* also had an affiliative effect, allowing subordinates to approach dominant individuals more closely (Figure 3). Interestingly, we noted that most individuals in the study group also frequently exhibited relaxed open-mouth display toward reserve staff during provisioning, suggesting possible affiliation and acceptance for easier food acquisition.

We also found that relaxed open-mouth display functioned as reassurance–a kind of affiliative signal displayed by dominant individuals towards subordinates to initiate closer proximity to each other (van Hooff, 1967; Wiper & Semple, 2007) (Figure 5). Dominant individuals can use this behavior to reassure and ease anxiety in subordinates who may treat the former as a potential threat (Cords, 1992; Das et al., 1998; Ren et al., 1990b). This behavior has also been reported when adult females care for their infants, when adult males or females solicit sexual partners for copulation, and when adult males pacify their own OMUs after conflict between two or more adults (Ren et al., 1990b). Thus, reassurance behavior may be instigated to reassure infants, sexual partners and unit members to gain fitness, social stability and self-assurance.

Within OMUs of *R. roxellana*, the exchange of relaxed open-mouth display between two individuals yielded more significant outcomes than when one individual displayed the behavior alone, allowing subordinates to approach dominant individuals for social activities such as sitting together, grooming and hugging (Figure 3), as well as reducing the distance between victims and aggressors after aggression (Bout & Thierry, 2005; van Hooff, 1967) (Figure 4). These findings are similar to observations in other non-human primates (Aureli, 1997; Bout & Thierry, 2005; Call et al., 1999; de Waal, 1986; de Waal & Luttrell, 1989; de Waal & Ren, 1988; de Waal & van Roosmalen, 1979; Wang, 2009; Wiper & Semple, 2007). Thus, *R. roxellana* appears to be a relatively mild and peaceful species with high intra-unit tolerance (Li et al., 2006; Wiper & Semple, 2007), and the exchange of relaxed open-mouth display helps maintain the stability and cohesion of the species' multi-level social organization (Qi et al., 2014).

We quantitatively analyzed the functions and hypotheses of relaxed open-mouth display within OMUs of free-ranging *R. roxellana*, which are essential for understanding the social dynamics and mechanisms of multi-level societies.

COMPETING INTERESTS

The authors declare that they have no competing interests.

AUTHORS' CONTRIBUTIONS

Y.J.Z. and Z.F.X. designed the study. Z.F.X. supervised the entire study. Y.J.Z. collected and analyzed behavioral data with H.C.C. and Y.X.C.'s additional methodological supports. Y. X.C. and Y.J.Z. wrote the manuscript and revised it accordingly. H.C.C., Y.C., H.Y. and W.J.Y. participated in behavioral data collection. H.Y., W.J.Y. and X.D.R. provided necessary logistical supports on field work. All authors read and approved the final version of the manuscript.

ACKNOWLEDGEMENTS

We thank the Administration Bureau of Shennongjia National Nature Reserve for their support, and Cheng Guo, Lang Lu and Bo Zhang for additional assistance on the study and manuscript. We are grateful for editor-in-chief, Yong-Gang Yao, and two anonymous reviewers who offer precious comments and suggestions on revision of the manuscript.

REFERENCES

Altmann SA.1962. A field study of the sociobiology of rhesus monkeys, *Macaca mulatta*. *Annals of New York Academy of Science*, **102**(2):338–435.

Altmann J. 1974. Observational study of behavior: Sampling methods. *Behavior*, **49**(3):227–267.

Aureli F, van Schaik CP. 1991. Post-conflict behavior in long-tailed macaques (*Macaca fascicularis*). *Ethology*, **89**(2):89–100.

Aureli F. 1997. Post-conflict anxiety in nonhuman primates: the mediating role of emotion in conflict resolution. *Aggressive Behavior*, **23**(5):315–328.

Bout N, Thierry B. 2005. Peaceful meaning for the silent bared-teeth displays of mandrills. *International Journal of Primatology*, **26**(6):1215–1228.

Call J, Aureli F, de Waal FBM. 1999. Reconciliation patterns among stump-tailed macaques: a multivariate approach. *Animal Behaviour*, **58**(1):165–172.

Cords M. 1992. Post-conflict reunions and reconciliation in long-tailed macaques. *Animal Behaviour*, **44**(1):57–61.

Cui DY, Niu KF, Tan CL, Yang MY, Zhang YY, Zhang JG, Yang YQ. 2014. Behavior coding and ethogram of Guizhou snub-nosed monkey (*Rhinopithecus brelichi*). *Sichuan Journal of Zoology*, **33**(6):815–828. (in Chinese)

Das M, Penke Z, van Hooff JARAM. 1998. Post-conflict affiliation and stress-related behavior of long-tailed macaque aggressors. *International Journal of Primatology*, **19**(1):53–71.

de Waal FBM, van Roosmalen A. 1979. Reconciliation and consolation among chimpanzees. *Behavioral Ecology and Sociobiology*, **5**(1):55–66.

de Waal FBM. 1986. The integration of dominance and social bonding in primates. *The Quarterly Review of Biology*, **61**(4):459–479.

de Waal FB M, Ren RM. 1988. Comparison of the reconciliation behavior of stumptail and rhesus macaques. *Ethology*, **78**(2):129–142.

de Waal FBM, Luttrell LM. 1989. Toward a comparative socioecology of the genus *Macaca*: different dominance styles in rhesus and stumptail monkeys. *American Journal of Primatology*, **19**(2):83–109.

de Waal FBM. 1993. Reconciliation among primates: a review of empirical evidence and unresolved issues. *In*: Mass on W A, Mendoza S P. Primate Social Conflict. Albany, NY, USA: State University of New York Press, 111–144.

Guo S, Li B, Watanabe K. 2007. Diet and activity budget of *Rhinopithecus roxellana* in the Qinling Mountains, China. *Primates*, **48**(4):268–276.

Hinde RA, Rowell TE. 1962. Communication by posture and facial expression in the rhesus monkey (*Macaca mulatta*). *Proceedings of the Zoological Society of London*, **138**(1):1–21.

Li BG, Chen FG, Luo YS, Xie WZ. 1993. Major categories of vocal behaviour in wild Sichuan golden monkey (*Rhinopithecus roxellana*). *Acta Theriologica Sinica*, **13**(3):181–187. (in Chinese)

Li BG, Li HQ, Zhao DP, Zhang YH, Qi XG. 2006. Study on dominance hierarchy of the Sichuan snub-nosed monkey (*Rhinopithecus roxellana*) in Qinling Mountains. *Acta Theriologica Sinica*, **26**(1):18–25. (in Chinese)

Li Y, Ren BP, Li YH, Li DY, Hu J. 2013. Behavior ethogram and PAE coding system of *Rhinopithecus bieti*. *Sichuan Journal of Zoology*, **32**(5):641–650. (in Chinese)

Martin P, Bateson P. 1993. Measuring Behavior: An Introductory Guide. Cambridge: Cambridge University Press, 50–55.

Prud'Homme J. 1991. Group fission in a semifree-ranging population of Barbary macaques (*Macaca sylvanus*). *Primates*, **32**(1):9–22.

Qi XG, Garber PA, Ji WH, Huang ZP, Huang K, Zhang P , Guo ST, Wang XW, He G, Zhang P, Li BG. 2014. Satellite telemetry and social modeling offer new insights into the origin of primate multilevel societies. *Nature Communication*, **5**(5):5296.

Ren RM, Yan KH, Su YJ, Wang QW, Sun YZ. 1990a. Comparison of the patterns of social behavioral repertoire between *Macaca thibetana* and *Macaca mulatta*. *Acta Psychologica Sinica*, **22**(4):107–112. (in Chinese)

Ren RM, Yan KH, Su YJ, Qi HJ, Bao WY. 1990b. Social communication by positure and facial expressions in Golden monkey (*Rhinopithecus roxellanae*). *Acta Psychologica Sinica*, **22**(2):49–57. (in Chinese)

Ren RM, Su YJ, Yan KH, Qi HJ, Bao WY. 1990c. Social relationships among Golden monkeys in breeding cages. *Acta Psychologica Sinica*, **22**(3):55–60. (in Chinese)

Ren RM, Yan KH, Su YJ, Qi HJ, Liang B, Bao WY, de Waal FBM. 1991. The reconciliation behavior of Golden monkeys (*Rhinopithecus roxellanae roxellanae*) in small breeding groups. *Primates*, **32**(3):321–327.

Smucny DA, Price CS, Byrne EA. 1996. Heart rate correlates of reconciliation in captive adult female rhesus macaques (*Macaca mulatta*). Abstracts of XVIth International Primatology Society Congress, Wisconsin, Madison, 556.

van Hooff JARAM. 1967. The facial displays of the catarrhine monkeys and apes. *In*: Morris D. Primate Ethology. New Brunswick, NJ, USA: AldineTransaction, 7–68.

Wang H. 2009. Dominance Hierarchy and Affinitive Behavior of the *Trachypithecus francoisi* in Captivity. Master thesis. Guangxi Normal University, Guilin.

Wiper SM, Semple S. 2007. The function of teeth chattering in male Barbary macaques (*Macaca sylvanus*). *American Journal of Primatology*, **69**(10):1179–1188.

Xiang ZF, Yang BH, Yu Y, Yao H, Grueter CC, Garber PA, Li M. 2014. Males Collectively Defend Their One-Male Units Against Bachelor Males in a Multi-Level Primate Society. *American Journal of Primatology*, **76**(7):609–617.

Yan KH, Su YJ, Ren RM. 2006. Social behavioral repertoires and action patterns of Sichuan snub-nosed monkey (*Rhinopithecus roxellana*). *Acta Theriologica Sinica*, **26**(2):129–135. (in Chinese)

Yang B, Zhao HT, Wang CL, Wang XW, Wang KF, Li BG. 2013. The classification of face expression of the Sichuan snub-nosed monkey (*Rhinopithecus roxellana*) in Qinling Mountains. *Bulletin of Biology*, **48**(12):8–10. (in Chinese)

Yao H, Liu X, Stanford C, Yang J, Huang T, Wu F, Li Y. 2011. Male dispersal in a provisioned multilevel group of *Rhinopithecus roxellana* in Shennongjia Nature Reserve, China. *American Journal of Primatology*, **73**(12):1280–1288.

Yu Y, Xiang ZF, Yao H, Grueter CC, Li M. 2013. Female snub-nosed monkeys exchange grooming for sex and infant handling. *PLoS One*, **8**(9):e74822.

Zumpe D, Michael RP. 1986. Dominance index: A Simple measure of relative dominance status in primates. *American Journal of Primatology*, **10**(4):291–301.

Home range variation of two different-sized groups of golden snub-nosed monkeys (*Rhinopithecus roxellana*) in Shennongjia, China: implications for feeding competition

Peng-Lai Fan[1,2], Yi-Ming Li[3], Craig B. Stanford[4], Fang Li[1], Ze-Tian Liu[3], Kai-Hua Yang[5], Xue-Cong Liu[1,*]

[1] *College of Life Sciences, University of Chinese Academy of Sciences, Beijing* 100049*, China*
[2] *Institute of Ecology, College of Life Sciences, Beijing Normal University, Beijing* 100875*, China*
[3] *Key Laboratory of Animal Ecology and Conservation Biology, Institute of Zoology, Chinese Academy of Sciences, Beijing* 100101*, China*
[4] *Departments of Biological Sciences and Anthropology, Jane Goodall Research Center, University of Southern California, Los Angeles, California* 90089*, USA*
[5] *Shennongjia National Park, Shennongjia Hubei* 442421*, China*

ABSTRACT

Knowledge on the home range size of a species or population is important for understanding its behavioral and social ecology and improving the effectiveness of conservation strategies. We studied the home range size of two different-sized groups of golden snub-nosed monkeys (*Rhinopithecus roxellana*) in Shennongjia, China. The larger group (236 individuals) had a home range of 22.5 km^2 from September 2007 to July 2008, whereas the smaller group (62 individuals) occupied a home range of 12.4 km^2 from November 2008 to July 2009. Both groups exhibited considerable seasonal variation in their home range size, which was likely due to seasonal changes in food availability and distribution. The home range in any given season (winter, spring, summer, or winter+spring+summer) of the larger group was larger than that of the smaller group. As the two groups were studied in the same area, with the confounding effects of food availability thus minimized, the positive relationship between home range size and group size suggested that scramble feeding competition increased within the larger group.

Keywords: *Rhinopithecus roxellana*; Home range size; Group size; Feeding competition

INTRODUCTION

A home range is defined as the area in which animal individuals or groups spend their normal activities over a certain period in search of food and caring for young (Burt, 1943). Knowledge on the home range size of a species or population is of great importance for understanding its behavioral and social ecology (Isbell, 1991; Snaith & Chapman, 2007; Zhou et al., 2007) and for improving the effectiveness of conservation strategies (Bryant et al., 2017; Huang et al., 2017). The home range size of non-human primates (hereafter, primates) is influenced by a range of ecological and behavioral factors, including food availability and distribution (Curtis & Zaramody, 1998; Zhang et al., 2014; Zhou et al., 2007), group size (Dias & Strier, 2003; Gillespie & Chapman, 2001; Li et al., 2010), sleeping site location (Zhou et al., 2011), water availability (Scholz & Kappeler, 2004), parasite avoidance (Freeland, 1980), topography (Fan & Jiang, 2008), and intergroup relationships (Benadi et al., 2008).

Received: 04 December 2017; Accepted: 25 June 2018; Online: 28 June 2018

Foundation items: This study was supported by the Hubei Provincial Key Laboratory for Conservation Biology of Snub-nosed Monkeys, Scientific Research Grant for Youth Scholars from the University of Chinese Academy of Sciences, L.S.B. Leakey Foundation, and Primate Conservation Inc.

*Corresponding author, E-mail: xuecongliu@ucas.ac.cn

DOI: 10.24272/j.issn.2095-8137.2018.044

Spatiotemporal distribution of food resources can affect the home range size both between and within primate species (Clutton-Brock & Harvey, 1977; Zhang et al., 2014; Zhou et al., 2007). Because leaves are more abundant and evenly distributed than fruits, folivores, e.g., most colobines, generally occupy smaller home ranges than frugivores, e.g., *Pan troglodytes* and *Ateles* spp. (Clutton-Brock & Harvey, 1977; Stanford, 1991; Zhou et al., 2007). For species inhabiting seasonal environments, the home range size of a group usually exhibits seasonal variation due to seasonal changes in food availability and distribution (*Eulemur mongoz*: Curtis & Zaramody, 1998; *Trachypithecus francoisi*: Zhou et al., 2007; *Macaca leonina*: Albert et al., 2013; *Hoolock leuconedys*: Zhang et al., 2014).

The influence of group size on home range size has also been widely investigated, but with contradictory findings; home range size increases with group size in many species and populations (Dias & Strier, 2003; Fashing et al., 2007; Gillespie & Chapman, 2001; Kurihara & Hanya, 2015; Li et al., 2010; Teichroeb & Sicotte, 2009), but not in all (Struhsaker, 1975; Whitesides, 1989). Theoretically, when food resources are limited, the addition of feeding members should reduce the amount of food intake per capita and thus larger groups are expected to occupy larger home ranges to obtain adequate food for all group members (Chapman & Chapman, 2000a; Isbell, 1991; Janson & van Schaik, 1988). Researchers often infer intragroup scramble feeding competition (i.e., reduction of resources without direct conflicts) from a positive relationship between home range size and group size (Fashing et al., 2007; Isbell, 1991; Snaith & Chapman, 2007). It should be emphasized that the influence of group size on home range size is highly dependent on food availability; if food resources are abundant enough to compensate for having more mouths to feed, more feeding members in larger groups may not lead to increased competition and thus home range expansion (Chapman & Chapman, 2000b; Isbell, 1991; Snaith & Chapman, 2007). Researchers often control the confounding effects of food availability by studying different-sized groups foraging in the same habitat (Dias & Strier, 2003; Gogarten et al., 2014). Unlimited food availability may explain the absence of a relationship between home range size and group size in some species or populations, particularly those that tend to rely heavily on leaves, an abundant food source (reviewed in Isbell, 1991).

The golden snub-nosed monkey (*Rhinopithecus roxellana*) is an endangered colobine species endemic to China and includes three geographically isolated populations: Qinling, Sichuan-Gansu, and Shennongjia (Li et al., 2002, 2007). Its long-term survival is threatened by habitat loss and fragmentation, illegal poaching, and increasing human activities due to the rapid development of ecotourism (Guo et al., 2008; Li et al., 2002; Xiang et al., 2011; Zhang et al., 2016). *R. roxellana* diverges from most colobines in various ecological aspects. Unlike most colobines living in tropical or subtropical forests, it inhabits temperate forests in mountainous areas at high altitude (1 000–4 100 m), which exhibit strong seasonality with cold and snowy winters (Kirkpatrick & Grueter, 2010; Li et al., 2002). Forest phenology and food availability strongly affect its diet, with flowers, young leaves, mature leaves, fruits, seeds, and buds becoming available and subsequently the main dietary components (Guo et al., 2007; Li, 2006; Liu et al., 2013b). Furthermore, lichens, an uncommon food source for primates, constitute an important part of its diet throughout (or almost) the year. *R. roxellana* lives in extraordinarily large multi-level groups of up to several hundred individuals, with one-male multi-female units as the basic social and reproductive level (Qi et al., 2014), whereas most other colobines live in small groups containing 3–20 individuals (Bennett & Davies, 1994; Oates, 1994).

Previous studies of the Qinling population have shown that groups of *R. roxellana* have home ranges much larger than those of most colobines (rarely >1 km^2) (Li et al., 2000; Tan et al., 2007). For example, the West Ridge group in Yuhuangmiao (90 individuals) occupied a home range of 22.5 km^2 from April to October 1995 and December 1996 to September 1997 (Li et al., 2000), and the East Ridge group (112 individuals) exploited a home range of 18.3 km^2 from November 2002 to November 2003 (Tan et al., 2007). Both groups exhibited considerable variation in their seasonal home range size (Li et al., 2000; Tan et al., 2007). The home range size of the Shennongjia population has never been systematically studied. Su et al. (1998) provided the only preliminary report that the monkeys were observed in an area covering 40 km^2 from November to December 1991, March to April 1992, and October 1992 to the end of 1995, but the study subjects were from different groups.

In the present study, we investigated the home range size of two different-sized *R. roxellana* groups in Shennongjia. Our results are of particular significance for conservation as the Shennongjia population has a smaller distribution area, a smaller population size, and lower genetic diversity compared to the other two populations (Li et al., 2007; Liu et al., 2015; Luo et al., 2012). In addition, because the two groups foraged in the same area and thus the confounding effects of food availability were minimized, intergroup comparisons of home range size bear important implications for intragroup scramble feeding competition.

MATERIALS AND METHODS

Study site

Shennongjia National Nature Reserve (E110°03′–110°34′, N31°22′–31°37′) is separated into two parts by geographical features, main roads, and human residential districts (Figure 1). *R. roxellana* is found only within the western part and our study site, the Qianjiaping area (60 km^2), is located at the southeastern end of this part. The topography of this area is extremely rugged, with an elevational range of 1 500–2 663 m (Liu et al., 2013b). The vegetation is characterized by deciduous broadleaf and evergreen conifer mixed forests. The climate is highly seasonal. The mean temperature at the elevation of 1 700 m is lowest in January (ca. –5.5 °C) and highest in July (ca. 16.3 °C). Annual rainfall is approximately 1 800 mm, with the rainy season occurring between July and

September. Snow occurs from early November to middle March. Based on local climate, we defined spring from 21 March to 31 May, summer from 1 June to 31 August, autumn from 1 September to 31 October, and winter from 1 November to 20 March.

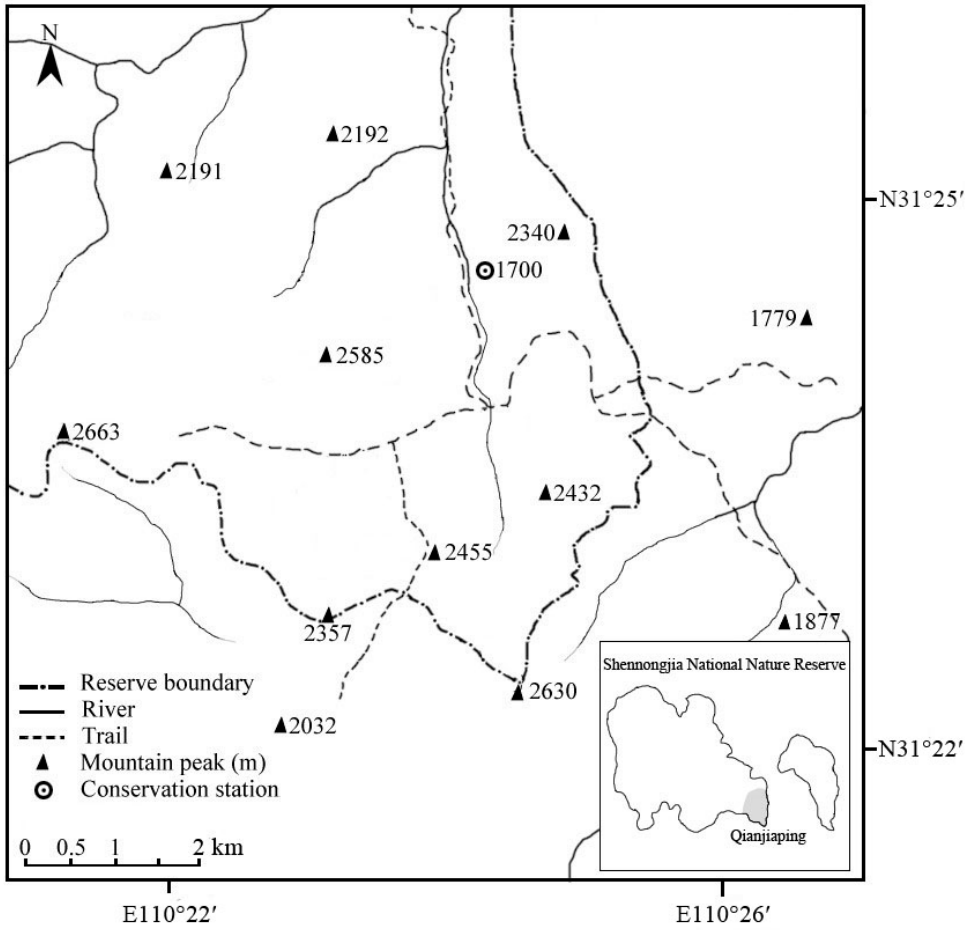

Figure 1 Topography of the Qianjiaping area of Shennongjia National Nature Reserve, China

Study groups

During the study period, the two different-sized groups of *R. roxellana* foraged mainly in the Qianjiaping area and occasionally in adjacent areas in the southeast (adjacent areas belong to Badong County). The larger group had been semi-habituated and studied periodically since 1999 (Li, 2001, 2002, 2004). We studied this group from September 2007 to July 2008, except for February 2008, and could approach it within 20–30 m. We lost this group at the end of July 2008 and did not contact it again in the study area during the study period. We looked for other potential monkey groups in the same area and found a much smaller one in November 2008. We followed this group through to July 2009, except for February 2009. Before this study, we had not observed this group foraging in the study area. The group had never been habituated or studied, and we could only approach it within about 100 m (the apparent differences in vigilance behavior indicated that this group was not a part separated from the larger group). Group sizes and compositions were determined when the monkeys crossed open areas or rivers, or when leaves of deciduous plants fell during winter (age-sex class definition following Li, 2007). During the study period, the larger group contained 236±38 individuals (n=8), including 106±12 adult males, 77±18 adult females, 35±10 juveniles, and 18±5 infants, whereas the smaller group contained 62±6 individuals (n=6), including 23±5 adult males, 22±3 adult females, 13±3 juveniles, and 4±3 infants. These counts may be biased because the monkey individuals were widely spread and our view was often obstructed.

Data collection

While following each group, we estimated the central locations of group spread at half-hourly intervals and obtained GPS coordinates (longitudes and latitudes) via a portable GPS unit

(Garmin GPSMap 60CSx 2.6-inch Mapping Handheld GPS). When we could not obtain a clear satellite signal due to dense canopy, we moved to a more open location (less than 20 m from the estimated group location). All study protocols adhered to the legal requirements of China and local management regulations of Shennongjia National Nature Reserve.

Data analysis

We employed the fixed kernel density estimation (KDE) to calculate the home range sizes during various periods for each group via ArcView 3.3 with the Animal Movement Analysis Extension (Hooge & Eichenlaub, 1997). KDE has several advantages over grid systems and minimum convex polygons (MCPs) in estimating home range size (Caillaud et al., 2014; Fashing et al., 2007). KDE is less sensitive to sample size and the presence of outlying points. MCPs often overestimate home range size by including large areas never used, while grid systems largely depend on arbitrarily chosen grid dimensions. Therefore, KDE is also preferable for comparison analyses of home range size between groups or populations and has been widely employed to estimate home range size in primate studies (e.g., Caillaud et al., 2014; Fashing et al., 2007; Scholz & Kappeler, 2004). KDE computes the spatial utilization distribution based on a random sample of group locations (Seaman et al., 1999; Worton, 1989). We estimated home range sizes based on 95% volume contours of kernel probability density surfaces with a smoothing parameter selected by least squares cross validation, as used in other studies (Campera et al., 2014; Fashing et al., 2007; Hanya & Bernard, 2016; Scholz & Kappeler, 2004).

We first calculated the overall (i.e., annual for the larger group and winter to summer for the smaller group) and seasonal home range sizes for each group. For intergroup comparisons, we then estimated the home range size from winter to summer for the larger group. We also calculated the overlapping sizes of the above parameters (i.e., winter to summer, winter, spring, and summer home range sizes) between the two groups.

RESULTS

We recorded 613 locations (winter: 192; spring: 137; summer: 106; autumn: 178) on 147 days for the larger group and 837 locations (winter: 258; spring: 303; summer: 276) on 130 days for the smaller group during the study period. The annual home range size of the larger group was 22.5 km^2 (Table 1; Figure 2). The home range size of the larger group from winter to summer was 21.5 km^2, much larger than that of the smaller group, 12.4 km^2. Furthermore, the home range of the smaller group from winter to summer was almost entirely included within that of the larger group, with the overlapping range occupying 91.9% of the home range of the smaller group.

The seasonal home ranges varied in size in a similar pattern for both groups: autumn (for the larger group only) > spring > summer > winter (Table 1; Figure 2). On the other hand, for the larger group, spring and autumn home ranges were comparable in size and accounted for 82.7% and 86.2% of the annual home range, respectively. Winter and summer home ranges were much smaller and accounted for 54.7% and 64.4% of the annual home range, respectively. For the smaller group, spring and summer home ranges were similar in size and occupied 96.8% and 94.4% of the overall home range, respectively, whereas winter home range was much smaller and occupied 48.4% of the overall home range.

The home range of the larger group in any given season (winter, spring, or summer) was larger than that of the smaller group. Furthermore, spring and summer home ranges of the smaller group were largely included within those of the larger group, with the overlapping ranges accounting for 89.2% and 67.5% of the home ranges of the smaller group, respectively. In winter, the two groups foraged primarily in different areas, with the overlapping range occupying 17.9% of the home range for the larger group and 36.7% for the smaller group.

DISCUSSION

Our study showed that the home range of *R. roxellana* in Shennongjia was large and comparable with that of the Qinling population (Li et al., 2000; Tan et al., 2007). It appears that colobines living in temperate habitats have larger home ranges than most other colobines in tropical or subtropical habitats, probably because food resources in temperate forests are less abundant and more spread out (Bishop, 1979; Grueter et al., 2008; reviewed in Kirkpatrick et al., 1998). For example, hanuman langurs (*Semnopithecus entellus*) in the Himalaya occupy home ranges up to 12 km^2, whereas the home range sizes of the same species in Sri Lanka are only 2–3 hm^2 (Bennett & Davies, 1994). The black-and-white snub-nosed monkey (*Rhinopithecus bieti*) is a colobine species endemic to temperate forests in China, and the home range size of a *R. bieti* group in the Samage Forest was reported to be 32 km^2 over a 14.5-month period (Grueter et al., 2008).

Similar to the Qinling population, *R. roxellana* in Shennongjia exhibited considerable variation in home range size among seasons (Li et al., 2000; Tan et al., 2007). Seasonal changes in food availability and distribution were likely the primary driver for the seasonal variation in home range size in this study, as reported in the Qinling population (Li et al., 2000; Tan et al., 2007) and many other primates (Albert et al., 2013; Curtis & Zaramody, 1998; Zhang et al., 2014; Zhou et al., 2007). According to our previous studies in the same area, besides lichens, a fallback food available year-round, *R. roxellana* mainly eats young leaves and buds in spring, and fruits and pine seeds (*Pinus armandii*) in autumn (Li, 2006; Liu et al., 2013b, 2016). Our previous preliminary vegetation survey showed that these food types tend to be widely distributed across the study area (Yang et al., 2014), and thus the home ranges of *R. roxellana* in spring and autumn were larger than those in summer and winter. In summer, mature leaves are abundant and evenly distributed and become an important dietary component, and thus the home range largely contracted correspondingly. In winter, probably because of the shortage of food resources and/or being less active to save energy in the cold and snowy weather, the monkeys exploited the smallest home range.

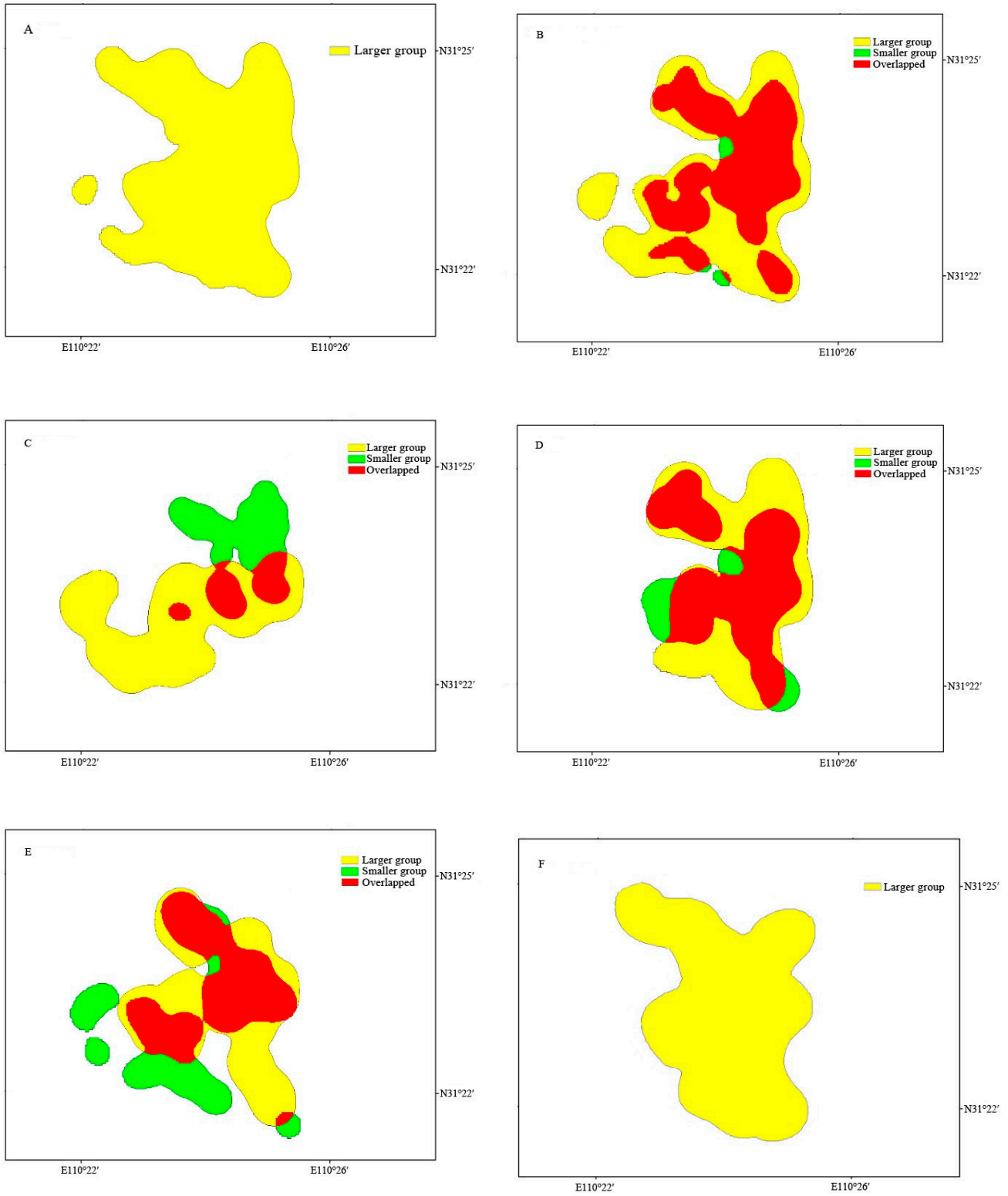

Figure 2 Home ranges of the two different-sized groups of *Rhinopithecus roxellana* in Shennongjia, China

Study period: September 2007 to July 2008 for the larger group, November 2008 to July 2009 for the smaller group. A: Annual; B: Winter+Spring+Summer; C: Winter; D: Spring; E: Summer; F: Autumn.

Table 1 Home range sizes (km^2) of the two different-sized groups of *Rhinopithecus roxellana* in Shennongjia, China

	Period					
	Annual	Winter+Spring+Summer	Winter	Spring	Summer	Autumn
Larger group	22.5	21.5	12.3	18.6	14.5	19.4
Smaller group	N/A	12.4	6.0	12.0	11.7	N/A
Overlapped	N/A	11.4	2.2	10.7	7.9	N/A

Study period: September 2007 to July 2008 for the larger group, November 2008 to July 2009 for the smaller group. N/A: Not available.

The home range size during the period from winter to summer increased with group size. However, the two groups were studied in different years and thus the relationship between home range size and group size may have been confounded by food availability (Chapman & Chapman, 2000b; Isbell, 1991; Snaith & Chapman, 2007) as the availability of some important food types (e.g., pine seeds) can vary between years (Li, 2006). Therefore, it is more reasonable to infer the effects of group size from intergroup comparisons of seasonal home ranges. The home range sizes in winter, spring, and summer all increased with group size. In particular, spring and summer home ranges of the larger group were almost an expansion of those of the smaller group. In the study area, the abundances of important foods, including young leaves, mature leaves, buds, and lichens, in spring and summer (June to July in particular) are not likely to vary between years (Li, 2006; Liu et al., 2013b). Thus, we believe the confounding effects of food availability were not significant. These results suggested positive effects of group size on home range size, at least in spring and summer. The sensitivity of home range size to group size is supported by previous findings that food distribution density in the study area is quite low (Yang et al., 2014). Food plants occupying $\geq$5.0% of the seasonal diet account for only a small proportion of the total basal area (varying from 4.2% in summer to 11.5% in winter) and total shrub coverage (varying from 1.3% in autumn to 13.9% in spring). Furthermore, only 11.5% of trees and 18.9% of shrubs are encumbered by lichens.

The positive effects of group size on home range size suggested increased scramble feeding competition within the larger group. In addition to *R. roxellana*, *R. bieti* also has a large proportion of lichens in its diet (Ding & Zhao, 2004; Grueter et al., 2009a, 2009b; Huang ZP et al., 2017; Kirkpatrick, 1996; Xiang et al., 2007) and lives in extraordinarily large multilevel groups (Cui et al., 2007; Kirkpatrick, 1996; Kirkpatrick et al., 1998). It has been hypothesized that intragroup feeding competition is weak due to the ubiquitous availability, even distribution, and low quality of lichens (similar to mature leaves), thus allowing the formation of large groups (Grueter & van Schaik, 2010; Kirkpatrick, 1996). However, detailed data on the availability and distribution of both lichen and plant foods are still lacking for most populations of the two species. There is increasing evidence showing that intragroup feeding competition in these two species may be more significant than previously hypothesized; for example, several indices of foraging efforts increase with group size, including home range size (Li et al., 2010; this study), daily travel distance (Grueter & van Schaik, 2010), and time allocated for feeding and moving (Liu et al., 2013a).

Finally, it is worth mentioning that almost the whole home range of the smaller group was also used by the larger group during winter to summer in different years. This observation suggested that the quality of the range used by both groups might be higher than that of the surrounding range within the study area. Furthermore, there might be intergroup competition for this higher quality range and the smaller group filled the range only after the larger group ranged out of it. Intergroup feeding competition has seldom been investigated in *R. roxellana* probably because intergroup encounters are very rare due to the extremely large home ranges (Qi et al., 2014; unpublished data).

COMPETING INTERESTS

The authors declare that they have no competing interests.

AUTHORS' CONTRIBUTIONS

X.C.L. designed the study and collected the data. Y.M.L. and C.B.S. supervised the study. X.C.L. and Z.T.L. performed the data analyses. P.L.F. and X.C.L. wrote the manuscript. F.L. and K.H.Y. revised the manuscript. All authors read and approved the final version of the manuscript.

ACKNOWLEDGEMENTS

We appreciate the anonymous reviewers for their valuable comments on the previous version of this manuscript. We also appreciate Ruo-Shuang Liu, Li-Na Yi, Yong-Fa Li, and Yi-Guo Sun for their help in data collection and analysis.

REFERENCES

Albert A, Huynen MC, Savini T, Hambuckers A. 2013. Influence of food resources on the ranging pattern of northern pig-tailed macaques (*Macaca leonina*). *International Journal of Primatology*, **34**(4): 696–713.

Benadi G, Fichtel C, Kappeler P. 2008. Intergroup relations and home range use in Verreaux's sifaka (*Propithecus verreauxi*). *American Journal of Primatology*, **70**(10): 956–965.

Bennett EL, Davies AG. 1994. The ecology of Asian colobines. *In*: Davies AG, Oates JF. Colobine Monkeys: Their Ecology, Behaviour and Evolution. Cambridge, UK: Cambridge University Press, 129–172.

Bishop NH. 1979. Himalayan langurs: Temperate colobines. *Journal of Human Evolution*, **8**(2): 251–281.

Bryant JV, Zeng XY, Hong XJ, Chatterjee HJ, Turvey ST. 2017. Spatiotemporal requirements of the Hainan gibbon: Does home range constrain recovery of the world's rarest ape? *American Journal of Primatology*, **79**(3): e22617.

Burt WH. 1943. Territoriality and home range concepts as applied to mammals. *Journal of Mammalogy*, **24**(3): 346–352.

Caillaud D, Ndagijimana F, Giarrusso AJ, Vecellio V, Stoinski TS. 2014. Mountain gorilla ranging patterns: Influence of group size and group dynamics. *American Journal of Primatology*, **76**(8): 730–746.

Campera M, Serra V, Balestri M, Barresi M, Ravaolahy M, Randriatafika F, Donati G. 2014. Effects of habitat quality and seasonality on ranging patterns of collared brown lemur (*Eulemur collaris*) in littoral forest fragments. *International Journal of Primatology*, **35**(5): 957–975.

Chapman CA, Chapman LJ. 2000a. Determinants of group size in social primates: the importance of travel costs. *In*: Boinski S, Garber P. Group Movement in Social Primates and Other Animals: Patterns, Processes and Cognitive Implications. Chicago: University of Chicago Press, 24–42.

Chapman CA, Chapman LJ. 2000b. Constraints on group size in red colobus and red-tailed guenons: examining the generality of the ecological constraints model. *International Journal of Primatology*, **21**(4): 565–584.

Clutton-Brock TH, Harvey PH. 1977. Species differences in feeding and ranging behaviour in primates. *In*: Clutton-Brock TH. Primate Ecology: Studies of Feeding and Ranging Behaviour in Lemurs, Monkeys and Apes. London: Academic Press, 557–584.

Cui LW, Huo S, Zhong T, Xiang ZF, Xiao W, Quan RC. 2007. Social organization of black-and-white snub-nosed monkeys (*Rhinopithecus bieti*) at Deqin, China. *American Journal of Primatology*, **70**(2): 169–174.

Curtis DJ, Zaramody A. 1998. Group size, home range use, and seasonal variation in the ecology of *Eulemur mongoz*. *International Journal of Primatology*, **19**(5): 811–835.

Dias LG, Strier KB. 2003. Effects of group size on ranging patterns in *Brachyteles arachnoides hypoxanthus*. *International Journal of Primatology*, **24**(2): 209–221.

Ding W, Zhao QK. 2004. *Rhinopithecus bieti* at Tacheng, Yunnan: Diet and daytime activities. *International Journal of Primatology*, **25**(3): 583–598.

Fan PF, Jiang XL. 2008. Effects of food and topography on ranging behavior of black crested gibbon (*Nomascus concolor jingdongensis*) in Wuliang Mountain, Yunnan, China. *American Journal of Primatology*, **70**(9): 871–878.

Fashing PJ, Mulindahabi F, Gakima J, Masozera M, Mununura I, Plumptre AJ, Nguyen N. 2007. Activity and ranging patterns of *Colobus angolensis ruwenzorii* in Nyungwe Forest, Rwanda: Possible costs of large group size. *International Journal of Primatology*, **28**(3): 529–550.

Freeland WJ. 1980. Mangabey (*Cercocebus albigena*) movement patterns in relation to food availability and fecal contamination. *Ecology*, **61**(6): 1297–1303.

Gillespie TR, Chapman CA. 2001. Determinants of group size in the red colobus monkey (*Procolobus badius*): An evaluation of the generality of the ecological-constraints model. *Behavioral Ecology and Sociobiology*, **50**(4): 329–338.

Gogarten JF, Bonnell TR, Brown LM, Campenni M, Wasserman MD, Chapman CA. 2014. Increasing group size alters behavior of a folivorous primate. *International Journal of Primatology*, **35**(2): 590–608.

Grueter CC, Li DY, Ren BP, Wei FW, van Schaik CP. 2009a. Dietary profile of *Rhinopithecus bieti* and its socioecological implications. *International Journal of Primatology*, **30**(4): 601–624.

Grueter CC, Li DY, Ren BP, Wei FW, Xiang ZF, van Schaik CP. 2009b. Fallback foods of temperate-living primates: a case study on snub-nosed monkeys. *American Journal of Physical Anthropology*, **140**(4): 700–715.

Grueter CC, Li DY, van Schaik CP, Ren BP, Long YC, Wei FW. 2008. Ranging of *Rhinopithecus bieti* in the Samage Forest, China. I. Characteristics of range use. *International Journal of Primatology*, **29**(5): 1121–1145.

Grueter CC, van Schaik CP. 2010. Evolutionary determinants of modular societies in colobines. *Behavioral Ecology*, **21**(1): 63–71.

Guo ST, Ji WH, Li BG, Li M. 2008. Response to a group of Sichuan snub-nosed monkeys to commercial logging in the Qinling Mountains, China. *Conservation Biology*, **22**(4): 1055–1064.

Guo ST, Li BG, Watanabe K. 2007. Diet and activity budget of *Rhinopithecus roxellana* in the Qinling Mountains, China. *Primates*, **48**(4): 268–276.

Hanya G, Bernard H. 2016. Seasonally consistent small home range and long ranging distance in *Presbytis rubicunda* in Danum Valley, Borneo. *International Journal of Primatology*, **37**(3): 390–404.

Hooge PN, Eichenlaub B. 1997. Animal movement extension to ArcView. Alaska Science Center – Biological Science Office, U.S. Geological Survey, Anchorage, AK, USA. http://gcmd.nasa.gov/records/USGS_animal_mvmt.html.

Huang ZH, Yuan PS, Huang HL, Tang XP, Xu WJ, Huang CM, Zhou QH. 2017. Effect of habitat fragmentation on ranging behavior of white-headed langurs in limestone forest in Southwest China. *Primates*, **58**(3): 423–434.

Huang ZP, Scott MB, Li YP, Ren GP, Xiang ZF, Cui LW, Xiao W. 2017. Black-and-white snub-nosed monkey (*Rhinopithecus bieti*) feeding behavior in a degraded forest fragment: clues to a stressed population. *Primates*, **58**(4): 517–524.

Isbell LA. 1991. Contest and scramble competition: Patterns of female aggression and ranging behavior among primates. *Behavioral Ecology*, **2**(2): 143–155.

Janson CH, van Schaik CP. 1988. Recognizing the many faces of primate food competition: methods. *Behaviour*, **105**(1-2): 165–186.

Kirkpatrick RC. 1996. Ecology and Behavior of the Yunnan Snub-nosed Langur *Rhinopithecus bieti* (Colobinae). Ph.D. dissertation, University of California, Davis.

Kirkpatrick RC, Grueter CC. 2010. Snub-nosed monkeys: multilevel societies across varied environments. *Evolutionary Anthropology,* **19**(3): 98–113.

Kirkpatrick RC, Long YC, Zhang T, Xiao L. 1998. Social organization and range use in the Yunnan snub-nosed monkey *Rhinopithecus bieti*. *International Journal of Primatology*, **19**(1): 13–51.

Kurihara Y, Hanya G. 2015. Comparison of feeding behavior between two different-sized groups of Japanese macaques (*Macaca fuscata yakui*). *American Journal of Primatology*, **77**(9): 986–1000.

Li BG, Chen C, Ji WH, Ren BP. 2000. Seasonal home range changes of the Sichuan snub-nosed monkey (*Rhinopithecus roxellana*) in the Qinling Mountains of China. *Folia Primatologica*, **71**(6): 375–386.

Li BG, Pan RL, Oxnard CE. 2002. Extinction of snub-nosed monkeys in China during the past 400 years. *International Journal of Primatology*, **23**(6): 1227–1244.

Li DY, Ren BP, Li BG, Li M. 2010. Range expansion as a response to increasing group size in the Yunnan snub-nosed monkey. *Folia Primatologica*, **81**(6): 315–329.

Li M, Liu ZJ, Gou JX, Ren BP, Pan RL, Su YJ, Funk SM, Wei FW. 2007. Phylogeography and population structure of the golden monkeys (*Rhinopithecus roxellana*): inferred from mitochondrial DNA sequences. *American Journal of Primatology*, **69**(11): 1195–1209.

Li YM. 2001. The seasonal diet of the Sichuan snub-nosed monkey (*Pygathrix roxellana*) in Shennongjia Nature Reserve, China. *Folia Primatologica*, **72**(1): 40–43.

Li YM. 2002. The seasonal daily travel in a group of Sichuan snub-nosed monkey (*Pygathrix roxellana*) in Shennongjia Nature Reserve, China. *Primates*, **43**(4): 271–276.

Li YM. 2004. The effect of forest clear-cutting on habitat use in Sichuan snub-nosed monkey (*Rhinopithecus roxellana*) in Shennongjia Nature Reserve, China. *Primates*, **45**(1): 69–72.

Li YM. 2006. Seasonal variation of diet and food availability in a group of Sichuan snub-nosed monkeys in Shennongjia Nature Reserve, China. *American Journal of Primatology*, **68**(3): 217–233.

Li YM. 2007. Terrestriality and tree stratum use in a group of Sichuan snub-nosed monkeys. *Primates*, **48**(3): 197–207.

Liu XC, Li F, Jiang J, Wang XJ, Li YM. 2016. Age-sex analysis for the diet of Sichuan snub-nosed monkeys (*Rhinopithecus roxellana*) in Shennongjia National Nature Reserve, China. *Primates*, **57**(4): 479–487.

Liu XC, Stanford CB, Li YM. 2013a. Effect of group size on time budgets of Sichuan snub-nosed monkeys (*Rhinopithecus roxellana*) in Shennongjia National Nature Reserve, China. *International Journal of Primatology*, **34**(2): 349–360.

Liu XC, Stanford CB, Yang JY, Yao H, Li YM. 2013b. Foods eaten by the Sichuan snub-nosed monkey (*Rhinopithecus roxellana*) in Shennongjia National Nature Reserve, China, in relation to nutritional chemistry. *American Journal of Primatology*, **75**(8): 860–871.

Liu ZJ, Liu GJ, Roos C, Wang ZM, Xiang ZF, Zhu PF, Wang BS, Ren BP, Shi FL, Pan HJ, Li M. 2015. Implications for genetics and current protected areas for conservation of 5 endangered primates in China. *Conservation Biology*, **29**(6): 1508–1517.

Luo MF, Pan HJ, Liu ZJ, Li M. 2012. Balancing selection and genetic drift at major histocompatibility complex class II genes in isolated populations of golden snub-nosed monkey (*Rhinopithecus roxellana*). *BMC Evolutionary Biology*, **12**: 207.

Oates JF. 1994. The natural history of African colobines. *In*: Davies AG, Oates JF. Colobine Monkeys: Their Ecology, Behaviour and Evolution. Cambridge, UK: Cambridge University Press, 75–128.

Qi XG, Garber PA, Ji WH, Huang ZP, Huang K, Zhang P, Guo ST, Wang XW, He G, Zhang P, Li BG. 2014. Satellite telemetry and social modeling offer new insights into the origin of primate multilevel societies. *Nature Communications*, **5**: 5296.

Scholz F, Kappeler PM. 2004. Effects of seasonal water scarcity on the ranging behavior of *Eulemur fulvus rufus*. *International Journal of Primatology*, **25**(3): 599–613.

Seaman DE, Millspaugh JJ, Kernohan BJ, Brundige GC, Raedeke KJ, Gitzen RA. 1999. Effects of sample size on kernel home range estimates. *Journal of Wildlife Management*, **63**(2): 739–747.

Snaith TV, Chapman CA. 2007. Primate group size and interpreting socioecological models: Do folivores really play by different rules? *Evolutionary Anthropology*, **16**(3): 94–106.

Stanford CB. 1991. The capped langur in Bangladesh: Behavioural ecology and reproductive tactics. *Contributions to Primatology*, **26**: 1–179.

Struhsaker TT. 1975. The Red Colobus Monkey. Chicago: University of Chicago Press.

Su YJ, Ren RM, Yan KH, Li JJ, Zhou Y, Zhu ZQ, Hu ZL, Hu YF. 1998. Preliminary survey of the home range and ranging behavior of golden monkeys (*Rhinopithecus* [*Rhinopithecus*] *roxellana*) in Shennongjia National Nature Reserve, Hubei, China. *In*: Jablonski NG. The Natural History of the Doucs and Snub-nosed Monkeys. Singapore: World Scientific Publishing, 255–268.

Tan CL, Guo ST, Li BG. 2007. Population structure and ranging patterns of *Rhinopithecus roxellana* in Zhouzhi National Nature Reserve, Shaanxi, China. *International Journal of Primatology*, **28**(3): 577–591.

Teichroeb JA, Sicotte P. 2009. Test of the ecological-constraints model on ursine colobus monkeys (*Colobus vellerosus*) in Ghana. *American Journal of Primatology*, **71**(1): 49–59.

Whitesides GH. 1989. Interspecific associations of Diana monkeys, *Cercopithecus diana*, in Sierra Leone, West Africa: biological significance or chance? *Animal Behaviour*, **37**(Part 5): 760–776.

Worton BJ. 1989. Kernel methods for estimating the utilization distribution in home-range studies. *Ecology*, **70**(1): 164–168.

Xiang ZF, Huo S, Xiao W, Quan RC, Grueter CC. 2007. Diet and feeding behavior of *Rhinopithecus bieti* at Xiaochangdu, Tibet: adaptations to a marginal environment. *American Journal of Primatology*, **69**(10): 1141–1158.

Xiang ZF, Yu Y, Yang M, Yang JY, Liao MY, Li M. 2011. Does flagship species tourism benefit conservation? A case study of the golden snub-nosed monkey in Shennongjia National Nature Reserve. *Chinese Science Bulletin*, **56**(24): 2553–2558.

Yang JY, Liu XC, Liao MY. 2014. Food distribution for a group of *Rhinopithecus roxellana* in Shennongjia, China. *Chinese Journal of Zoology*, **49**(4): 465–475. (in Chinese).

Zhang D, Fei H, Yuan S, Sun W, Ni Q, Cui L, Fan P. 2014. Ranging behavior of eastern hoolock gibbon (*Hoolock leuconedys*) in a northern montane forest in Gaoligongshan, Yunnan, China. *Primates*, **55**(2): 239–247.

Zhang P, Hu KJ, Yang B, Yang DH. 2016. Snub-nosed monkeys (*Rhinopithecus* spp.): conservation challenges in the face of environmental uncertainty. *Science Bulletin*, **61**(5): 345–348.

Zhou QH, Huang CM, Li YN, Cai XW. 2007. Ranging behavior of the Francois' langur (*Trachypithecus francoisi*) in the Fusui Nature Reserve, China. *Primates*, **48**(4): 320–323.

Zhou QH, Tang XP, Huang HL, Huang CM. 2011. Factors affecting the ranging behavior of white-headed langurs (*Trachypithecus leucocephalus*). *International Journal of Primatology*, **32**(2): 511–523.

Effects of age, sex and manual task on hand preference in wild *Rhinopithecus roxellana*

Wei-Wei Fu[1], Xiao-Wei Wang[1,*], Cheng-Liang Wang[1], Hai-Tao Zhao[1], Yi Ren[1], Bao-Guo Li[2,3,*]

[1] *Shaanxi Key Laboratory for Animal Conservation, Shaanxi Institute of Zoology, Xi'an Shaanxi* 710032*, China*
[2] *Shaanxi Key Laboratory for Animal Conservation, College of Life Sciences, Northwest University, Xi'an Shaanxi* 710069*, China*
[3] *Center for Excellence in Animal Evolution and Genetics, Chinese Academy of Sciences, Kunming Yunnan* 650223*, China*

ABSTRACT

Golden snub-nosed monkeys (*Rhinopithecus roxellana*), as typical arboreal group-living Old World monkeys, provide an appropriate animal model to research manual laterality and explore the factors affecting hand preference in non-human primates (NHP). This study investigated hand preference based on 63 subjects and four spontaneous manual tasks (including unimanual and bimanual feeding and grooming), and assessed the effects of age, gender and type of task on handedness in *R. roxellana*. A population-level left-handedness was found not only in the bimanual coordinated tasks (bimanual feeding and grooming), but also in one unimanual reaching task (unimanual feeding). There were no significant differences between the sexes in either direction or strength of hand preference among any task. However, a significant difference between adults and juveniles was found in the unimanual feeding task. This is the first report on handedness in unimanual and bimanual feeding tasks that require bipedal posture in wild *R. roxellana.* Furthermore, this study demonstrated spontaneous feeding tasks reported previously only in the quadrupedal posture in this species, supporting the importance of factors such as posture and task complexity in the evolution of primate manual lateralization.

Keywords: Handedness; Unimanual reaching; Bimanual coordination; Sex; Age

INTRODUCTION

Hand dominance is defined as a tendency to use one hand over the other to perform most activities. In humans, strong lateralization in handedness was found early and was considered the most obvious example of cerebral lateralization and an exclusive characteristic (Perelle & Ehrman, 2005). Over the past 20 years, however, numerous systematic investigations of handedness in non-human primates (NHP) have been published (Regaiolli et al., 2016). Interestingly, these studies have not shown a similar strong hand preference in NHP as observed in humans, with contradictory findings reported thus far (Regaiolli et al., 2018). Therefore, further study on manual laterality and the factors that affect hand preference in NHP is required.

As typical arboreal group-living Old World primates, golden snub-nosed monkeys (*Rhinopithecus roxellana,* Colobinae, Cercopithecidae) have been studied broadly in regard to hand preference in the wild (Liang & Zhang, 1998; Ma et al., 1988) and in captivity (Zhao et al., 2008, 2010). So far, remarkable achievements, such as the postural origins theory (MacNeilage et al., 1987) and task complexity theory (Fagot & Vauclair, 1991), have been obtained from research on hand preference in non-human primates (NHP). The postural origins theory proposes that arboreal primates preferentially use their left-hand for manual tasks (e.g., grasping food) (MacNeilage et al., 1987). The task complexity theory proposes that preferences

Received: 01 December 2017; Accepted: 29 October 2018; Online: 28 November 2018

Foundation items: This study was supported by the Major Program of National Natural Science Foundation of China (31730104), the National Natural Science Foundation of China (31572278, 31472014), the Foundation of Shaanxi Academy of Sciences of China (2016K-20) and the National Key Research and Development Program of China, Ministry of Science and Technology (2016YFC0503200)

[*]Corresponding authors, E-mail: wxw8008@126.com; baoguoli@nwu.edu.cn

DOI: 10.24272/j.issn.2095-8137.2019.023

and group-level biases of manual laterality more likely appear in bimanual coordinated tasks than in unimanual tasks (Fagot & Vauclair, 1991). Although these two theories are supported in *R. roxellana* (Zhao et al., 2008, 2010), some issues on the handedness of this species remain unclear. First, previous studies on NHP report that bipedal posture can elicit stronger hand preference than quadrupedal posture (Fagot & Vauclair, 1991; MacNeilage, 2008; Sanford et al., 1984). However, unimanual feeding tasks in *R. roxellana* have only been investigated in quadrupedal posture (Zhao et al., 2008), with existing research not yet revealing the influence of bipedal posture on handedness. Second, many studies on NHP species (e.g., chimpanzees (*Pan troglodytes*): Boesch, 1991; orangutans (*Pongo pygmaeus*): Cunningham et al., 1989; Rogers & Kaplan, 1996; *Hylobates* species (*Hylobates syndactylus*, *H. concolor* and *H. lar*): Stafford et al., 1990; tufted capuchin monkeys (*Cebus apella*): Lacreuse & Fragaszy, 1996, Westergaard & Suomi, 1993; Japanese macaques (*Macaca fuscata*): Kubota, 1990 and pig-tailed macaques (*M. leonina*): Zhao et al., 2016) have reported that the strength of hand preference is positively correlated with age. The maturation theory suggests different rates in the maturity of the two hemispheres from the fetal period (Hopkins & Bard, 1993), which has been widely accepted to explain the influence of age on handedness. Based on this theory, different growth rates affect the initial muscle movements of the fetus, with greater strength and unanimous direction of hand preference more likely found in mature individuals (Hopkins & Bard, 1993). Regarding *R. roxellana*, only one captive study has reported no age difference in hand preference (Liang & Zhang, 1998). In addition, although research has reported no significant effect of gender on hand preference in NHP (e.g., Meguerditchian et al., 2015; Meunier & Vauclair, 2007; Wells, 2002), several studies have reported significant differences between the sexes (e.g., Morino et al., 2017; Pan et al., 2011, 2013; Spinozzi & Truppa, 2002). Gender influence on hand preference has only been reported in *R. roxellana* based on one unimanual reaching task (Liang & Zhang, 1998; Ma et al., 1988; Zhao et al., 2008). Thus, the contradictory results of the influence of age and gender on hand preference in *R. roxellana* limit our understanding and highlight the need for further research on handedness in this species under different settings and manual tasks.

In this study, we observed handedness in a population of wild *R. roxellana* in relation to four spontaneous manual tasks (i.e., unimanual feeding, bimanual feeding, unimanual grooming and bimanual grooming). Based on the task complexity theory (Fagot & Vauclair, 1991) and previous reports on bimanual tasks in *R. roxellana* (Zhao et al., 2008, 2010), we hypothesized that hand biases of *R. roxellana* would be similarly evident for bimanual feeding, which has not been reported in this species previously. We also tested whether hand preference for feeding in the bipedal posture would be more biased than that in the quadrupedal posture based on earlier studies (Fagot & Vauclair, 1991; MacNeilage, 2008; Sanford et al., 1984). Importantly, we compared the age and gender differences in hand preference with previous studies on *R. roxellana* (Liang & Zhang, 1998; Ma et al., 1988; Zhao et al., 2008) as well as handedness differences between *R. roxellana* and other NHP, including closely related *R. bieti* (Pan et al., 2011, 2013; Jablonski, 1998). This study on hand preference in *R. roxellana* will provide additional behavioral evidence on the evolution of handedness in NHP.

MATERIALS AND METHODS

Study site and species

This study was carried out in Zhouzhi National Nature Reserve on the northern slopes of the Qinling Mountains, Shaanxi, China. Two wild troops of *R. roxellana* live at the study site, i.e., the East Ridge troop and West Ridge troop (WRT). Our focus population was provisioned at Sanchakou (1 646 m a.s.l.) in Gongnigou valley (N33°48′68″, E108°16′18″) within the WRT. Field assistants searched for the focal population and attracted the monkeys to the provisioning site at 0900 h every day. Approximately 200 g of dispersed food (corn, apples and radishes) were provided per monkey per day at three time points (1000 h, 1200 h and 1400 h). Compared with the total daily diet of *R. roxellana*, the energy intake of the provisioned food was small and thus its influence on natural behavior was minimal (Li & Zhao, 2007). When the focal population was well habituated to the presence of observers, we identified all focal individuals via physical characteristics and maintained a distance of 5–50 m (Li et al., 2000; Zhang et al., 2006). The focal individuals were divided into four classes: juvenile females (1–3 years), juvenile males (1–5 years), adult females (>5 years) and adult males (>7 years) (Zhang et al., 2006). In total, 63 individuals were involved, consisting of 15 adult males, 27 adult females, 12 juvenile males and 9 juvenile females in 11 one-male multi-female units and the sole all-male unit in the study.

Data collection

The data were collected over 138 d. A total of 6 030 manual observational data from 63 subjects from September 2010 to May 2011 were collected by focus animal sampling (Altmann, 1974) and behavioral sampling (Martin & Bateson, 2007). Four types of manual task were identified and collected. Under common conditions, one hand is considered dominant and the other hand is considered subordinate. Thus, data were recorded as left-dominant/right-subordinate (L) or right-dominant/left-subordinate (R) in all types of task.

(1) Unimanual feeding: This simple reaching task was observed when a subject fed on the ground in the bipedal posture. The hand that first grasped the food and brought it to its mouth was deemed dominant, whereas the other hand, which was unused or placed on its hind limb, was deemed subordinate. Data were recorded when a focal individual first made contact with food at the same site.

(2) Bimanual feeding: Bimanual feeding was defined as a coordinated bimanual action and was frequently observed when feeding in trees. One hand (subordinate) was used to draw thin branches to the focal individual, while the opposite hand (dominant) was used to pick leaves or bark from the branches and bring them to its mouth (Meguerditchian et al.,

2010). If the focal individual continued feeding in the same position, the behavior was only recorded once. If the focal individual changed position, like in the unimanual feeding task, the behavior was recorded a second time.

(3) Unimanual grooming: Grooming is a common behavior in highly social primates. As described previously, unimanual grooming was recorded when the focal individual used only one hand (dominant) to perform grooming, with the other hand (subordinate) placed on its hind limbs or used for postural support (Hopkins et al., 2007). Following the method described by Hopkins et al. (2007), real-time recording over a 5-min observation period was used for data collection on one focal individual. Within the 5-min observation period, data on the focal individual were collected every 15 s. During observation, mouths were sometimes involved in the grooming action, which was ignored due to its low frequency and limited influence on the determination of hand preference. Observation ceased if the focal individual stopped grooming within the 5-min observation period and did not groom in the following 30 s. A new 5-min observation period was continued if the focal individual did not stop grooming after the initial 5-min observation period, and when no other individuals performed grooming within visible distance.

(4) Bimanual grooming: Bimanual grooming was defined as coordinated bimanual action in which the individual used both hands to perform grooming. The dominant hand performed grooming while the subordinate hand was used to hold or stabilize the area around the grooming site (Hopkins et al., 2007). Data collection during bimanual grooming also met the criteria mentioned above for unimanual grooming.

Data analyses

Three important indexes were used for the determination of hand preference. First, to identify the degree of individual lateral bias, the handedness index (HI) for each focal subject was calculated based on the following formula: (right-hand use–left-hand use)/(right-hand use+left-hand use). The HI varied between -1.0 and 1.0, indicating left- and right-hand bias, respectively. Second, the absolute value of HI (ABS-HI) was used to reflect the strength of individual-level hand preference. Third, the binomial Z-scores were used to determine whether the frequency of left- or right-hand use exceeded that expected by chance (50% right-hand use). Based on the Z-scores, our subjects were categorized as right-handed ($z \geq 1.96$), left-handed ($z \leq -1.96$) or ambipreferent ($1.96 > z > -1.96$).

One-sample *t*-tests of the HI scores were used to evaluate whether the group was ambipreferent or lateralized in hand use for each task (Hopkins, 1999) and Mann-Whitney *U*-tests were used for determination of age and gender effects on hand preference. The Spearman correlation test was applied to evaluate the relationship between the number of data points per subject and HI/ABS-HI scores. SPSS v.23.0 and two-tailed significance at $P \leq 0.05$ were used in all analyses.

RESULTS

There was no significant correlation between sample size and HI scores (unimanual feeding: $r=0.327$, $P=0.111$; bimanual feeding: $r=-0.109$, $P=0.699$; unimanual grooming: $r=0.003$, $P=0.992$; bimanual grooming: $r=0.084$, $P=0.598$) and ABS-HI scores (unimanual feeding: $r=-0.324$, $P=0.114$; bimanual feeding: $r=-0.109$, $P=0.699$; unimanual grooming: $r=0.131$, $P=0.655$; bimanual grooming: $r=0.136$, $P=0.409$), suggesting that individual differences in the total number of responses did not skew the distribution of handedness values.

For unimanual feeding, the mean number of manual data per subject was 49.92 ± 2.29 (range: 31–67) and the mean HI and ABS-HI scores were -0.21 ± 0.05 (range: -0.51–0.33) and 0.29 ± 0.03 (range: 0.10–0.51), respectively (Table 1); for bimanual feeding, the mean number of manual data per subject was 57.93 ± 6.98 (range: 30–126) and the mean HI and ABS-HI scores were -0.39 ± 0.06 (range: -0.88 to -0.05) and 0.39 ± 0.06 (range: 0.05–0.88), respectively (Table 2); for unimanual grooming, the mean number of manual data per subject was 46.57 ± 5.96 (range: 30–111) and the mean HI and ABS-HI scores were -0.13 ± 0.07 (range: -0.60–0.29) and 0.23 ± 0.05 (range: 0.00–0.60), respectively (Table 3); for bimanual grooming, the mean number of manual data per subject was 77.54 ± 5.66 (range: 30–163) and the mean HI and ABS-HI scores were -0.25 ± 0.04 (range: -0.85–0.54) and 0.33 ± 0.03 (range: 0.01–0.85), respectively (Table 4).

When using Z-scores as the index for hand preference classification to determine individual-level hand preference, 38% individuals in unimanual feeding, 67% in bimanual feeding, 36% in unimanual grooming and 67% in bimanual grooming showed left-handed preference (Figure 1). No individual showed right-handed preference in bimanual feeding, and only 12%, 7% and 10% showed right-handed preference in unimanual feeding, unimanual grooming and bimanual grooming, respectively. One sample *t*-tests on the HI scores revealed significant population-level left-hand preferences for unimanual feeding task ($t_{24}=-4.447$, $P<0.001$), bimanual feeding task ($t_{14}=-6.325$, $P<0.001$) and bimanual grooming task ($t_{41}=-5.722$, $P<0.001$) but not for unimanual grooming task ($t_{13}=-1.859$; $P=0.086$).

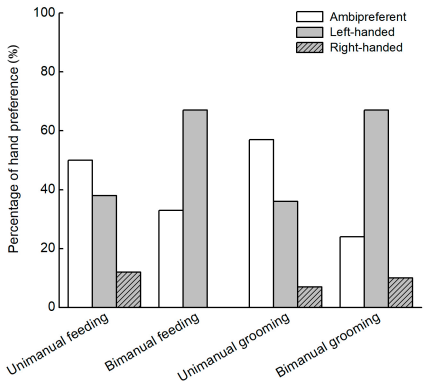

Figure 1 Percentage of subjects exhibiting right-hand, left-hand and ambidextrous preference in unimanual feeding (*n*=25), bimanual feeding (*n*=15), unimanual grooming (*n*=14) and bimanual grooming (*n*=42) tasks in *R. roxellana*

Table 1 Hand preference for unimanual feeding task in *R. roxellana* (*n*=25)

Animal ID	Age	Sex	L[a]	R[b]	Percentage (%)[c]	HI	ABS-HI	Z-scores	Preference[d]
BHX	Adult	F	21	12	63.64	−0.27	0.27	−1.57	Ambi
BX	Adult	F	38	23	62.30	−0.25	0.25	−1.92	Ambi
DAH	Adult	F	34	26	56.67	−0.13	0.13	−1.03	Ambi
F2	Adult	F	36	29	55.38	−0.11	0.11	−0.87	Ambi
HUT	Adult	F	36	16	69.23	−0.38	0.38	−2.77	Left
JD	Adult	F	34	26	56.67	−0.13	0.13	−1.03	Ambi
WSF1	Adult	F	27	12	69.23	−0.38	0.38	−2.40	Left
ZFX	Adult	F	20	39	66.10	0.32	0.32	2.47	Right
JB	Adult	M	28	19	59.57	−0.20	0.20	−0.90	Ambi
RX	Adult	M	36	29	55.38	−0.11	0.11	−0.87	Ambi
SH	Adult	M	34	20	62.96	−0.37	0.37	0.32	Ambi
WX	Adult	M	34	28	54.84	−0.10	0.10	−0.64	Ambi
XH	Adult	M	30	20	60.00	−0.19	0.19	−1.66	Ambi
BB	Adult	M	31	16	65.96	−0.32	0.32	−2.19	Left
FP	Adult	M	22	40	64.52	0.29	0.29	2.29	Right
HT	Adult	M	15	30	66.67	0.33	0.33	2.24	Right
JBJ20	Juvenile	F	22	17	56.41	−0.13	0.13	−0.80	Ambi
RXJ20	Juvenile	F	24	13	64.86	−0.30	0.30	−1.81	Ambi
BBJ20	Juvenile	F	26	11	70.27	−0.41	0.41	−2.47	Left
BBJ30	Juvenile	F	27	10	72.97	−0.46	0.46	−2.79	Left
JBJ30	Juvenile	F	30	12	71.43	−0.43	0.43	−2.78	Left
SH	Juvenile	F	49	18	73.13	−0.51	0.51	−3.20	Left
GPJ21	Juvenile	M	22	17	56.41	−0.13	0.13	−0.80	Ambi
JBJ41	Juvenile	M	41	17	70.69	−0.41	0.41	−3.15	Left
RXJ41	Juvenile	M	23	8	74.19	−0.48	0.48	−2.69	Left

[a]: Number of responses made with the left hand. [b]: Number of responses made with the right hand. [c]: Percentage of use of the preferred hand. [d]: Category of hand preference based on Z-scores. M: Male; F: Female.

Table 2 Hand preference for bimanual feeding task in *R. roxellana* (*n*=15)

Animal ID	Age	Sex	L[a]	R[b]	Percentage (%)[c]	HI	ABS-HI	Z-scores	Preference[d]
XL	Adult	F	27	21	0.56	−0.13	0.13	−0.87	Ambi
DBC	Adult	F	27	18	0.60	−0.20	0.20	−1.34	Ambi
QQ	Adult	F	24	15	0.62	−0.23	0.23	−1.44	Ambi
RH	Adult	F	21	13	0.62	−0.24	0.24	−1.37	Ambi
XBC	Adult	F	21	19	0.53	−0.05	0.05	−0.32	Ambi
HH	Adult	F	42	24	0.64	−0.27	0.27	−2.22	Left
GTT	Adult	F	42	12	0.78	−0.56	0.56	−4.08	Left
DH	Adult	F	27	3	0.90	−0.80	0.80	−4.38	Left
BB	Adult	M	78	48	0.62	−0.24	0.24	−2.67	Left
JB	Adult	M	78	27	0.74	−0.49	0.49	−4.98	Left
WS	Adult	M	48	27	0.64	−0.28	0.28	−2.42	Left
SH	Adult	M	54	18	0.75	−0.50	0.50	−4.24	Left
WB	Adult	M	45	3	0.94	−0.88	0.88	−6.06	Left
JBJ41	Juvenile	M	33	12	0.73	−0.47	0.47	−3.13	Left
XD	Juvenile	M	33	9	0.79	−0.57	0.57	−3.70	Left

[a]: Number of responses made with the left hand. [b]: Number of responses made with the right hand. [c]: Percentage of use of the preferred hand. [d]: Category of hand preference based on Z-scores. M: Male; F: Female.

Table 3 Hand preference for unimanual grooming task in *R. roxellana* (*n*=14)

Animal ID	Age	Sex	L[a]	R[b]	Percentage (%)[c]	HI	ABS-HI	Z-scores	Preference[d]
HB	Adult	F	24	27	0.53	0.06	0.06	0.42	Ambi
HH	Adult	F	18	15	0.55	−0.09	0.09	−0.52	Ambi
WSF1	Adult	F	12	18	0.60	0.20	0.20	1.10	Ambi
WS	Adult	M	23	42	0.65	0.29	0.29	2.36	Right
BB	Adult	M	48	15	0.76	−0.52	0.52	−4.16	Left
JB	Adult	M	33	12	0.73	−0.47	0.47	−3.13	Left
GP	Adult	M	69	42	0.62	−0.24	0.24	−2.56	Left
SH	Adult	M	24	31	0.56	0.13	0.13	0.94	Left
SHJ30	Juvenile	F	21	12	0.64	−0.27	0.27	−1.57	Ambi
RXJ20	Juvenile	F	18	12	0.60	−0.20	0.20	−1.10	Ambi
GPJ20	Juvenile	F	24	6	0.80	−0.60	0.60	−3.29	Left
GPJ21	Juvenile	M	20	16	0.56	−0.11	0.11	−0.67	Ambi
XD	Juvenile	M	21	19	0.53	−0.05	0.05	−0.32	Ambi
WSJ21	Juvenile	M	15	15	0.50	0.00	0.00	0.00	Ambi

[a]: Number of responses made with the left hand. [b]: Number of responses made with the right hand. [c]: Percentage of use of the preferred hand. [d]: Category of hand preference based on Z-scores. M: Male; F: Female.

The effects of sex on the direction and strength of hand preference were assessed using the HI and ABS-HI scores, respectively. For unimanual feeding, the mean HI score per subject was −0.26, *SE*=0.06 for females, −0.15, *SE*=0.08 for males; the mean ABS-HI score per subject was 0.30, *SE*=0.04 for females and 0.27, *SE*=0.04 for males; there were no differences between the sexes in HI (N_a=14, N_b=11; *U*=56.5, *P*=0.261) or ABS-HI scores (N_a=14, N_b=11; *U*=64.00, *P*=0.475) (Figure 2A). For bimanual feeding, the mean HI score per subject was −0.31, *SE*=0.09 for females and −0.49, *SE*=0.08 for males; the mean ABS-HI score per subject was 0.31, *SE*=0.09 for females and 0.49, *SE*=0.08 for males; no differences were found between the sexes in HI (N_a=8, N_b=7; *U*=12.50, *P*=0.073) or ABS-HI scores (N_a=8, N_b=7; *U*=12.50, *P*=0.073) (Figure 2B). For unimanual grooming, the mean HI score per subject was −0.15, *SE*=0.11 for females and −0.12, *SE*=0.09 for males; the mean ABS-HI score per subject was 0.24, *SE*=0.08 for females and 0.23, *SE*=0.07 for males; no differences were found between the sexes in HI (N_a=6, N_b=8; *U*=22.00, *P*=0.795) or ABS-HI scores (N_a=6, N_b=8; *U*=24.00, *P*=1.000) (Figure 2C). For bimanual grooming, the mean HI score per subject was −0.24, *SE*=0.05 for females and −0.25, *SE*=0.07 for males; the mean ABS-HI score per subject was 0.32, *SE*=0.04 for females and 0.35, *SE*=0.03 for males; there were no differences between the sexes in HI (N_a=27, N_b=17; *U*=186.00, *P*=0.497) or ABS-HI scores (N_a=25, N_b=17; *U*=173.00, *P*=0.311) (Figure 2D).

The effects of age on hand preference were also assessed using the HI and ABS-HI scores. For unimanual feeding, the mean HI score per subject was −0.16, *SE*=0.06 for adults and −0.36, *SE*=0.05 for juveniles, and juveniles showed more left-handedness than adults (N_a=30, N_b=12; *U*=137.50, *P*=0.236); the mean ABS-HI score per subject was 0.24, *SE*=0.03 for adults and 0.36, *SE*=0.05 for juvenile, and juveniles showed a stronger hand preference than adults (N_a=16, N_b=9; *U*=30.00, *P*=0.017) (Figure 3A). For bimanual feeding, the mean HI score per subject was −0.37, *SE*=0.07 for adults and −0.52, *SE*=0.05 for juveniles; the mean ABS-HI score per subject was 0.37, *SE*=0.07 for adults and 0.52, *SE*=0.05 for juveniles; there were no differences between juveniles and adults in HI (N_a=13, N_b=2; *U*=7.00, *P*=0.308) or ABS-HI scores (N_a=13, N_b=2; *U*=7.00, *P*=0.308) (Figure 3B). For unimanual grooming, the mean HI score per subject was −0.08, *SE*=0.10 for adults and −0.21, *SE*=0.08 for juveniles; the mean ABS-HI score per subject was 0.25, *SE*=0.06 for adults and 0.20, *SE*=0.08 for juveniles; no differences were found between juveniles and adults in HI (N_a=8, N_b=6; *U*=16.00, *P*=0.300) or ABS-HI scores (N_a=8, N_b=6; *U*=19.50, *P*=0.559) (Figure 3C). For bimanual grooming, the mean HI score per subject was −0.20, *SE*=0.05 for adults and −0.36, *SE*=0.07 for juveniles; the mean ABS-HI score per subject was 0.32, *SE*=0.03 for adults and 0.37, *SE*=0.06 for juveniles; there were no differences between juveniles and adults in HI (N_a=30, N_b=12; *U*=137.50, *P*=0.236) or ABS-HI scores (N_a=30, N_b=12; *U*=167.00, *P*=0.717) (Figure 3D).

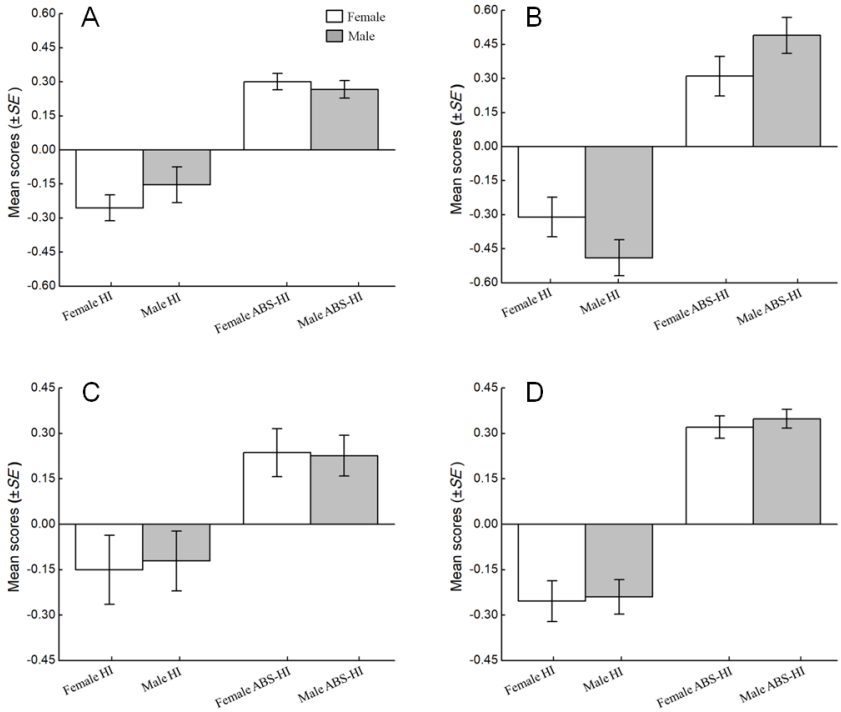

Figure 2 Influence of sex on hand preference among four types of task in *R. roxellana*

A: Unimanual feeding task; B: Bimanual feeding task; C: Unimanual grooming task; D: Bimanual grooming task. Values are means±*SE*.

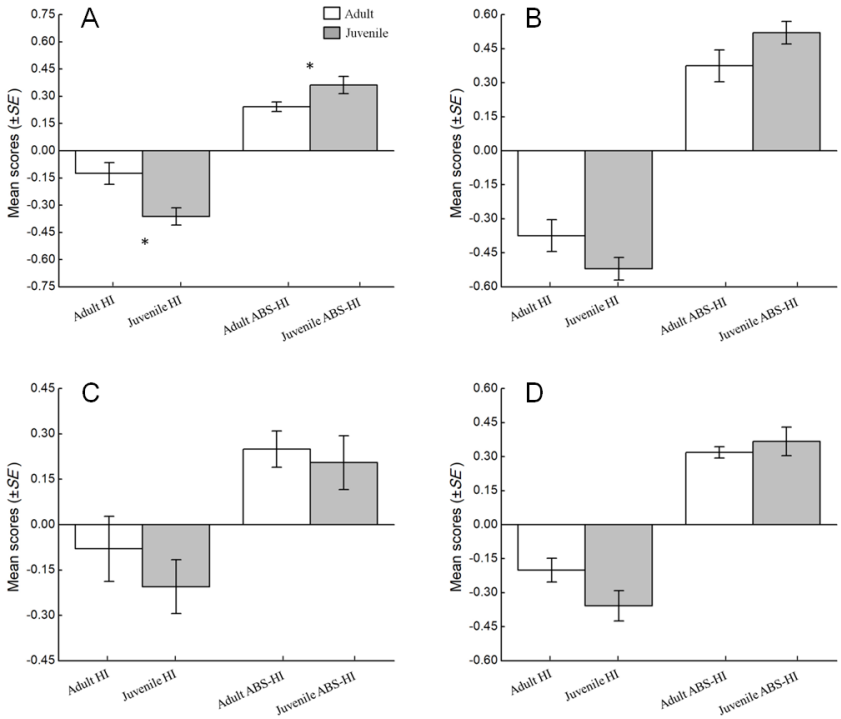

Figure 3 Influence of age on hand preference among four types of task in *R. roxellana*

A: Unimanual feeding task; B: Bimanual feeding task; C: Unimanual grooming task; D: Bimanual grooming task. Values are means±*SE*. * indicates significant difference between adults and juveniles (P<0.05).

Table 4 Hand preference for bimanual grooming task in *R. roxellana* (*n*=42)

Animal ID	Age	Sex	L[a]	R[b]	Percentage (%)[c]	HI	ABS-HI	Z-scores	Preference[d]
BHX	Adult	F	59	58	0.50	−0.01	0.01	−0.09	Ambi
GPF6	Adult	F	37	31	0.54	−0.09	0.09	−0.73	Ambi
JD	Adult	F	46	55	0.54	0.09	0.09	0.9	Ambi
NZ	Adult	F	32	47	0.59	0.19	0.19	1.69	Ambi
FF	Adult	F	18	51	0.74	0.48	0.48	3.97	Right
KK	Adult	F	41	61	0.60	0.2	0.2	1.98	Right
DBC	Adult	F	78	47	0.62	−0.25	0.25	−2.77	Left
DH	Adult	F	41	16	0.72	−0.44	0.44	−3.31	Left
GGT	Adult	F	23	11	0.68	−0.35	0.35	−2.06	Left
HB	Adult	F	49	23	0.68	−0.36	0.36	−3.06	Left
HH	Adult	F	34	19	0.64	−0.28	0.28	−2.06	Left
HUT	Adult	F	52	32	0.63	−0.24	0.24	−2.09	Left
HX	Adult	F	68	26	0.72	−0.45	0.45	−4.33	Left
LZ	Adult	F	99	38	0.72	−0.45	0.45	−5.21	Left
RH	Adult	F	50	27	0.65	−0.3	0.3	−2.62	Left
WXF1	Adult	F	83	36	0.70	−0.39	0.39	−4.31	Left
WXF2	Adult	F	95	54	0.64	−0.28	0.28	−3.36	Left
YL	Adult	F	67	38	0.64	−0.28	0.28	−2.83	Left
ZFX	Adult	F	92	43	0.68	−0.36	0.36	−4.22	Left
BZT	Adult	M	26	23	0.53	−0.06	0.06	−0.43	Ambi
YB	Adult	M	22	10	0.69	−0.38	0.38	−2.12	Ambi
FP	Adult	M	16	54	0.77	0.54	0.54	4.54	Right
JB	Adult	M	29	49	0.63	0.26	0.26	2.26	Right
FQ	Adult	M	29	15	0.67	−0.33	0.33	−1.98	Left
GP	Adult	M	47	16	0.75	−0.49	0.49	−3.91	Left
SH	Adult	M	107	56	0.66	−0.31	0.31	−3.99	Left
WS	Adult	M	34	15	0.69	−0.39	0.39	−2.71	Left
XH	Adult	M	35	18	0.66	−0.32	0.32	−2.34	Left
BBJ40	Juvenile	F	32	22	0.59	−0.19	0.19	−1.36	Ambi
SHJ40	Juvenile	F	28	13	0.68	−0.37	0.37	−2.34	Left
AMUJ412	Juvenile	M	32	23	0.58	−0.16	0.16	−1.21	Ambi
BBJ20	Juvenile	M	19	21	0.53	0.05	0.05	0.32	Ambi
GPJ31	Juvenile	M	20	10	0.67	−0.33	0.33	−1.83	Ambi
GPJ20	Juvenile	M	38	3	0.93	−0.85	0.85	−5.47	Left
HSJ20	Juvenile	M	75	29	0.72	−0.44	0.44	−4.51	Left
JBJ41	Juvenile	M	83	54	0.61	−0.21	0.21	−2.48	Left
RXJ41	Juvenile	M	57	21	0.73	−0.46	0.46	−4.08	Left
RXJ410	Juvenile	M	25	11	0.69	−0.39	0.39	−2.33	Left
SHJ20	Juvenile	M	26	6	0.81	−0.63	0.63	−3.54	Left
WSSJ	Juvenile	M	33	17	0.66	−0.32	0.32	−2.26	Left

[a]: Number of responses made with the left hand. [b]: Number of responses made with the right hand. [c]: Percentage of use of the preferred hand. [d]: Category of hand preference based on Z-scores. M: Male; F: Female.

DISCUSSION

Bimanual feeding was the first task reported in hand preference research and the third spontaneous bimanual task, after bimanual mount reaching and grooming, reported in *R. roxellana* (Zhao et al., 2008, 2010). Population-level hand preference in bimanual feeding and grooming tasks supports our hypothesis that hand preference in bimanual feeding would be similar to that in bimanual grooming (Zhao et al., 2010). In addition, the population-level hand preference in bimanual feeding and bimanual grooming, but not in unimanual grooming, are in accordance with the task complexity theory (Fagot & Vauclair, 1991). Based on that theory, population-level hand preference is not elicited in simple reaching tasks (e.g., unimanual grooming), which has also been reported in other studies (Meguerditchian et al., 2010; Zhao et al., 2008, 2010). Therefore, our unimanual feeding results are not consistent with the task complexity theory. This could be explained by the relative complexity of our unimanual feeding task, in which the main provisioned food (corn) was very small and light, requiring precision grasping. Accurate operation is a determinant for complex tasks (Blois-Heulin et al., 2006; Meunier & Vauclair, 2007). Therefore, feeding on corn might be motorically more complex than feeding on other foods (e.g., apples and radishes), and is thus more likely to elicit greater hand preference.

In the current study, *R. roxellana* exhibited more left-handedness than right-handedness in all four tasks, which supports the postural origins theory (MacNeilage et al., 1987). Moreover, the finding that the proportion of ambidextrously-handed individuals was higher than left-handed or right-handed individuals in both unimanual tasks (based on individual Z-scores) may be linked to the increase in time spent on the ground. This is because increased activities on the ground can relax selective pressure on the strong hand to support body weight and increase opportunities to use both hands (Morino et al., 2017).

We also reported unimanual feeding in the bipedal posture and a population-level hand preference in this posture, different from individual-level hand preference observed in the quadrupedal posture for the same species (Zhao et al., 2008). This finding supports our hypothesis and is in accordance with other studies reporting that bipedal posture can elicit stronger hand preference than quadrupedal posture (Fagot & Vauclair, 1991; MacNeilage, 2008; Sanford et al., 1984). The reason for the increase of hand preference in the bipedal posture is that this posture can constrain the choice of left or right hand due to postural demands, which results in the hand being used to support the body not being used for reaching (Fagot & Vauclair, 1991; MacNeilage, 2008; Sanford et al., 1984). However, previous research on *R. bieti* implies increased right-hand bias in the bipedal posture compared to that in the quadrupedal posture (Pan et al., 2013), in disagreement with our result. These discrepancies may be related to the different species or different wild and captive settings.

There were no differences in the direction or strength of hand preference between the sexes in any task in *R. roxellana*, which agrees with previous research on the same species (in captivity: Liang & Zhang, 1998; in the wild: Zhao et al., 2008) and is also supported by several other studies (e.g., chimpanzees: Chapelain & Hogervorst, 2009; Corp & Byrne, 2004; gorillas (*Gorilla gorilla*): Meguerditchian et al., 2010; white-faced capuchins (*C. capucinus*): Meunier & Vauclair, 2007; pig-tailed macaques (*M. leonina*): Zhao et al., 2016). These findings reveal similar hemisphere specialization between the sexes in NHP. However, previous findings on *R. bieti* suggest that males prefer the left hand significantly more often than do females, with the sex effect on hand preference even shown to be task- (Pan et al., 2011) and posture-specific (Pan et al., 2013). The differential findings between *R. roxellana* and *R. bieti* might correlate to the sexual dimorphism between the two species (Pan et al., 2011). As *R. bieti* is sexually more dimorphic than *R. roxellana* (Jablonski & Pan, 1995), this might lead to a stronger sex effect on hand preference (Pan et al., 2011).

The current study also showed no significant differences between juvenile and adult *R. roxellana* in the direction or strength of hand preference for all tasks, except for unimanual feeding, in which more left-handedness and greater handedness were found in juveniles than in adults. Based on Morino et al. (2017), an increase in time spend on the ground by individuals can increase opportunities to use both hands (Morino et al., 2017). Therefore, the increase in time spent on the ground by adults resulted in greater liberation of their right hand compared with that of juveniles, which may explain the more ambidextrous adults (62.5%) than juveniles (33.3%) (Table 1) in this arboreal primate. Correspondingly, the greater ambidexterity in adults led to a decrease in the rate of one hand usage and showed a weakening in the strength of hand preference compared with that observed in juveniles. Moreover, our findings on the effects of age on hand preference did not support the maturation theory (Hopkins & Bard, 1993) and the difference may relate to the selection of subjects. Unfortunately, we failed to collect data on infant behaviors in the study. The main reason is that infants rarely groomed others or themselves and often fed on the ground alone. Thus, the existing data did not allow us to further analyze age influence on hand preference and prevented further explanation of the ontogenetic development of hand preference in NHP (Hopkins & Bard, 1993). A manual task shared among all age-classes will be needed in future studies of this arboreal primate species.

In conclusion, this is the first report on spontaneous unimanual and manual feeding in the bipedal posture in wild *R. roxellana*, with results showing population-level handedness in both tasks. The unimanual feeding results may be linked to the need for accurate operation when feeding on corn on the ground and the bipedal posture therefore elicited greater hand preference than quadrupedal posture. A population-level handedness was also found in manual grooming, but not in unimanual grooming, which is in accordance with previous study on *R. roxellana* (Zhao et al., 2010), with both supporting the theory of task complexity (Fagot & Vauclair, 1991). Moreover, there were no significant differences in the direction or strength of hand preference between the sexes in any

of the tasks. Furthermore, a significant effect of age on the direction and strength of hand preference was only found in unimanual feeding. We did not compare the level of individual hand specialization in different manual tasks because only three out of 63 individuals (5%) were observed in all four tasks. Further study should focus on individual hand specialization among tasks and investigate tasks shared among all age-classes in *R. roxellana* to clarify hand preference in NHP and facilitate comparative research between non-human and human primates.

COMPETING INTERESTS

The authors declare that they have no competing interests.

AUTHORS' CONTRIBUTIONS

B.G.L., X.W.W., and W.W.F. conceived and designed the study. W.W.F., C.L.W., and H.T.Z. collected the data. W.W.F., X.W.W., and Y.R. revised the manuscript. All authors read and approved the final version of the manuscript.

ACKNOWLEDGEMENTS

We thank to the Director and staff of Zhouzhi National Nature Reserve for their permission to conduct this research. We also thank to Song-Tao Guo, Xiao-Guang Qi, Pei Zhang, Kang Huang, Dong Zhang, and Wei Wei from College of Life Sciences, Northwest University for their help during the study.

REFERENCES

Altmann J. 1974. Observational study of behavior: sampling methods. *Behaviour,* **49**(3): 227–267.

Blois-Heulin C, Guitton JS, Nedellec-Bienvenue D, Ropars L, Vallet E. 2006. Hand preference in unimanual and bimanual tasks and postural effect on manual laterality in captive red-capped mangabeys (*Cercocebus torquatus torquatus*). *American Journal of Primatology,* **68**(5): 429–444.

Boesch C. 1991. Handedness in wild chimpanzees. *International Journal of Primatology,* **12**(6): 541–558.

Chapelain AS, Hogervorst E. 2009. Hand preferences for bimanual coordination in 29 bonobos (*Pan paniscus*). *Behavioural Brain Research,* **196**(1): 15–29.

Corp N, Byrne RW. 2004. Sex difference in chimpanzee handedness. *American Journal of Physical Anthropology,* **123**(1): 62–68.

Cunningham D, Forsythe C, Ward JP. 1989. A report of behavioral lateralization in an infant orang-utan (*Pongo pygmaeus*). *Primates,* **30**(2): 249–253.

Fagot J, Vauclair J. 1991. Manual laterality in nonhuman primates: a distinction between handedness and manual specialization. *Psychological Bulletin,* **109**(1): 76–89.

Hopkins WD, Bard KA. 1993. The ontogeny of lateralized behavior in nonhuman primates with special reference to chimpanzees (*Pan troglodytes*). *In*: Ward JP, Hopkins WD. Primate Laterality: Current Behavioral Evidence of Primate Asymmetries. New York: Springer Verlag, 251–265.

Hopkins WD. 1999. On the other hand: statistical issues in the assessment and interpretation of hand preference data in nonhuman primates. *International Journal of Primatology,* **20**(6): 851–866.

Hopkins WD, Russell JL, Remkus M, Freeman H, Schapiro SJ. 2007. Handedness and grooming in *Pan troglodytes*: comparative analysis between findings in captive and wild individuals. *International Journal of Primatology,* **28**(6): 1315–1326.

Jablonski NG. 1998. The evolution of doucs and snub-nosed monkeys and the question of phyletic unity of the odd-nosed colobines. *In*: Jablonski NJ. The Natural History of the Doucs and Snub-Nosed Monkeys. Singapore: World Scientific, 13–52.

Jablonski NG, Pan R. 1995. Sexual dimorphism in the snub-nosed langurs (*Colobinae: Rhinopithecus*). *American Journal of Physical Anthropology*, **96**(3): 251–272.

Kubota K. 1990. Preferred hand use in the japanese macaque troop, arashiyama-R, during visually guided reaching for food pellets. *Primates,* **31**(3): 393–406.

Lacreuse A, Fragaszy DM. 1996. Hand preferences for a haptic searching task by tufted capuchins (*Cebus apella*). *International Journal of Primatology,* **17**(4): 613–632.

Li BG, Chen C, Ji WH, Ren BP. 2000. Seasonal home range changes of the Sichuan snub-nosed monkey (*Rhinopithecus roxellana*) in the Qinling Mountains of China. *Folia Primatological* (*Basel*), **71**(6): 375–386.

Li BG, Zhao DP. 2007. Copulation behavior within one-male groups of wild *Rhinopithecus roxellana* in the Qinling Mountains of China. *Primates*, **48**(3): 190–196.

Liang B, Zhang SY. 1998. Hand preference in food reaching in Sichuan golden monkeys (*Rhinopithecus roxellana*). *Acta Theriol Sinica,* **18**(2): 107–111.

Ma YY, Tian YF, Deng ZY. 1988. The hand preference of *Presbytis* (PR), *Rhinopithecus* (RH), and *Hylobates* (HY) in picking up food. *Acta Anthropol Sinica,* **7**(2): 177–181. (in Chinese)

MacNeilage PF, Studdert-Kennedy MG, Lindblom B. 1987. Primate handedness reconsidered. *Behavioral and Brain Sciences,* **10**(2): 247–263.

MacNeilage PF. 2008. Present status of the postural origins theory. *In*: Hopkins WD. The Evolution of Hemispheric Specializations in Primates. Amsterdam: Elsevier, 59–92.

Martin P, Bateson P. 2007. Measuring Behaviour: An Introductory Guide. 3rd ed. Cambridge: Cambridge University Press.

Meguerditchian A, Calcutt SE, Lonsdorf EV, Ross SR, Hopkins WD. 2010. Brief communication: captive gorillas are right-handed for bimanual feeding. *American Journal of Physical Anthropology,* **141**(4): 638–645.

Meguerditchian A, Phillips KA, Chapelain A, Mahovetz LM, Milne S, Stoinski T, Bania A, Lonsdorf E, Schaeffer J, Russell J, Hopkins WD. 2015. Handedness for unimanual grasping in 564 great apes: the effect on grip morphology and a comparison with hand use for a bimanual coordinated task. *Frontiers in Psychology,* **6**: 1794.

Meunier H, Vauclair J. 2007. Hand preferences on unimanual and bimanual tasks in white-faced capuchins (*Cebus capucinus*). *American Journal of Primatology,* **69**(9): 1064–1069.

Morino L, Uchikoshi M, Bercovitch F, Hopkins WD, Matsuzawa T. 2017. Tube task hand preference in captive hylobatids. *Primates,* **58**(3): 403–412.

Pan J, Xiao W, Zhao QK. 2011. Hand preference by black-and-white snub-nosed monkeys (*Rhinopithecus bieti*) in captivity: influence of tasks and sexes. *Laterality*: *Asymmetries of Body*, *Brain and Cognition,* **16**(6):

656–672.

Pan J, Xiao W, Talbert MH, Scott MB. 2013. Foot use and hand preference during feeding in captive black-and-white snub-nosed monkeys (*Rhinopithecus bieti*). *Integrative Zoology,* **8**(4): 378–388.

Perelle IB, Ehrman L. 2005. On the other hand. *Behavior Genetics,* **35**(3): 343–350.

Regaiolli B, Spiezio C, Hopkins WD. 2016. Hand preference on unimanual and bimanual tasks in Strepsirrhines: the case of the ring-tailed lemur (*Lemur catta*). *American Journal of Primatology*, **78**(8): 851–860.

Regaiolli B, Spiezio C, Hopkins WD. 2018. Hand preference on unimanual and bimanual tasks in Barbary macaques (*Macaca sylvanus*). *American Journal of Primatology*, **80**(5): e22745.

Rogers LJ, Kaplan G. 1996. Hand preferences and other lateral biases in rehabilitated orang-utans, *Pongo pygmaeus pygmaeus*. *Animal Behaviour,* **51**(1): 13–25.

Sanford C, Guin K, Ward JP. 1984. Posture and laterality in the bushbaby (*Galago senegalensis*). *Brain, Behavior and Evolution,* **25**(4): 217–224.

Spinozzi G, Truppa V. 2002. Problem-solving strategies and hand preferences for a multicomponent task by tufted capuchins (*Cebus apella*). *International Journal of Primatology,* **23**(3): 621–638.

Stafford DK, Milliken GW, Ward JP. 1990. Lateral bias in feeding and brachiation in *Hylobates*. *Primates,* **31**(3): 407–414.

Wells DL. 2002. Hand preference for feeding in captive *Colobus guereza*. *Folia Primatological* (*Basel*), **73**(1): 57–59.

Westergaard GC, Suomi SJ. 1993. Hand preference in capuchin monkeys varies with age. *Primates,* **34**(3): 295–299.

Zhang P, Watanabe K, Li BG, Tan CL. 2006. Social organization of Sichuan snub-nosed monkeys (*Rhinopithecus roxellana*) in the Qinling Mountains, Central China. *Primates,* **47**(4): 374–382.

Zhao DP, Ji WH, Watanabe K, Li BG. 2008. Hand preference during unimanual and bimanual reaching actions in Sichuan snub-nosed monkeys (*Rhinopithecus roxellana*). *American Journal of Primatology,* **70**(5): 500–504.

Zhao DP, Gao X, Li BG. 2010. Hand preference for spontaneously unimanual and bimanual coordinated tasks in wild Sichuan snub-nosed monkeys: Implication for hemispheric specialization. *Behavioural Brain Research,* **208**(1): 85–89.

Zhao DP, Wang Y, Wei XY. 2016. Hand preference during bimanual coordinated task in northern pig-tailed macaques *Macaca leonina*. *Current Zoology,* **62**(4): 385–391.

Interchange between grooming and infant handling in female Tibetan macaques (*Macaca thibetana*)

Qi Jiang[1], Dong-Po Xia[2], Xi Wang[1], Dao Zhang[1], Bing-Hua Sun[1], Jin-Hua Li[1,3,*]

[1] *School of Resource and Environmental Engineering, Anhui University, Hefei Anhui* 230601*, China*
[2] *School of Life Science, Anhui University, Hefei Anhui* 230601*, China*
[3] *School of Life Science, Hefei Normal University, Hefei Anhui* 241000*, China*

ABSTRACT

In some non-human primates, infants function as a social tool that can bridge relationships among group members. Infants are a desired commodity for group members, and mothers control access to them. The biological market theory suggests that grooming is widespread and represents a commodity that can be exchanged for infant handling. As a limited resource, however, the extent to which infants are interchanged between mothers (females with an infant) and non-mothers (potential handlers, females without an infant) remains unclear. In this study, we collected behavioral data to investigate the relationship between grooming and infant handling in free-ranging Tibetan macaques (*Macaca thibetana*) at Mt. Huangshan, China. Our results showed that females with infants received more grooming than females without infants. After her infant was handled, mother females received more grooming than they did during daily grooming interactions. However, with the increasing number of infants within the social group, both the grooming that mothers received and the grooming that non-mothers invested for handling infants decreased. We also found that non-mothers invested more time in grooming to gain access to younger infants than older infants. Our results provide evidence that infants are social commodities for both mother and non-mother females. Mothers use infants for obtain grooming and non-mothers use grooming to gain access to infants. The current study implies a bidirectional and complex interchange pattern between grooming and infant handling to compensate for the dyadic grooming disparity in non-human primates.

Keywords: Tibetan macaques (*Macaca thibetana*); Interchange; Infant handling; Grooming; Biological market theory

INTRODUCTION

While female attraction to infants represents a common feature in non-human primate species, maternal responses to infant handling show a certain degree of variability (Maestripieri, 1994; Nicolson, 1987). In some species, such as Asian colobines, females allow their newborn infants to be held frequently and carried for long durations by other group members (infant caretaking) (Nicolson, 1987; Stanford, 1992). In other species, such as baboons and macaques, mothers are much more restrictive in allowing access their young offspring (Altmann, 2002; Nicolson, 1987), despite persistent attempts by group members to interact with their infant (Frank & Silk, 2009; Gumert, 2007a; Henzi & Barrett, 2002). It is well documented that infants can be used as social tools to buffer agonistic interactions (Dunbar, 1984; Taub, 1980) and to facilitate social bonds (Dunayer & Berman, 2017; Hsu et al., 2016; Manson, 1999). Therefore, the infant handling concept may be indicative of the behavioral pattern that exists between an infant and a non-mother group member (Hsu et al., 2016; Jin et al., 2015; Maestripieri, 1994).

In recent decades, studies on the social function of infant handling within the framework of the biological market theory have gained increasing interest (Ueno, 2017; Wei et al., 2013; Yu et al., 2013). Biological market theory proposes that the infant can be considered as a social commodity,

Received: 01 November 2017; Accepted: 26 April 2018; Online: 28 June 2018

Foundation items: This study was supported in part by grants from the National Natural Science Foundation of China (31772475; 31672307; 31401981; 31372215)

*Corresponding author, E-mail: jhli@ahu.edu.cn

DOI: 10.24272/j.issn.2095-8137.2018.049

and thus interchange relationships between infant handling and behavioral commodities may exist. For example, in chacma baboons (*Papio cynocephalus ursinus*), Henzi & Barrett (2002) proposed that female A will groom female B more often if female B has a newborn infant in order to gain access. Yu et al. (2013) described similar findings in golden snub-nosed monkeys (*Rhinopithecus roxellana*), indicating that infant handling might be interchanged for grooming. Infant handling is also reported as a social commodity to interchange for affiliation, e.g., embracing in spider monkeys (*Ateles geoffroyi yucatanensis*) (Slater et al., 2007).

Grooming is a measure of affiliative social relationships among non-human primates (Dunbar, 2010). In some species, grooming accounts for as much as 10%–20% of an individual's total daily activity budget (Lehmann et al., 2007). Previous studies have demonstrated that grooming can be interchanged for support in agonistic encounters (Seyfarth & Cheney, 1984), mating opportunities (Barrett & Henzi, 2001; Gumert, 2007b), tolerance (Gumert & Ho, 2008), food (Watts, 2002), and infant handling (Gumert, 2007a; Henzi & Barrett, 2002; Tiddi et al., 2010). In tufted capuchin monkeys (*Cebus apella nigritus*), Tiddi et al. (2010) proposed that grooming is interchanged for infant handling among females, with grooming given by potential handlers increasing the likelihood of subsequent infant handling opportunities. Similar results have also been found in wild baboons (*P. anubis*) (Frank & Silk, 2009), long-tail macaques (*Macaca fascicularis*) (Gumert, 2007a), and golden snub-nosed monkeys (Wei et al., 2013).

These previous studies suggest that both grooming and infant handling opportunities are valuable commodities in primates. Infant handling consists of an infant and adult female other than its mother. The groomer (female A) may interchange grooming to gain access to the groomee's infant (female B, the infant's mother). Accordingly, as a limited-competition resource, infants could be interchanged between the groomee (supplier, infant's mother) and groomer (demander, potential handler, non-mother). However, the extent to which individuals perform grooming for infant handling or provide infant handling for grooming among females remains unclear.

We used the biological market perspective to examine the interchange relationships between grooming and infant handling in Tibetan macaques (*M. thibetana*). Tibetan macaques live in multi-male-multi-female social groups (mean group size=33.8±6.79), with female philopatry and male dispersion (Li, 1999). Tibetan macaques devote approximately 20% of their daily activity budget to grooming and thus it can be considered as a behavioral commodity in their social groups (Xia et al., 2012, 2013). Similar to other macaque species, group members persistently attempt to interact with infants in multiple ways (Li, 1999).

We hypothesized the existence of bidirectional and complex interchange patterns between grooming and infant handling in Tibetan macaques. We tested the following predictions: if an infant is a limited and valuable commodity, (1) females with infants will be more attractive than females without infants, and females will receive more but provide less grooming after giving birth than before parturition; (2) with an increase in the number of infants, females with infants will receive less grooming from females without infants; (3) females with infants will receive more grooming if they first allow their infant to be handled; if grooming is an effective way to gain access to an infant, (4) females will obtain more infant handling opportunities after grooming the infant's mother than they have under baseline social conditions.

MATERIALS AND METHODS

Study site and subjects

This study was conducted at Mt. Huangshan National Reserve in Anhui Province, China. The reserve is a World Culture and Nature Heritage site and well-known tourist destination, as well as research site for the study of Tibetan macaques.

The study site can be found within the reserve in an area known as the "Valley of the Monkeys". There are two groups at the site: Yulingkeng A1 (YA1, target group in this study) and Yulingkeng A2 (YA2). Matrilineal kinship is known from historic and demographic data collected daily since 1986 (Li, 1999). The target group has been thoroughly habituated to close observation (i.e., from <1 m) and all individuals can be recognized using physical features (i.e., scars, hair color patterns, or facial/body contours) without disturbance or capture. During the study period, the group consisted of eleven adult males, thirteen adult females, five subadults/juveniles, thirteen yearlings, and eleven infants $\leq$6-months-old (Table 1). We selected thirteen adult females and two subadult females for this study.

Table 1 Birth records of infants in the YA1 group during the study period

No.	Name	Date of birth	Date of death	Sex	Mother
1	TQY	2016–03–04	N/A	F	TXX
2	TFH	2016–03–27	N/A	F	THY
3	YXC	2016–04–16	2016–10–04	M	YCY
4	THL	2016–05–18	N/A	F	TRY
5	YXY	2016–05–29	2016–10–21	M	YH
6	TQYE	2016–06–05	2016–10–27	F	TXH
7	TXT	2016–09–18	2016–12–20	M	TH
8	HXY	2017–02–15	N/A	F	HH
9	THR	2017–02–16	2017–04–15	M	TR
10	YXM	2017–03–11	N/A	M	YCLA
11	YXD	2017–04–17	N/A	F	YCY

N/A: Not available. M: Male; F: Female.

Data collection

This study was conducted from July 2016 to January 2017 and from March to May 2017. All behavioral data were collected during an intensive study period over 201 days (average=25.1day/month, range=24–27). The social group was followed from dawn to dusk, and behavioral observations began at approximately 0700–0800 h and ended at 1700–1800

h each day (depending on the time of year). The observer maintained an observation distance of 5–10 m from the monkeys.

Focal animal sampling and continuous recording (using a digital voice recorder) were used to score the daily activity of the focal individual (Altmann, 1974), with the recorded data used as the baseline. Focal sample duration was set at 15 min (Li et al., 2007). We followed the sampling rules of Xia et al. (2012, 2013) to avoid the influence of humans and double-counting social interactions.

To investigate whether non-mothers were more likely to handle infants after grooming their mothers, we collected post-grooming (PG) samples. The PG samples consisted of 15-min focal observations of a non-mother who had just groomed a mother. To investigate whether infant handling by non-mothers increased subsequent grooming investment given to mothers, we collected post-infant handling (PH) samples. The PH samples consisted of 15-min focal observations of a non-mother who had just handled an infant of a mother. On the next day, at the same time, we conducted 15-min matched control (MC) focal observations matched with a PG or PH sample, with no grooming or infant handling preceding the focal observation (De Waal & Yoshihara, 1983). We collected MC samples only if the two participants were in proximity (within 5 m). If the two participants were not in proximity during the MC observations and/or were involved in handling or grooming interactions within the 5 min preceding a planned MC or in the first 5 min of an ongoing MC, we postponed the MC until all conditions were meet. If a MC observation could not be conducted within one week of the PG or PH, the PG or PH was discarded.

We used *ad libitum* sampling to collect data on duration of all grooming bouts between mothers and non-mothers that involved infant handling. We categorized an interaction as a grooming-infant handling interchange if a non-mother groomed a mother and handled her infant. This could occur in any order and any number of times. The interaction finished when the two individuals moved >5 m away from each other. We measured the total duration of grooming until the two females departed each other. We recorded the dyadic social relationships immediately when an interaction ended. According to Xia et al. (2012; 2013), we defined grooming as any act in which a macaque (groomer) used its hand or mouth to touch, clean, or manipulate the fur of another individual (groomee). Infant handling behaviors included inspect, teeth-chatter, hold, groom, and bridge (Table 2).

We used *ad libitum* sampling to record aggressive and submissive behaviors to determine dominance relationships. Aggressive interactions were defined as an individual threatening, chasing, slapping, grabbing, or biting another individual (Berman et al., 2007). Submissive behaviors were scored when an individual showed fearful interactions, such as fear grin, cower, mock leave, avoid, flee, or scream (Berman et al., 2004). All records of agonism were tallied for each focal female and divided into aggression given and aggression received.

Data analysis

We reported baseline data as mean±*SE* grooming duration (min/h) and infant handling frequency (times/h). We used a one sample Kolmogorov-Smirnov test to examine whether the data conformed to normal distribution ($P>0.05$).

Table 2 Definitions of infant handling behaviors

Behavior	Definition
Inspect	Handler brought its face within 15 cm of an infant and peered at it or smelt the genital area.
Teeth-chatter	Handler was in proximity to an infant and made clicking sounds with their teeth toward the infant.
Hold	Handler grabbed an infant using one or both hands.
Groom	Handler manipulated an infant's hair with its hand and/or mouth (except for momentary touching), sometimes removing and eating small items found in the infant's fur.
Bridge	Handler in proximity to the mother and glancing at the infant, with the infant carried by either the mother or handler. The pair held the infant between them and simultaneously licked the infant's genitals or body while teeth-chattering vigorously.

Infant handling behavior definitions were modified from Manson (1999) and Li (1999).

We used the baseline data and calculated the duration of grooming received by mothers from non-mothers and given to non-mothers by mothers before parturition and six months after giving birth. Data were compared using paired *t*-tests to analyze whether mothers were groomed for longer periods after giving birth than before parturition, and whether mothers groomed non-mothers less after giving birth than before parturition.

We collected data on 11 of the 15 females investigated for PG and PH. No data were collected for three adult females (TT, YZ, YM), who were older and less socially active in regard to infant handling and did not give birth or become pregnant during the study. One subadult female (THX) was not observed to engage in a grooming-infant handling interchange. We used paired *t*-test to compare the duration of grooming between focal samples and PH samples, and between MC samples and PH samples to determine if non-mothers handling infants promoted the non-mothers to groom mothers. We used paired *t*-test to compare the frequency of infant handling between focal samples and PG samples, and between MC samples and PG samples to determine if non-mothers grooming mothers promoted non-mother infant handling.

We used the *ad libitum* data collected on grooming-infant handling interchange to investigate whether the number of infants per female was negatively correlated with duration of non-mothers grooming mothers during the interaction. We used linear regression to determine relationships between grooming and the number of infants per female.

We analyzed grooming-infant handling interchange data to elucidate the effect of infant age on the duration of non-mothers grooming mothers during the interaction. We used linear regression to determine the relationship between infant age

and duration of non-mothers grooming mothers. We assessed individual dominance rank by calculating David's Score (DS). We also calculated linearity for the obtained dominance hierarchy (De Vries, 1995; Gammell et al., 2003) Rank distance is the number of individuals ranking between the focal animal and a given partner, plus 1 (Castles et al., 1999). In our study, the rank distance was the number of individuals ranking between the mother and non-mother, using the mother's rank as the standard. We determined the sequence of social ranks based on the DS values, according to Gammell et al. (2003). YH was the highest ranked, followed by YXX, YCY, YM, TXH, TH, TXX, YCLA, HH, TR, TRY, THX, TT, YZ, and THY.

We analyzed grooming-infant handling interchange data and used linear regression analysis to test the relationship between rank distance and duration of non-mothers grooming mothers. To investigate whether kinship between non-mother and mother affected the duration of non-mothers grooming mothers when infant handling, we used paired *t*-tests to compare the duration of non-mothers grooming mothers between kin and non-kin.

To account for potential bias caused by pseudoreplication, we used factorial ANOVA to test for variation across individuals and number of infants, infant age, and rank distance on the duration of non-mothers grooming mothers. We found a significant effect of number of infants, infant age, and rank distance on grooming duration, but no significant effect on individuals or interaction effects. We found no evidence that individual variation existed and therefore no support that individual idiosyncrasies solely accounted for the results. Thus, pseudoreplication did not seriously affect the results.

RESULTS

During the study period, we collected 90 valid PG-MC samples, 86 valid PH-MC samples, and 148 grooming-infant handling interchanges.

Grooming variation among females

The mean duration of mothers grooming non-mothers before birth (1.04±0.05 min/h) (mean±*SE*) was significantly longer than after birth (0.62±0.07 min/h) (paired *t*-test: t=6.233, df=5, P=0.002), whereas the mean duration of non-mothers grooming mothers after birth (1.27±0.17 min/h) was significantly longer than that before birth (0.66±0.09 min/h) (paired *t*-test: t=–4.218, df=5, P=0.008) (Figure 1).

Grooming variation between PH and baseline

For focal sample observations, the mean duration of non-mothers grooming mothers was 1.52±0.13 min/h (mean±*SE*). After non-mothers handled infants of mothers, the mean duration of non-mothers grooming mothers was 3.02±0.22 min/h (mean±*SE*). The duration of grooming was significantly higher in PH samples than in focal samples (paired *t*-test: t=7.679, df=10, P<0.001). In MC sample observations, the mean duration of non-mothers grooming mothers was 1.74±0.08 min/h (mean±*SE*). The duration of grooming was significantly higher in PH samples than in MC samples (paired *t*-test: t=6.475, df=10, P<0.001) (Figure 2).

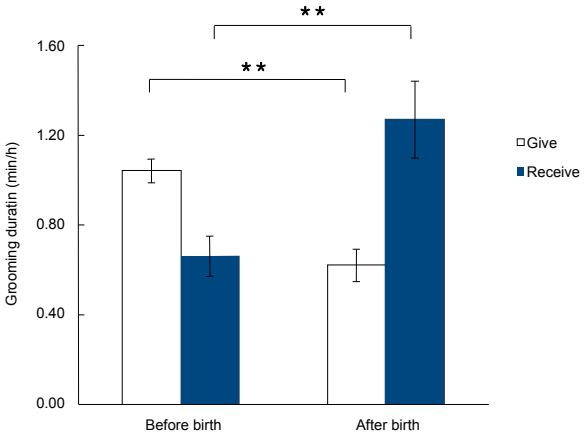

Figure 1 Duration of grooming females gave and received before birth and after birth (mean±*SE*)

**: P<0.01.

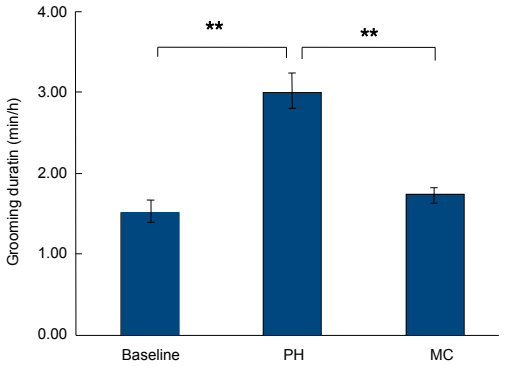

Figure 2 Duration of non-mothers grooming mothers (mean±*SE*)

Baseline represents the mean from focal sample data. PH represents the mean from post-infant handling sample data. MC represents the mean from MC sample data where mothers and non-mothers were in proximity. **: P<0.01.

Grooming variation with number of infants

The number of infants per female was negatively correlated with the duration of non-mothers grooming mothers during grooming-infant handling interchange (linear regression: R=0.624, F=93.271, P<0.001, R^2=0.390, df=147) (Figure 3).

Variation of infant handling

In focal sample observations, the mean frequency of non-mother infant handling was 2.07±0.48 times/h (mean±*SE*). After non-mothers groomed mothers, the mean frequency of non-mother infant handling was 6.20±0.65 times/h (mean±*SE*). The mean frequency of infant handling was significantly higher in PG samples than in focal samples (paired *t*-test: t=7.642, df=10, P<0.001). In MC sample observations, the mean frequency of infant handling was 2.60±0.36 times/h (mean±*SE*). The mean frequency of infant handling was significantly higher in PG samples than in MC samples (paired *t*-test: t=5.858, df=10, P<0.001) (Figure 4).

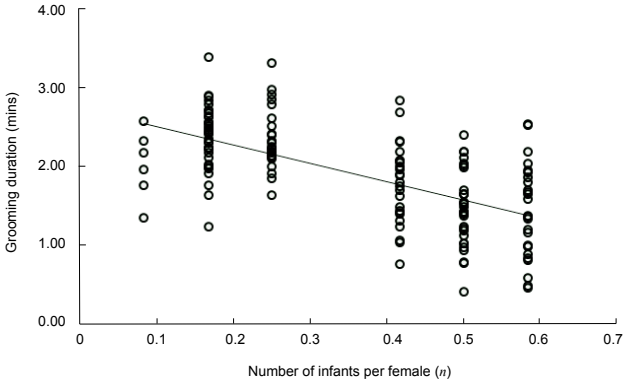

Figure 3 Duration of non-mothers grooming mothers was negatively correlated with the number of infants per female (mean±*SE*)

Linear regression: R=0.624, F=93.271, $P<0.001$, $R^2=0.390$, $df=147$.

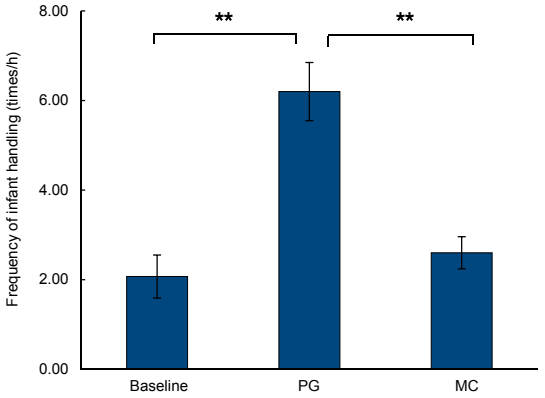

Figure 4 Frequency of non-mother infant handling (mean±*SE*)

Baseline represents the mean from focal sample data, PG represents the mean from post-grooming sample data, MC represents the mean from MC sample data where mothers and non-mothers were in proximity. **: $P<0.01$.

Effect of infant age

Infant age was negatively correlated with the duration of non-mothers grooming mothers during grooming-infant handling interchanges (linear regression: R=0.634, F=98.128, $P<0.001$, $R^2=0.402$, $df=147$) (Figure 5). The duration of non-mothers grooming mothers decreased significantly with infant age.

Effect of rank and kin

The rank distance between mothers and non-mothers was negatively correlated with the duration of non-mothers grooming mothers (linear regression: R=0.277, F=12.088, $P=0.001$, $R^2=0.076$, $df=147$) (Figure 6).

There was no significant difference in the duration of non-mothers grooming mothers when infant handling between kin and non-kin (paired t-test: $t=0.758$, $df=4$, $P=0.491$).

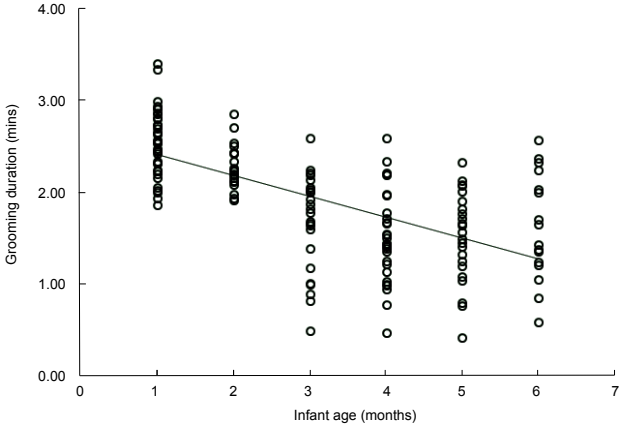

Figure 5 Duration of non-mothers grooming mothers was negatively correlated with infant age (mean±*SE*)

Linear regression: R=0.634, F=98.128, $P<0.001$, $R^2=0.402$, $df=147$.

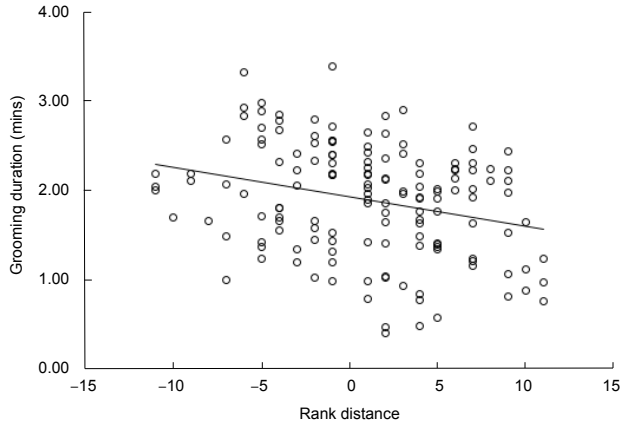

Figure 6 Duration of non-mothers grooming mothers was negatively correlated with rank distance between mothers and non-mothers (mean±*SE*)

Linear regression: R=0.277, F=12.088, $P=0.001$, $R^2=0.076$, $df=147$.

DISCUSSION

Infants are considered as commodities between a groomee (supplier, infant's mother) and groomer (demander, potential handler, non-mother). However, the extent to which individuals groom in exchange for infant handling or offer infant handling in exchange for grooming among females remains unclear. In this study, we found that mothers received more grooming from non-mothers after birth than before birth, and that mothers groomed non-mothers less after birth than before birth. These results supported the prediction that females with infants are more attractive than females without infants and that females will receive more but provide less grooming after birth than before parturition. These findings are similar to that reported for golden snub-nosed monkeys (*R. roxellana*) (Wei et al., 2013). Furthermore, after non-mothers handled infants, the duration of non-mothers grooming mothers was significantly higher than that observed under baseline conditions, supporting the prediction

that females with infants will receive more grooming if they first allow their infant to be handled. These results are similar to that reported for wild baboons (*P. anubis*) (Frank & Silk, 2009). We also demonstrated positive evidence for the prediction that females will gain higher infant handling opportunities after grooming an infant's mother compared with baseline interactions. Similar results have also been found in studies on golden snub-nosed monkeys (*R. roxellana*) and long-tailed macaques (*M. fascicularis*) (Gumert, 2007a; Yu et al., 2013). Thus, we concluded that infants are a limited and valuable commodity and can be used by mothers in exchange for grooming. Furthermore, grooming is an effective way for non-mothers to access infants. Our results showed bidirectional and complex interchange patterns between grooming and infant handling in Tibetan macaques, and that the adaptive investment of females will change based on their social characteristics and group dynamics.

A single behavioral exchange may not explain all behavioral relationships among individuals. In the case of reciprocity, pairs of actors are expected to form long-term and predictable social relationships so that, on average, the overall costs and benefits to each are relatively equal over time (Seyfarth, 1977; Xia et al., 2012). In contrast, under conditions in which individual actors have the opportunity to interact with a diverse set of social partners who vary in the quality of goods or services each can provide at any given moment in time, individuals are expected to seek out partners who provide the greatest benefit at the lowest cost (Noë et al., 1991; Wilkinson, 1984). These interactions can involve an exchange of the same goods or services (i.e., grooming in exchange for grooming) or the interchange of different goods or services. In Tibetan macaques, grooming can be exchanged for grooming (Xia et al., 2012, 2013) and interchanged for tolerance (Xia et al., 2012). In our study, grooming was interchanged for infant handling. However, we suggest that a single exchange may not fully explain the behavioral relationship between individuals. The behavioral exchange model is complex, reflecting the evolution of individual adaptability and promoting relationship maintenance and group stability in primate societies.

Market forces affect the interchange between grooming and infant handling. Infant age is a market force that can influence grooming payment. In our study, Tibetan macaque females groom other females for a longer period when they have a younger infant, with similar results also reported in studies on long-tailed macaques (*M. fascicularis*), tufted capuchin monkeys (*Cebus apella nigritus*), sooty mangabeys (*Cercocebus atys*), and vervet monkeys (*Chlorocebus aethiops*) (Fruteau et al., 2011; Gumert, 2007a; Tiddi et al., 2010). These results reflect that newborn infants are generally more attractive than older infants (Nicolson, 1987), with infants get older, their attractiveness declined. Market theory predicts that supply and demand will influence behavior exchange among group members by altering the value of the commodities traded (Noë et al., 2001). Under a biological market perspective, potential handlers attracted to infants represent the demand and infants represent the supply (Gumert, 2007a; Henzi & Barrett, 2002). In Tibetan macaques, with the increase in the number of infants, the duration of non-mothers grooming mothers for infant handling decreased significantly. Similar results have been reported in studies on chacma baboons (*P. cynocephalus ursinus*) and long-tailed macaques (*M. fascicularis*) (Gumert, 2007a; Henzi & Barrett, 2002).

Dominance hierarchy is a factor that has considerable influence on social interchange in non-human primates. Dominance relationships may make social commodities cheaper for higher-ranked individuals and more expensive for lower-ranked individuals (Gumert, 2007a; Henzi & Barrett, 2002; Tiddi et al., 2010; Wei et al., 2012). In Tibetan macaques, rank can affect the patterns of grooming reciprocity among females; within the context of a biological market, higher ranking females have a wider set of social options than middle and lower ranking females (Xia et al., 2012). Our study indicated that dominance also altered the interchange between grooming and infant handling in Tibetan macaques, by reducing the grooming investment that higher ranking non-mothers gave to mothers when infant handling and increasing the grooming investment that lower ranking non-mothers gave to mothers. These results indicate that, in an infant market, lower-ranked individuals will pay more for interacting with higher-ranked partners, and rank might corrupt a social market and skew social exchange to benefit higher-ranked individuals.

In Tibetan macaques, we found the interchange between grooming and infant handling to be bidirectional and to change with the age and number of infants. The interchange relationship between grooming and infant handling is an important part of social relationship maintenance and group stability in primate societies. It not only helps us to understand the characteristics of behavioral adaptation in adult individuals, but also highlights the social functions of infants.

COMPETING INTERESTS

The authors declare that they have no competing interests.

AUTHORS' CONTRIBUTIONS

Q.J. and D.P.X. designed the study. Q.J. and K.H.P. conducted data collection. Q.J. and K.H.P. performed statistical analysis, Q.J. and D.P.X. wrote the manuscript, and J.H.L. revised the manuscript. All authors read and approved the final version of the manuscript.

ACKNOWLEDGEMENTS

This study was conducted at Mt. Huangshan China. We give special thanks to Mr. HB Cheng and family for their outstanding logistical support during our study. We are also very grateful to Mr. SF Xie, YG Xie and the staff of Huangshan Monkey Center for their complete support and assistance.

REFERENCES

Altmann J. 1974. Observational study of behaviour sampling methods. *Behaviour*, **49**(3): 227–267.

Altmann J. 2002. Baboon mothers and infants. *African Journal of Ecology*, **40**(4): 417.

Barrett L, Henzi SP. 2001. The utility of grooming in baboon troops. *In*: Noë R, Van Hooff JARAM, Hammerstein P., Eds Economics in Nature: Social Dilemmas, Mate Choice and Biological Markets. Cambridge: Cambridge University Press, 119–145.

Berman CM, Ionica C, Li JH. 2007. Supportive and tolerant relationships among male Tibetan macaques at Huangshan, China. *Behaviour*, **144**(6) : 631–661.

Berman CM, Ionica C, Li JH. 2004. Dominance style among *Macaca thibetana* on Mt. Huangshan, China. *International Journal of Primatology*, **25**(6): 1283–1312.

Castles DL, Whiten A, Aureli F. 1999. Social anxiety, relationships and self-directed behaviour among wild female olive baboons. *Animal Behaviour,* **58**(6): 1207–1215.

De Vries H. 1995. An improved test of linearity in dominance hierarchies containing unknown or tied relationships. *Animal Behaviour*, **50**(5): 1375–1389.

De Wall FBM, Yoshihara D. 1983. Reconciliation and redirected affection in rhesus monkeys. *Behaviour*, **85**(3): 224–241.

Dunayer ES, Berman CM. 2017. Infant handling enhances social bonds in free-ranging rhesus macaques(*Macaca mulatta*). *Behaviour*, **154**(7–8): 875–907.

Dunbar RIM. 2010. The social role of touch in humans and primates: behavioural function and neurobiological mechanisms. *Neuroscience & Biobehavioral Reviews*, **34**(2): 260–268.

Dunbar RIM. 1984. Infant-use by male gelada in agonistic contexts: agonistic buffering, progeny protection or soliciting support? *Primates*, **25**(1): 28–35.

Frank RE, Silk JB. 2009. Grooming exchange between mothers and non-mothers: the price of natal attraction in wild baboons(*Papio anubis*). *Behaviour*, **146**(7): 889–906.

Fruteau C, van de Waal E, van Damme E, Noë R. 2011. Infant access and handling in sooty mangabeys and vervet monkeys. *Animal Behaviour*, **81**(1): 153–161.

Gammell MP, De Vries H, Jennings DJ, Carlin CM, Hayden TJ. 2003. David's score: A more appropriate dominance ranking method than Clutton-Brock et al.'s index. *Animal Behaviour,* **66**(3): 601–605.

Gumert MD. 2007a. Grooming and infant handling interchange in *Macaca fascicularis*: The relationship between infant supply and grooming payment. *International Journal of Primatology*, **28**(5): 1059–1074.

Gumert MD. 2007b. Payment for sex in a macaque mating market. *Animal Behaviour*, **74**(6): 1655–1667.

Gumert MD, Ho MHR. 2008. The trade balance of grooming and its coordination of reciprocation and tolerance in Indonesian long-tailed macaques(*Macaca fascicularis*). *Primates*, **49**(3): 176–185.

Henzi SP, Barrett L. 2002. Infants as a commodity in a baboon market. *Animal Behaviour*, **63**(5): 915–921.

Hsu MJ, Lin S, Lin JF, Lin TJ, Agoramoorthy G. 2016. Non-maternal infant handling in wild formosan macaques of mount longevity, Taiwan. *Folia primatologica*, **86**: 491–505.

Jin T, Wang DZ, Pan WS, Yao M. 2015. Nonmaternal infant handling in wild white-headed langurs(*Trachypithecus leucocephalus*). *International Journal of Primatology*, **36**(2): 269–287.

Lehmann J, Korstjens AH, Dunbar RIM. 2007. Group size, grooming and social cohesion in primates. *Animal Behaviour*, **74**(6): 1617–1629.

Li JH. 1999. The Tibetan Macaque Society: A Field Study. Hefei, Anhui University Press.(in Chinese)

Li JH, Yin H, Zhou L. 2007. Non-reproductive copulation behavior among Tibetan macaques (*Macaca thibetana*) at Huangshan, China. *Primates*, **48**(1): 64–72.

Maestripieri D. 1994. Social structure, infant handling, and mothering styles in group-living old world monkeys. *International Journal of Primatology*, **15**(4): 531–553.

Manson JH. 1999. Infant handling in wild *Cebus capucinus*: Testing bonds between females? *Animal Behaviour*, **57**(4): 911–921.

Nicolson NA. 1987. Infants, mothers, and other females. *In*: Smuts BB, Cheney DL, Seyfarth RM, Wrangham RW, Struhsaker T (Eds). Primate Societies. Chicago: University of Chicago Press, 330–342.

Noë R, van Schaik CP, van Hooff JARAM. 1991. The market effect: an explanation for pay-off asymmetries among collaborating animals. *Ethology*, **87**(1–2): 97–118.

Noë R, van Hooff JARAM, Hammerstein P. 2001. Economics in Nature: Social Dilemmas, Mate Choice and Biological Markets. Cambridge: Cambridge University Press.

Seyfarth RM, Cheney DL. 1984. Grooming, alliances and reciprocal altruism in vervet monkeys. *Nature*, **308**(5959): 541–543.

Seyfarth RM. 1977. A model of social grooming among adult female monkeys. *Journal of Theoretical Biology*, **65**(4): 671–698.

Slater KY, Schaffner CM, Aureli F. 2007. Embraces for infant handling in spider monkeys: evidence for a biological market? *Animal Behaviour*, **74**(3): 455–461.

Stanford CB. 1992. Costs and benefits of allomothering in wild capped langurs(*Presbytis pileata*). *Behavioral Ecology and Sociobiology*, **30**(1): 29–34.

Taub DM. 1980. Testing the 'agonistic buffering' hypothesis. *Behavioral Ecology and Sociobiology*, **6**(3): 187–197.

Tiddi B, Aureli F, Schino G. 2010. Grooming for infant handling in tufted capuchin monkeys: a reappraisal of the primate infant market. *Animal Behaviour*, **79**(5): 1115–1123.

Ueno M. 2017. Development of studies on grooming reciprocity in primates. *Japanese Journal of Animal Psychology*, **66**(2): 91–107.

Watts DP. 2002. Reciprocity and interchange in the social relationships of wild male chimpanzees. *Behaviour*, **139**: 343–370.

Wei W, Qi XG, Garber PA, Guo ST, Zhang P, Li BG. 2013. Supply and demand determine the market value of access to infants in the golden snub-nosed monkey(*Rhinopithecus roxellana*). *PLoS One*, **8**(6): e65962.

Wei W, Qi XG, Guo ST, Zhao DP, Zhang P, Huang K, Li BG. 2012. Market powers predict reciprocal grooming in golden snub-nosed monkeys(*Rhinopithecus roxellana*). *PLoS One*, **7**(5): e36802.

Wilkinson GS. 1984. Reciprocal food sharing in the vampire bat. *Nature*, **308**(5955): 181–184.

Xia DP, Li JH, Garber PA, Matheson MD, Sun BH, Zhu Y. 2013. Grooming reciprocity in male Tibetan macaques. *American Journal of Primatology*, **75**(10): 1009–1020.

Xia DP, Li JH, Garber PA, Sun LX, Zhu Y, Sun BH. 2012. Grooming reciprocity in female Tibetan macaques *Macaca thibetana. American journal of Primatology*, **74**(6): 568–572.

Yu Y, Xiang ZF, Yao H, Grueter CC, Li M. 2013. Female snub-nosed monkeys exchange grooming for sex and infant handling. *PLoS One*, **8**(9): e74822.

Zoological Research Editorial Board

ZOOLOGICAL RESEARCH
动物学研究
Bimonthly, Since 1980

Project for Enhancing International Impact of China STM Journals

中国精品科技期刊 2017 OUTSTANDING S&T JOURNALS OF CHINA
中国精品科技期刊
中国科技核心期刊
中国百强报刊

Editor-in-Chief: Yong-Gang Yao

Executive Editor-in-Chief: Yun Zhang

Editors: Su-Qing Liu Long Nie

Edited by Editorial Office of Zoological Research

(Kunming Institute of Zoology, Chinese Academy of Sciences, 32 Jiaochang Donglu, Kunming, Yunnan, Post Code: 650223 Tel: +86 871 65199026 E-mail: zoores@mail.kiz.ac.cn)

Sponsored by Kunming Institute of Zoology, Chinese Academy of Sciences; China Zoological Society©

Supervised by Chinese Academy of Sciences

Published by Science Press (16 Donghuangchenggen Beijie, Beijing 100717, China)

Printed by Kunming Xiaosong Plate Making & Printing Co, Ltd

Domestic distribution by Yunnan Post and all local post offices in China

International distribution by China International Book Trading Corporation (Guoji Shudian) P.O.BOX 399, Beijing 100044, China

Advertising Business License 广告经营许可证：滇工商广字66号

淘宝购买

微店购买

Domestic Postal Issue No.: 64-20

Price: 15.0 USD/80.0 CNY

遗传资源与进化国家重点实验室 State Key Laboratory of Genetic Resources and Evolution

AMHD

ISSN 2095-8137

9 772095 813193 03>